

IN²UB ANNUAL MEETING

BOOK OF ABSTRACTS

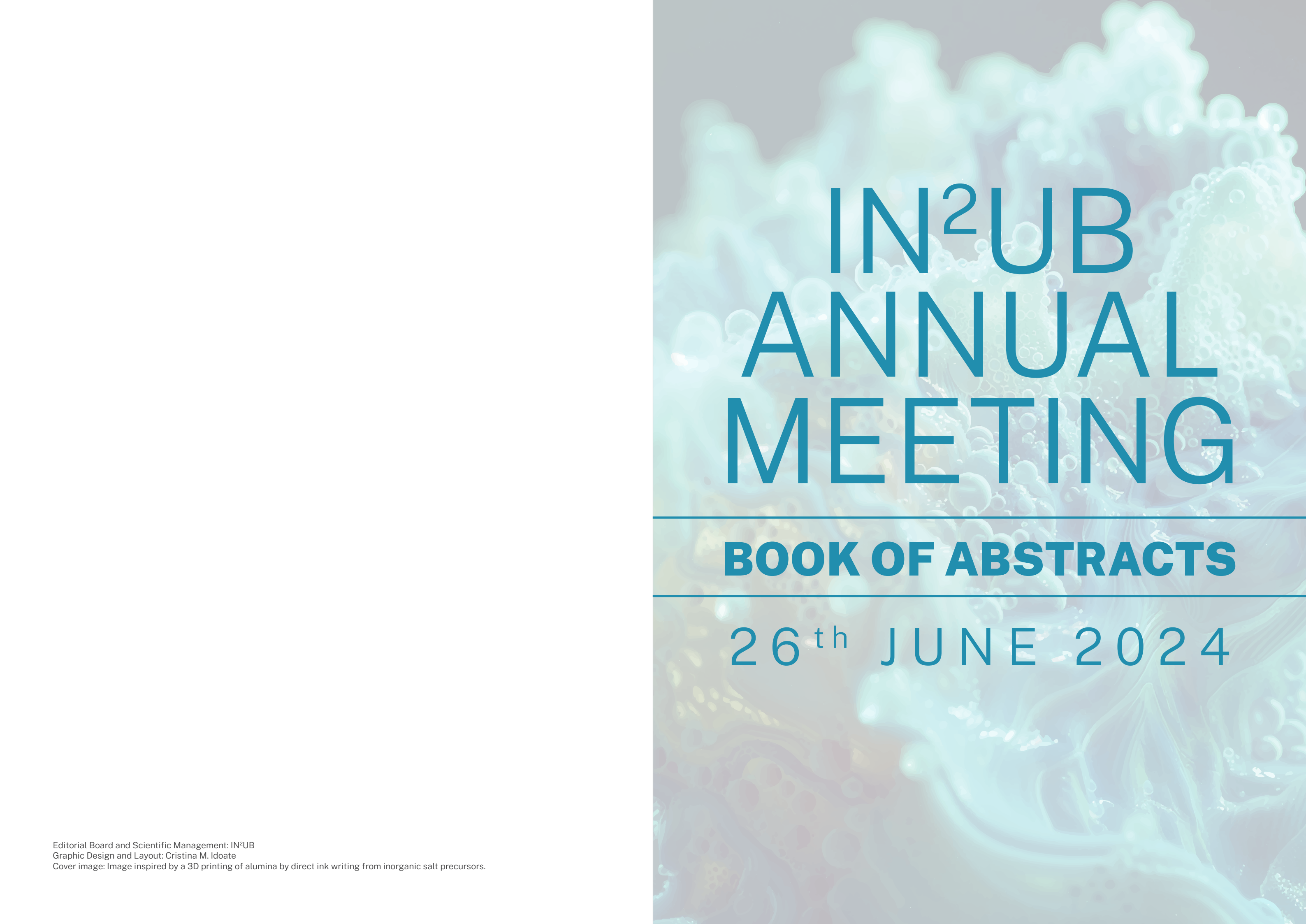
26th JUNE 2024



Institut de Nanociència
i Nanotecnologia



UNIVERSITAT DE
BARCELONA

The background of the entire page is a complex, abstract 3D printed structure of alumina. It features a dense network of interconnected, porous-looking filaments and spheres, creating a highly textured and intricate appearance. The color palette is a mix of light blues, greens, and soft purples, giving it a futuristic and scientific feel.

IN²UB ANNUAL MEETING

BOOK OF ABSTRACTS

26th JUNE 2024

FOREWORD

Dear IN²UB fellows,

It is a great pleasure to invite you to read through the program and book of abstracts for the 2024 IN²UB Annual Workshop. The tremendous success brought about by the high quality and attendance of this event reflects the vivacity and dynamism of our organization, which draws special value from the strongly multidisciplinary nature of the contributions. I believe that this program faithfully mirrors our diversity within the realm of Nanoscience and Nanotechnology, and the workshop is an ideal forum to capitalize on this diversity through fruitful collaborations.

I encourage you to take advantage of this opportunity, which will not only broaden your scientific horizons but also enhance the stature and raison d'être of IN²UB.

I would like to take this occasion to thank everyone who has made this event possible. First, I extend my gratitude to those directly involved in the organization, the selection of contributions, and the conduction of the workshop. I am also grateful to the young and senior researchers who have contributed their papers (whether posters or oral presentations). Finally, I thank all the researchers of IN²UB, whose efforts have produced the knowledge contained in this program and who will share their insights during the meeting.

On behalf of the IN²UB, I wish that you enjoy and take maximum profit from this celebration of our research.

Guillem Aromí

*Director of the Institute of Nanoscience and Nanotechnology
of the University of Barcelona (IN²UB)*

CONTENTS INDEX

PROGRAM 12

PLENARY LECTURE 14

PL

Zoom in: from seeing to experiment in a nanolaboratory

Prof. Francesca Peiró..... 15

ART 16

2022-ART grantee (ART1)

Development of chemoresistive gas sensors made from metal-organic frameworks (MOFs) for early thermal runaway detection in Lithium-ion batteries
Prof. Albert Romano.....18

2022-ART grantee (ART2)

Hierarchically nanostructured transition metal carbides and MXenes on carbon felt for CO₂ reduction and green H₂ production (2IPs)
Dr. Stefanos Chaitoglou, Dr. Xavier Vendrell.....19

2022-ART grantee (ART3)

Electronic and PHOTOelectronic properties of multifunctional Semiconducting nanostructures (ELPHOS)
Dr. Adriana Figueroa..... 20

2023-ART grantee (ART4)

Magnonic wrinkles
Dr. Blai Casals..... 21

ORAL PRESENTATIONS 22

O1

Anti-ferroelectric dark modes in an inverted plasmonic lattice

J. Rodríguez-Álvarez, A. Labarta, J. C. Idrobo, R. Dell'Anna, A. Cian, D. Giubertoni, X. Borrísé, A. Guerrero, F. Pérez-Murano, A. Fraile Rodríguez and X. Batlle 24

O2

Smart gel-dispersed calcium hydroxide-loaded nanoparticles for endodontics

X. Roig, L. Halbaut, M. Espina, J. A. González Sánchez, F. Duran-Sindreu, M. L. García, E. Sánchez-López..... 25

O3

Machine Learning Strategies for Low-Loss Electron Energy Loss Spectroscopy

V. Costa, D. del Pozo, C. Coll, J. Nogués, B. Sepulveda, L. Bocher, M. Kociak, J. Blanco-Portals, S. Estradé and F. Peiró 26

O4

Scanless and Camera-Free Fd-Flim With Frequency Encoded Light

L. Rodríguez-Suné, P. Ricci, A. Marchese, P. Saggau, M. Duocastella 27

O5

Mathematical model of fluid front dynamics driven by porous media pumps

A. Benavent-Claró, Y. Alvarez-Braña, F. Benito-Lopez, L. Basabe-Desmots and A. Hernandez-Machado 28

O6

Motion and control of virtual colloidal particles in confined chiral liquid crystals

J. Torres-Andrés, J. Ingés-Mullol, F. Sagués..... 29

O7

Magnetic nanocomposites for radar shielding applications

J. Calvo-de la Rosa, A. García-Santiago, J. M. Hernández, M. Vazquez-Aíge, J. M. Lopez-Villegas and J. Tejada 30

O8

Usage of Polypurine Reverse Hoogsteen Hairpins for Therapeutic Intervention Against SARS-CoV-2

C. J. Ciudad, S. Valiuska, J. M. Rojas, P. Nogales-Altozano, A. Aviñó, R. Eritja, M. Chillón, N. Sevilla and V. Noé 31

O9

Carbides, MAX and MXenes as co-catalysts in nanocomposites for the H₂ photoproduction from bioethanol

A. Sánchez, M. Gil, J. Serafin, P. Ramírez de la Piscina and N. Homs 32

POSTERS 34

NanoMet

P1 Unsupervised machine learning for nanoparticles in biological solutions 36

P2 Impact of an inhomogeneous concentration field on the transport and self-assembly of active particles 37

P3 Non-equilibrium thermodynamics of catalytic janus particles self-assembly 39

P4 Solid-state pyroelectric system for near-field energy conversion 40

P5 Investigating vacancies and anisotropic defects using STEM and iDPC imaging techniques 41

P6 Analysis of Optical Properties of HfO₂ Thin Layers with Rhombohedral, Monoclinic, and Hexagonal Structures Using EELS 43

NanoBio

P7 Probing active nematics with in situ microfabricated elastic inclusions 45

P8 Liposomal encapsulation and release for skin protection and treatment 46

P9 Targeting lncRNA Hotair with PPRHs in the context of breast cancer and tamoxifen resistance 47

P10 Towards the reduction of experimental costs through the use of Meta Learning 48

P11 3D culturing immortalized pulmonary fibroblasts within extracellular matrix hydrogels impacts their mechanical phenotype 49

P12 Cryosectioning of hydrogels as a reliable approach to increase yield and further tune mechanical properties 50

P13 Super-resolution laser scanning microscopy with photo-switchable fluorophores 52

P14 Microfluidic device for the study of angiogenesis in controlled 3d microenvironments 53

P15 On the total field characterization of highly focused beams in the far field. 54

NanoEnergy

P16 Fabrication of an alicu alloy by applying pulsed current without additives for decorative purposes 55

NanoMagnetism

P17 Unveiling the 3D magnetic vortex texture of iron oxide nanoflowers 56

P18 A supramolecular helicate with two independent Fe(II) switchable centres and a [Fe(anilate)₃]³⁺ guest 57

P19 Design of h-bonded supramolecular Fe(II) switchable materials 58

P20 Exploring size-dependent magnetic properties of non-stoichiometric Ni_{1-x}O nanoparticles 59

P21 Energy transfer dynamics in heterometallic [LnLn'Ln] trinuclear compounds. 60

P22 Slow magnetic relaxation and luminescence properties in β-diketonate lanthanide(III) complexes. Preparation of Eu(III) and Yb(III) OLED devices 61

P23 Strong spin-photon coupling in van der waals magnets 62

P24 Deep learning for magnetization dynamics 63

P25 Antiferromagnetic resonance in canted antiferromagnets 64

P26 Modulated spin dynamics of [Co₂] coordination helicates via differential strand composition 65

P27 Spin-crossover and supramolecular interactions: modulating structural changes 66

P28 Strain assisted magnetic domain wall motion 67

NanoPharmaMed

P29 Changes in the aggregation pathways and final conformation of α-synuclein induced by lipid environment 68

P30 Intracellular glutathione (GSH) detection using BODIPY-functionalized silicon oxide microchips 69

P31 Characterization of Poly(ε-caprolactone) nanoparticles for enhanced ocular drug delivery 70

P32 Formulation, characterization and evaluation of the anti-inflammatory efficacy of a chrysothol-loaded nanoemulsion for the treatment of atopic dermatitis	71
P33 Exploring the impact of titanium oxide nanoparticles: unveiling their phototoxic behaviour in a keratinocyte cell line	72
P34 Supramolecular gels for photodynamic therapy	73
P35 Novel riluzole loaded nanostructured lipid carriers for the treatment of psoriasis	74
P36 Crucial role of PrP ^{Sc} in triggering oligomerization of A β peptides	75
P37 3D spheroids induced by superhydrophobicity as cell-derived strategies for therapeutical targets	76
P38 In-vitro PrP ^{Sc} aggregates alter α -synuclein aggregation pattern	77
P39 Dually active apigenin-loaded nanostructured lipid carriers with rosehip oil for cancer treatment	78
P40 Development and characterization of PLGA nanoparticles loaded with <i>phlomis crinita</i> extract: promising potential for enhanced skin treatments	79
P41 Cubic liquid crystalline-based emulsions for bakuchiol topical delivery	80
P42 Novel optimized clobetasol-loaded lipid nanoparticles for dermal applications	81
P43 Ruthenium (II) thiocyanate complexes: moving from dye-sensitized solar cells to photodynamic therapy for cancer treatment	82
P44 Application of nanomedicine for the development of a novel diclofenac formulation for proliferative diseases	83

NanoPhotoElectro

P45 Unlocking the potential of metal oxide nanowires: tailored synthesis and integration for advanced applications	84
---	----

P46 ZIF-8 based surface plasmon resonance sensors for chemical vapor optical detection	85
P47 Coupled optical modes in twisted triskelia nanostructures	87
P48 Lead-Free Perovskite-Based Optoelectronic Devices: Advancements in Flexible Inkjet Printing	88
P49 Non-invasive light guiding in uniform and scattering media via photoacoustic excitation	90
P50 Mueller matrix polarization spatial frequency domain imaging system (pSFDI) for mapping biological tissues	91
P51 3D shape control of laser-printed parts with substrate reshaping	92
P52 Insights into inkjet-printed 2d tin iodide perovskite: optical and optoelectronic analyses	93
P53 Guiding light deep in scattering media with shaped ultrasound waves	94
P54 Structural and optical characterization of inkjet-printed CsCu ₂ I ₃ thin films	95
P55 Triphenylene metal-organic frameworks as a platform for catalysis applications	96
P56 Synchronization dynamics in optomechanical crystal cavities	97
P57 Studying triphenylene derivative MOFs for room-temperature greenhouse gas sensing	98
P58 Two-dimensional transition metal dichalcogenides for gas sensing applications	99

NanosMat

P59 Phosphane gold (I) complexes: structural configuration vs luminescent properties	100
P60 Synthesis and photophysical characterization of novel heterometallic gold(I)-copper(I) complexes	101
P61 Boosting supercapacitive performance using defect-engineered ZnO nanorods anchored on graphene nanowalls hybrid electrodes	102

P62 Optical studies on anisotropic Bi ₂ S ₃ and hybrid Bi ₂ S ₃ @Au theragnostic nanocomposites	103
--	-----

P63 Luminescent gold(I) naphthalimide derivatives	104
--	-----

P64 SiNWs-MoOX hybrid electrodes: advancing Li-ion battery technology through surface modification	105
---	-----

P65 Mo ₂ C nanostructures anchored on carbon nanotubes for enhanced electrocatalytic hydrogen evolution	106
---	-----

P66 CoFe ₂ O ₄ /Cu- and Ce-DOPED SnO ₂ Composites for Sonophotocatalytic Degradation of Organic Pollutants	107
--	-----

P67 Electrochemical fabrication and functionalization of BiOI for photocatalytic water decontamination	108
---	-----

P68 Doped ZnO/Ni photocatalysts for the removal of pharmaceutical pollutants via pms activation	109
--	-----

P69 No switching cooperativity on complexes with bis-coordinated azo ligands having a {M ^{II} (dppp)} ²⁺ (M = PD, PT) scaffold	110
---	-----

P70 Flower-like hydroxyapatite: hydrothermal preparation and functionalization with aminophosphate compounds	111
---	-----

P71 Biomimetic sunflower pollen-based heterostructured photocatalyst for enhanced visible-light-driven photocatalytic degradation of pharmaceuticals	112
---	-----

P72 Enhancing organic field-effect transistors: a study on triindole-based semiconductors using advanced processing techniques and device architectures	113
--	-----

AUTHOR INDEX

114

PROGRAM

9:00h. – 9:30h. **REGISTRATION**

9:30h. – 9:40h. **WELCOME & OPENING**

Prof. Guillem Aromí, Director of Institute of Nanoscience and Nanotechnology (IN²UB).

SESSION I

9:40h. – 10:40h. **PLENARY (TBA)**
ZOOM IN: FROM SEEING TO EXPERIMENT IN A NANOLABORATORY

Prof. Francesca Peiró
LENS-MIND, Department of Electronics and Biomedical Engineering and Institute of Nanoscience and Nanotechnology (IN²UB), University of Barcelona (UB).

10:45h. – 11:10h. **2022-ART GRANTEE (ART1)**
DEVELOPMENT OF CHEMORESISTIVE GAS SENSORS MADE FROM METAL-ORGANIC FRAMEWORKS (MOFs) FOR EARLY THERMAL RUNAWAY DETECTION IN LITHIUM-ION BATTERIES

Prof. Albert Romano, MIND group. (NanoPhotoElectro&NanosMat collaboration). (* as the Group Responsible, the IP can't attend).

11:10h. – 11:50h. **COFFEE BREAK & POSTER SESSION I**

SESSION II

11:50h. – 12:15h. **2022-ART GRANTEE (ART2)**
HIERARCHICALLY NANOSTRUCTURED TRANSITION METAL CARBIDES AND MXENES ON CARBON FELT FOR CO₂ REDUCTION AND GREEN H₂ PRODUCTION (2IPs)

*Dr. Stefanos Chaitoglou**, ENPHOCAMAT group (NanosMat) & *Dr. Xavier Vendrell*, MATCAT group (NanoEnergy) (* Speaker).

12:15h. – 12:35h. **ORAL (O1)**
ANTI-FERROELECTRIC DARK MODES IN AN INVERTED PLASMONIC LATTICE

Javier Rodríguez, Group of Magnetic Nanomaterials (NanoMagnetics).

12:35h. – 12:55h. **ORAL (O2)**
SMART GEL-DISPERSED CALCIUM HYDROXIDE-LOADED NANOPARTICLES FOR ENDODONTICS

Xavier Roig, Nanostructured systems for controlled drug delivery group (NanoPharmaMed).

12:55h. – 13:15h. **ORAL (O3)**
MACHINE LEARNING STRATEGIES FOR LOW-LOSS ELECTRON ENERGY LOSS SPECTROSCOPY

Vanessa Costa, LENS-MIND group (NanoMet).

13:15h. - 15:00h. **LUNCH & NETWORKING**

SESSION III

15:00h. - 15:25h. **2022-ART GRANTEE (ART3)**
ELECTRONIC AND PHOTOELECTRONIC PROPERTIES OF MULTIFUNCTIONAL SEMICONDUCTING NANOSTRUCTURES (ELPHOS)

Dr. Adriana Figueroa, Group of Magnetic Nanomaterials (NanoMagnetics&NanoPhotoElectro&NanoBio Collaboration).

15:25h. - 15:50h. **2023-ART GRANTEE (ART4)**
MAGNONIC WRINKLES

Dr. Blai Casals, Grup de Magnetisme (NanoMagnetics&NanoEnergy Collaboration).

15:50h. - 16:10h. **ORAL (O4)**
SCANLESS AND CAMERA-FREE Fd-FLIM WITH FREQUENCY ENCODED LIGHT

Laura Rodríguez, LASER-Micro and Nanotechnology and Nanoscopies for Electronic and Electrophotonic Devices (MIND) (NanoPhotoElectro).

16:10h. - 16:30h. **ORAL (O5)**
MATHEMATICAL MODEL OF FLUID FRONT DYNAMICS DRIVEN BY POROUS MEDIA PUMPS

Andreu Benavent, Physics in Nanobiophysics (NanoBio).

16:30h. - 17:10h. **COFFEE BREAK & POSTER SESSION II**

SESSION IV

17:10h – 17:30h. **ORAL (O6)**
MOTION AND CONTROL OF VIRTUAL COLLOIDAL PARTICLES IN CONFINED CHIRAL LIQUID CRYSTALS

Joel Torres, SOC&SAM group (NanosMat).

17:30h - 17:50h. **ORAL (O7)**
MAGNETIC NANOCOMPOSITES FOR RADAR SHIELDING APPLICATIONS

Jaume Calvo, Grup de Magnetisme (NanoMagnetics).

17:50h – 18:10h. **ORAL (O8)**
USAGE OF POLYPURINE REVERSE HOOGSTEEN HAIRPINS FOR THERAPEUTIC INTERVENTION AGAINST SARS-CoV-2

Verónica Noé, Cancer Therapy Group (NanoBio).

18:10h – 18:30h. **ORAL (O9)**
CARBIDES, MAX AND MXENES AS CO-CATALYSTS IN NANOCOMPOSITES FOR THE H₂ PHOTOPRODUCTION FROM BIOETANOL SAGE

Adrià Sánchez, MATCAT group (NanoEnergy).

18:30h. – 18:50h. **POSTER AWARD**

18:50h. – 19:00h. **CLOSING REMARKS**

Prof. Martí Duocastella, IN²UB Deputy Director.

PLENARY LECTURE

PLENARY LECTURE

PL

ZOOM IN: FROM SEEING TO EXPERIMENT IN A NANOLABORATORY

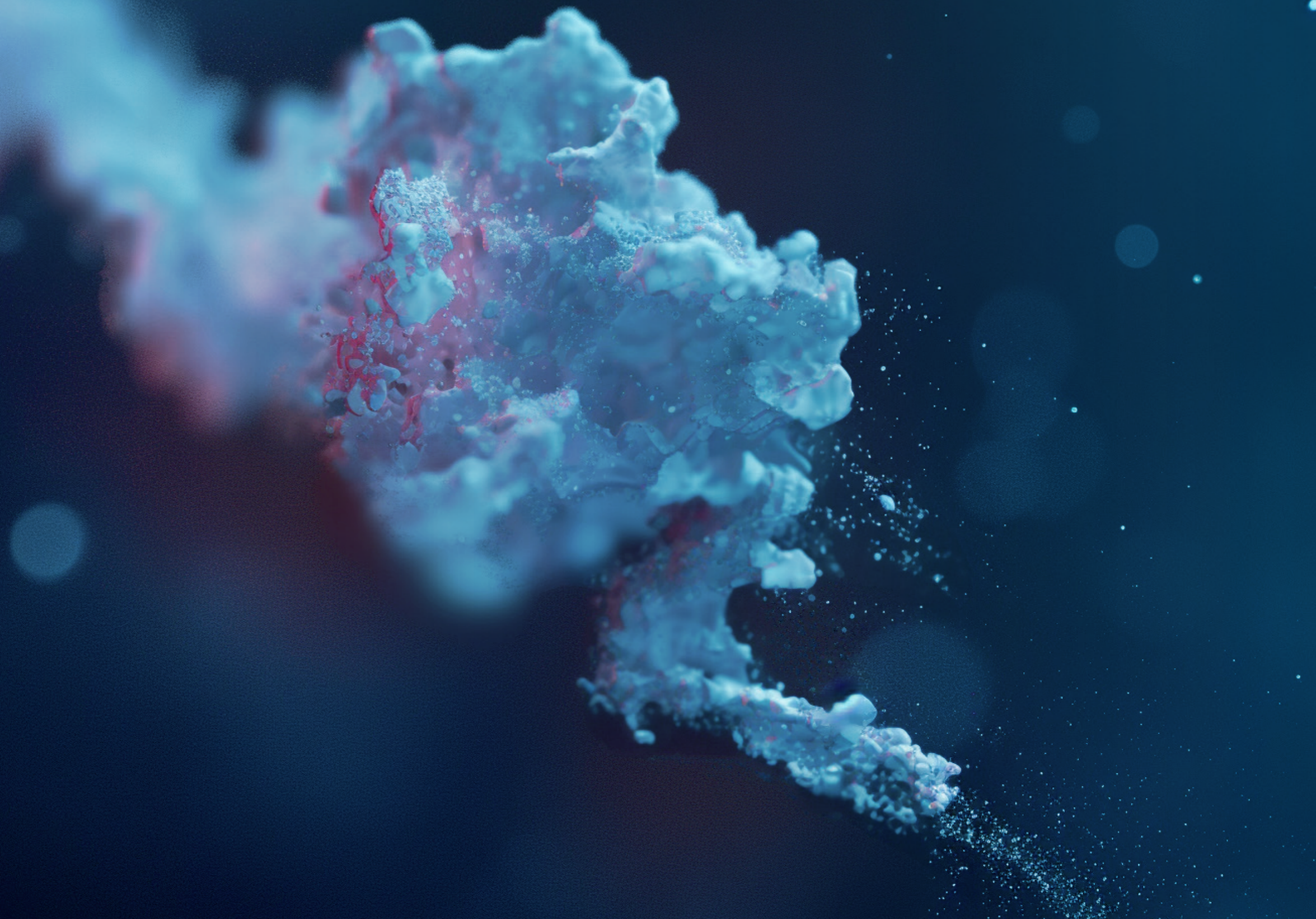
✉ francesca.peiro@ub.edu

Prof. Francesa Peiró

LENS-MIND, Department of Electronics and Biomedical Engineering and Institute of Nanoscience and Nanotechnology (IN²UB), University of Barcelona (UB).

Scanning and transmission electron microscopy (STEM) has been an indispensable tool for exploring matter with atomic-scale spatial resolution, benefiting both materials science and life sciences. With recent instrumental developments, methodological innovations, and the application of artificial intelligence tools, electron microscopy now enables us to interrogate matter in unprecedented ways. It allows not only for the precise determination of the position and nature of atoms but for the measurement of material properties (electrical, magnetic, optoelectronic, mechanical, and others) at unparalleled resolutions, even in three dimensions. The use of cold electron emission guns with different acceleration voltages and controlled doses, high-speed direct detection cameras, and X-ray detectors and energy filters enables multimodal signal acquisition. AI plays a fundamental role in efficiently exploiting this comprehensive set of data. STEM microscopy has evolved into a nanolaboratory for experimenting, observing, and measuring dynamic processes at the highest spatial and energy resolutions. As the scientific community says: a synchrotron has been brought to the heart of the TEM.

ART GRANTEES



ART CALL

ART1 (2022–ART grantee)

DEVELOPMENT OF CHEMORESISTIVE GAS SENSORS MADE FROM METAL-ORGANIC FRAMEWORKS (MOFs) FOR EARLY THERMAL RUNAWAY DETECTION IN LITHIUM-ION BATTERIES

✉ albert.romano@ub.edu

I. Fort-Grandas^{1,2,3}, S. Aljemazi², S. T. Navale^{1,2}, A. Estany-Macià^{1,2}, Y. Mendoza^{1,2,3}, P. Pellegrino^{1,2}, M. López^{1,2}, Christophe Serre^{1,2}, A. Grabulosa-Rodríguez^{1,3}, M. Moreno-Sereno^{1,2}, D. Sainz^{1,3}, A. Vidal-Ferran^{1,3,4}, G. Domènech-Gil^{1,2}, A. Romano-Rodríguez^{1,2}

¹ Institute of Nanoscience and Nanotechnology, Universitat de Barcelona, 08028 Barcelona, Spain

² Dept. of Electronic and Biomedical Engineering, Universitat de Barcelona, 08028 Barcelona, Spain

³ Dept. of Inorganic and Organic Chemistry, Universitat de Barcelona, 08028 Barcelona, Spain

⁴ Catalan Institution of Research and Advanced Studies (ICREA), 08010 Barcelona, Spain

Lithium-ion batteries (LIBs) are widely used nowadays in several fields such as electrical vehicles, laptops, mobile phones, ... One of their main drawbacks is the thermal runaway due to overcharging, internal/external short circuiting, and thermal failure, which present the risks of fire and explosion. The battery emits toxic and flammable gases during the initial stages of these runaway processes, mainly CO₂, C_xH_y, H₂, CO, and VOCs [1], whose detection could help in preventing the associated hazards.

Chemoresistive sensors are solid state devices whose resistance changes in the presence of certain gases. These devices present high sensitivity to several gases, cost-efficient, small size, easy operation and integration capabilities, but usually require high operating temperatures. Promising chemoresistive materials for room temperature (RT) operation could be metal-organic frameworks (MOFs) [2]. In this work, we present the results of synthesis, gas sensor fabrication and their response to CO₂, H₂, and CH₄.

Materials & Methods

2 ml of distilled water was added to a 10 ml glass vial containing 0.022 mM of a 2,3,6,7,10,11-hexahydroxytriphenylene (HOTP) and 0.039 mM of Cu(C₂H₃O₂)₂·H₂O, which was sonicated for 10 minutes. Subsequently, 0.15 ml of DMF was added dropwise into the mixture, and the resulting solution further sonicated for 10 minutes. The capped vial was next kept inside an oven at 80 °C for 6 hrs, followed by natural cooling to RT. Finally, a black powder product was collected by centrifugation, washed several times with distilled water and ethanol, and dried under nitrogen flow.

The obtained powders were structurally and chemically characterised to confirm the MOFs formation. For the fabrication of the sensor devices, the MOFs powder was dispersed in water and drop casted onto fused silica substrate containing interdigitated Cr/Au electrodes.

Results and Discussion

The structural characterisation results confirm the crystalline nature of the MOFs, presenting an hexagonal structures with an in-plane lattice parameter of about 2 nm, and with a crystallite size in the range of few to several hundreds of nanometres. The chemoresistive sensing behaviour of these devices is demonstrated by exposing, e.g., to a 5-minute pulse of 300 ppm of CO₂ diluted in dry air, showing a resistance increase of about 2%, while the baseline resistance is almost recovered after removal of the gas, suggesting poisoning of the sensors.

The complete gas sensing response of the devices will be presented and discussed during the presentation and a critical discussion of the feasibility of these devices for LiB will be carried out.

References

- [1] C. Essl, L. Seifert, M. Rabe, A. Fuchs, *Batteries* **7**, 25 (2021)
 [2] W.T. Koo, J.S. Jang, I.D. Kim. *Chem.* **5**, 1938-1963 (2019)
 [3] M.G. Campbell, D. Sheberla, S.F. Liu, et al., *Angew. Chem. Inter. Ed.* **54**, 4349–4352 (2015)

ART2 (2022–ART grantee)

HIERARCHICALLY NANOSTRUCTURED TRANSITION METAL CARBIDES AND MXENES ON CARBON FELT FOR CO₂ REDUCTION AND GREEN H₂ PRODUCTION (2IPs)

✉ stefanoschaitoglou@ub.edu ✉ xavier.vendrell@ub.edu

S. Chaitoglou¹, X. Vendrell², A. Ventura-Crespin², R. Ospina¹, Y. Ma¹, R. Amade¹, E. Bertran-Serra¹, L. Mestres², N. Homs², P. Ramírez de la Piscina²

¹ Department of Applied Physics, University of Barcelona, Spain

² Department of Inorganic & Organic Chemistry, University of Barcelona, Spain

The proposed multidisciplinary project focuses on the preparation of nanostructured transition metal carbides and MXenes decorated on a carbon felt-based support to study their viability as catalysts for CO₂ reduction by the reverse water gas shift reaction [1] and for the green H₂ production through the electrocatalytic hydrogen evolution reaction [2]. The selected materials exhibit features typically in the order of micro-to-nanometer, therefore, because of the small size, the ratio of surface area to volume is much higher than in conventional catalysts. In addition, carbon felt (CF), exhibiting microporosity and microstructure features, is used as support for TMCs and MXenes offering a cheap and ecological approach to green H₂ production and CO₂ reduction.

Materials & Methods

CF, transition metal chlorides and MAX phases in powder form were purchased. In a first approach, vertical graphene nanowalls were deposited on the CF by ICP-CVD. Then, the sample was impregnated in a solution containing MoCl₅ dispersed in isopropanol, followed by transfer in an oven for the carburization step via thermal annealing. Detailed description of the experimental procedures can be found in [3]. In a second approach different metals (Co, Cu and Ni) were immobilised into de CF by using the drop casting technique and a posterior heat treatment. All the catalysts were evaluated in the hydrogen evolution

reaction (HER) and in the reverse water gas shift reaction (RWGS) and characterized by X-ray diffraction, Scanning Electron Microscopy and X-ray Photoelectron Spectroscopy among other techniques commonly used in electrochemistry and

Results & Discussion

The role of the GNWs here is dual, since they act as both a support system with a very high specific surface area and a carbon precursor for the carburization of Mo during high temperature annealing. The crystal defects present on the graphene lattice facilitate the enhanced anchoring of MoCl₅ precursor molecules, as quantified by EDS measurements. Microscopy characterization reveals that Mo₂C particles are preferentially bound on the defective edges of the graphene nanostructure. The resulting compounds are tested as catalyst electrodes towards hydrogen evolution reaction. They require just 141 mV for the generation of 10 mA/cm², a value that exceeds the performance of most Mo₂C/graphene hybrids found in literature up today. The remarkable stability of the Mo₂C on GNWs hybrid under the experimental conditions adds further appeal to its potential application as an efficient and durable electrocatalyst. The negligible decrease in current density after prolonged operation indicates that the hybrid material maintains its catalytic activity over extended periods. On the other hand, we are presently investigating the impact of various MAX and transition metals supported on carbon felts on both the HER and RWGS reactions. Our latest findings indicate that the pairing of MAX phases or transition metals with carbonaceous fiber support significantly amplifies the catalytic performance in RWGS and HER reactions. These promising results motivate us to further explore the synergistic effects between the carbonaceous support and the catalyst.

References

- [1] Elsermagaw, O. Y. H. et al. *J. CO₂ Util.* **41** (2020) 101280 (2020)
 [2] Yu, F. et al. *Mater. Today Phys.* **7** (2018)121–138
 [3] Chaitoglou, S. et al. *Journal of Alloys and Compounds* **972** (2024) 172891

ART3

ELECTRONIC AND PHOTOELECTRONIC PROPERTIES OF MULTIFUNCTIONAL SEMICONDUCTING NANOSTRUCTURES (ELPHOS)

✉ aifigueroa@ub.edu

A. I. Figueroa^{1,2}, J. A. Ruiz-Torres^{1,2}, C. Moya^{1,2},
E. Carranza-Botey¹, R. Millán-Solsona^{2,3,4},
J. D. Forero^{2,3}, A. Fraile-Rodríguez^{1,2}, B. Garrido^{2,3},
S. Hernández^{2,3}, G. Gomila^{2,3,4}, A. Labarta^{1,2}, X. Batlle^{1,2}

¹ Departament de Física de la Matèria Condensada,
Martí i Franquès 1, 08028 Barcelona, Spain

² Institut de Nanociència i Nanotecnologia, Universitat
de Barcelona, 08028 Barcelona, Spain

³ Departament d'Enginyeria Electrònica i Biomèdica,
Universitat de Barcelona, 08028 Barcelona, Spain

⁴ Institut de Bioenginyeria de Catalunya (IBEC), The
Barcelona Institute of Science and Technology
(BIST), 08028 Barcelona, Spain

Semiconductor nanostructures have an enormous potential for applications in diverse areas of modern technologies due to their versatility and possibility of tuning their properties as desired. Bi₂S₃, in particular, has a small direct bandgap between 1-2 eV which allows the absorption of visible and infrared light, of relevance for applications in areas including biomedical therapies, energy storage, optoelectronics and thermoelectric technologies [1, 2]. In this work, we delve into the properties of Bi₂S₃ and hybrid Bi₂S₃-Au nanostructures through advanced electrical and optical methods, to explore and exploit their electronic and optoelectronic properties. Bi₂S₃ with different morphology, with and without Au inclusions, were prepared from protocols based on hot injection of Bi₂S₃ [1]. Optimization of the optoelectronic response in these nanostructures, as obtained by UV-Vis spectroscopy and photoluminescence, was achieved through modification of their shapes, sizes, and Au inclusion. Our results demonstrate that: i) the gap energy values of the nanostructures are larger than that of bulk Bi₂S₃; ii) their optical properties depend strictly on the width-to-length ratio; and iii) Au presence enhances light absorption in the infrared range. Moreover, advanced characterization through local electrostatic force microscopy strongly indicates electronic transfer between Au and Bi₂S₃ in the hybrid Bi₂S₃-Au systems, in agreement with the optical absorption enhancement observed in the nanostructures. These remarkable results will not only promote the current research and advances towards biomedical applications of these systems, but they will also open novel scenarios for their incorporation into electronic devices with other multiple functionalities.

References

- [1] Escoda-Torroella, M. et al. *Phys. Chem. Chem. Phys.*, **25**, 3900-3911 (2023).
[2] Ajiboye T.O. & Onwudiwe D. C.. *Results Chem.* **3**,100151 (2021).

ART4

MAGNONIC WRINKLES

✉ bcasals@ub.edu

B. Casals^{1,2}, R. Galceran^{1,2}, F. Macià^{2,3},
J. Bertomeu^{1,2}, J. M. Hernández^{2,3}

¹ Dept. of Applied Physics, University of Barcelona,
08028 Barcelona, Spain

² Institute of Nanoscience and Nanotechnology
(IN²UB), University of Barcelona, 08028 Barcelona,
Spain.

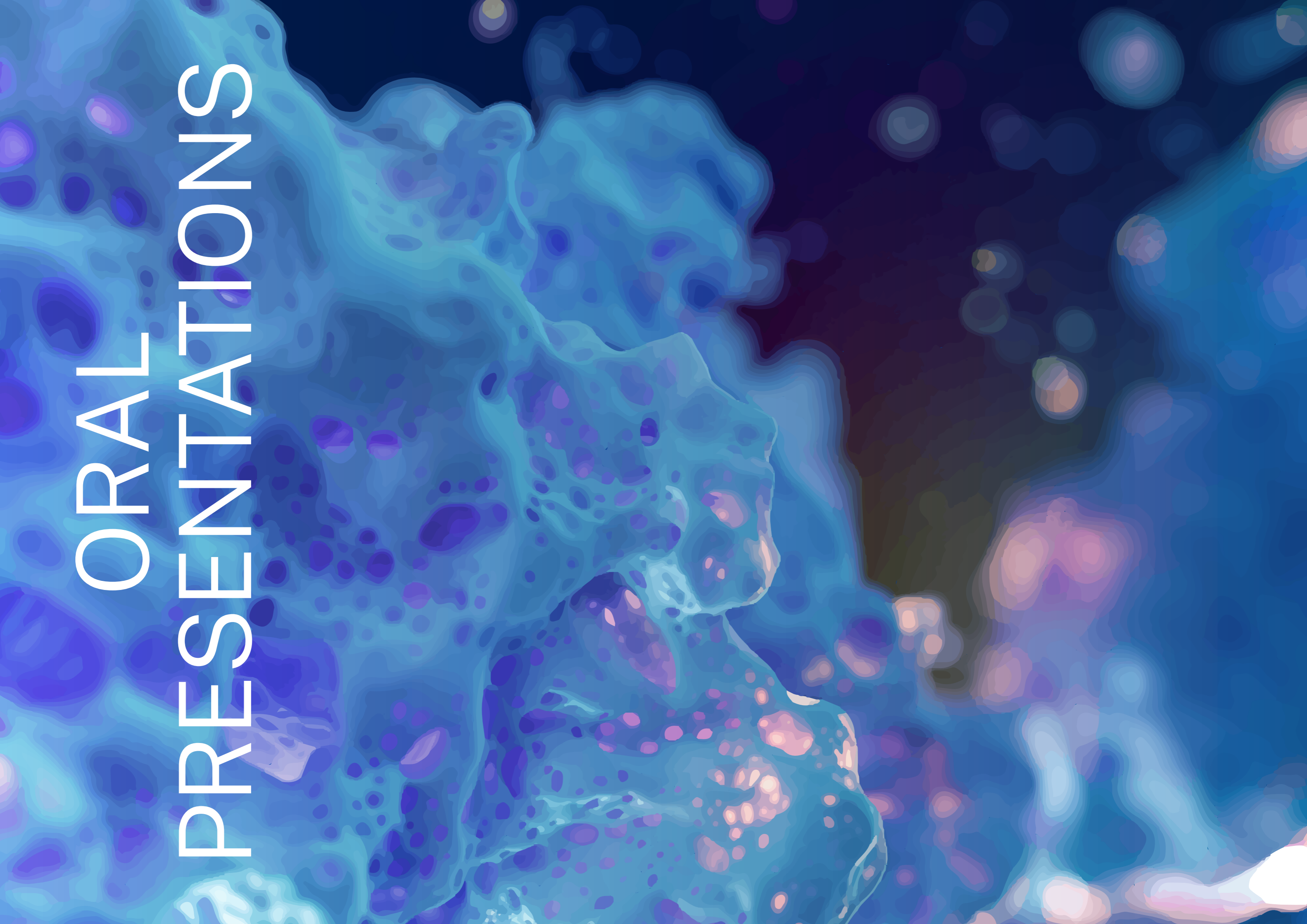
³ Dept. of Condensed Matter Physics, University of
Barcelona, 08028 Barcelona, Spain

The “Magnonic wrinkles” ART granted project aims to understand and control magnetization dynamics and magnonic dispersion created by film wrinkles in ferromagnetic films deposited on flexible substrates. Magnonic crystals are magnetic metamaterials that control and manipulate spin waves (magnons), in a similar way that photonic crystals control light waves. Magnons are collective excitations of electron spins and are a powerful tool for information transport and processing [1] because of its low energy consumption and its easy integrability to CMOS technology. Magnon propagation can be controlled by engineering artificial periodic structures at the micro-nanoscale in magnetic materials. The fabrication of the periodic structures requires a combination of expensive lithographic and nanofabrication techniques. However, when flexible substrates are used, wrinkles appear as a periodic corrugation on films and serve to accommodate a compressive strain. The spatial periodicity of the wrinkles ranges from tens of nanometers to micrometers, which matches well with wavelengths of spin waves in ferromagnetic materials. The project explores and exploits the coupling between periodic spatial deformation (wrinkles) and magnetic waves in different magnetic materials, with the final goal of understanding and controlling the magnonic dispersion created by the wrinkles. Our proposed work consists, on the one hand, in growing magnetic thin films (Cobalt, Iron or Nickel) on flexible substrates that generate a tunable wrinkle orientation and periodicity, and, on the other hand, determining the magnetic properties induced by the wrinkled films, focusing on the coupling with dynamical magnetization modes.

References

- [1] Pirro, P. et al. Advances in coherent magnonics. *Nature Reviews Materials* 6 (2021).

ORAL PRESENTATIONS



01

ANTI-FERROELECTRIC DARK MODES IN AN INVERTED PLASMONIC LATTICE

✉ javier.rodriiguez@ub.edu

Rodríguez-Álvarez, J.^{1,2}, Labarta, A.^{1,2}, Idrobo, J. C.³, Dell'Anna, R.⁴, Cian, A.⁴, Giubertoni, D.⁴, Borrisé, X.⁵, Guerrero, A.⁵, Pérez-Murano, F.⁵, Fraile Rodríguez, A.^{1,2}, Batlle, X.^{1,2}

¹ Departament de Física de la Matèria Condensada, Universitat de Barcelona, 08028 Barcelona, Spain

² Institut de Nanociència i Nanotecnologia (IN²UB), Barcelona, 08028, Spain

³ Materials Science and Engineering Department, University of Washington, Seattle, WA, 98195, USA

⁴ Sensors & Devices Center, FBK - Bruno Kessler Foundation, via Sommarive, 18, Povo, TN 38123 Italy

⁵ Institut de Microelectrónica de Barcelona (IMB-CNM, CSIC), Bellaterra, 08193, Spain

We present a detailed study of dark and bright modes in the visible and near-infrared energy regime of an inverted plasmonic honeycomb lattice by a combination of state-of-the-art Au⁺ focused ion beam lithography, optical and electron spectroscopy, and finite-difference time-domain simulations. The lattice consists of slits carved in an Au thin film, exhibiting a plethora of resonances in the visible and near-infra-

red ranges (see Figure 1). A detailed description of the charge distribution and near-field enhancement has been given by virtue of the good agreement between the electron energy loss spectroscopy (EELS) measurements, the optical measurements, and simulations. The most remarkable result is the finding of dark modes that may be caused by antiferroelectric arrangements of the slit polarizations, giving rise to charge arrangements with a unit cell two times larger than that of the original honeycomb lattice (Figure 1b and 1e). Additionally, bright plasmonic modes exhibiting hotspots far from the metal slits are also found. The studied plasmonic resonances take place within 0.5 and 2 eV energy range, indicating that they could be suitable for a synergistic coupling with excitons in 2D transition metal dichalcogenides materials or for designing nanoscale sensing platforms based on near-field enhancement over a metallic surface. For example, the exciton energies for 2D WSe₂ and MoS₂ on an Au substrate, 1.75 and 1.9 eV, respectively [1], could be targeted by easily tuning manufacturing parameters such as the pitch of the lattice, thus changing the spectral position of the plasmonic resonances.

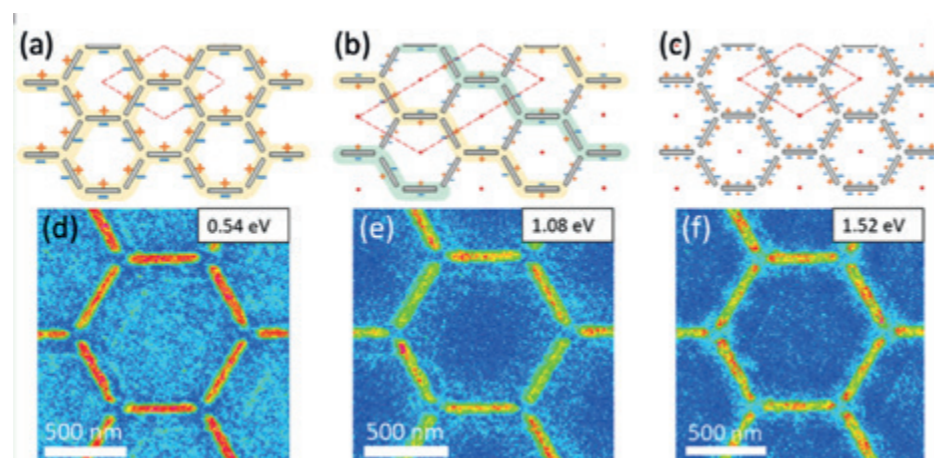


Figure 1. (a), (b) and (c) panels show schematic representations of the charge distributions associated with a bright mode and extended and local dark modes in the structure, respectively. Panels (d), (e) and (f) present the EELS mapping measured for each of the modes.

References

[1] Rodríguez-Álvarez, et al., ACS Nano, 2023, 17(9), 8123-8132.

02

SMART GEL-DISPERSED CALCIUM HYDROXIDE-LOADED NANOPARTICLES FOR ENDODONTICS

✉ xavier.roig.soriano@ub.edu

X. Roig¹, L. Halbaut¹, M. Espina^{1,2}, J. A. González Sánchez³, F. Duran-Sindreu³, M. L. García^{1,2}, E. Sánchez-López^{1,2}

¹ Department of Pharmacy, Pharmaceutical Technology and Physical Chemistry, Faculty of Pharmacy and Food Sciences, University of Barcelona, Barcelona, Spain

² Institute of Nanoscience and Nanotechnology (IN²UB), University of Barcelona, Barcelona, Spain

³ Department of Endodontics, Faculty of Dentistry, Universitat Internacional de Catalunya, Barcelona, Spain

Aim

Endodontics is the field of dentistry that treats the disorders of the dental pulp and its consequences and endodontic infections are one of the most relevant pathologies in dentistry. However, more than 15 % of the infections are not properly treated [1]. This may be due to the fact that Ca(OH)₂, the gold-standard medication does not properly arrive to the target site. For this reason, the aim of this work is to encapsulate Ca(OH)₂ in polylactic-co-glycolic acid (PLGA) nanoparticles (NPs) and disperse them in smart-gels (Ca(OH)₂-NPs-gel) able to be applied in liquid form and increase their mucoadhesion in contact with the tissues [2], [3]. Moreover, in vitro and ex vivo assessments were also carried out to confirm their safety and evaluate penetration capacity into dentinal tubules in comparison to free Ca(OH)₂.

Methodology

Ca(OH)₂-NPs properties were studied by measuring average size, polydispersity index, zeta potential and entrapment efficiency of three different batches and tolerance was assessed by means of the HET-CAM test [2]. In vitro Ca(OH)₂ release was studied by direct dialysis in an aqueous media monitoring the amount of Ca(OH)₂ released. Moreover, permeation across dentinal tubules was developed by applying Ca(OH)₂-NPs-gel labelled with Rhodamine to extracted human teeth and observed by confocal microscopy.

Results

Ca(OH)₂-NPs-gel demonstrated to be reproducible with an average size below 200 nm, a homogeneous NPs population, negative surface charge and high entrapment efficiency. Ca(OH)₂-NPs-gel showed a prolonged Ca(OH)₂ release which fitted the Korsmeyer-Peppas equation. In addition, HET-CAM test confirmed that Ca(OH)₂-NPs-gel were non-irritant [2]. Finally, penetration depth inside the dentinal tubules was significantly enhanced, especially in the middle-apical sections where free Ca(OH)₂ was unable to arrive. This is especially relevant since bacteria causing endodontic infections tend to accumulate and form biofilms in this apical areas [2].

Conclusion

Calcium hydroxide-loaded PLGA NPs dispersed in a smart gel have been characterized, were non-irritant and show enhanced penetration inside dentinal tubules. Therefore, they may constitute a suitable alternative as an intracanal antibacterial drug.

References

- [1] Tibúrcio-Machado, C.S.; Michelon, C.; Zanatta, F.B.; Gomes, M.S.; Marin, J.A.; Bier, C.A. The global prevalence of apical periodontitis: a systematic review and meta-analysis. *Int. Endod. J.* **2021**, *54*, 712–735, doi:10.1111/iej.13467.
- [2] Roig, X.; Halbaut, L.; Elmsmari, F.; Pareja, R.; Arrien, A.; Duran-Sindreu, F.; Delgado, L.M.; Espina, M.; García, M.L.; Sánchez, J.A.G.; et al. Calcium hydroxide-loaded nanoparticles dispersed in thermosensitive gel as a novel intracanal medicament. *Int. Endod. J.* **2024**, 1–15.
- [3] Elmsmari, F.; González Sánchez, J.A.; Duran-Sindreu, F.; Belkadi, R.; Espina, M.; García, M.L.; Sánchez-López, E. Calcium hydroxide-loaded PLGA biodegradable nanoparticles as an intracanal medicament. *Int. Endod. J.* **2021**, *54*, 2086–2098, doi:10.1111/iej.13603.

03

MACHINE LEARNING STRATEGIES FOR LOW-LOSS ELECTRON ENERGY LOSS SPECTROSCOPY

V. Costa Ledesma¹, D. del Pozo Bueno¹, C. Coll Benejam², J. Nogués², B. Sepulveda³, L. Bocher⁴, M. Kociak⁴, J. Blanco-Portals¹, S. Estradé Albiol¹, F. Peiró

¹ LENS-MIND, Department of Electronics and Biomedical Engineering and Institute of Nanoscience and Nanotechnology (IN²UB), University of Barcelona (UB), Barcelona, Spain

² Catalan Institution for Research and Advanced studies, ICREA Academia, Bellaterra, Spain

³ Instituto de Microelectrónica de Barcelona (IMB-CNM, CSIC)Campus UAB, Bellaterra, Spain

⁴ Laboratoire de Physique des Solides (LSP), Microscopie électronique STEM, Orsay, France

Localised Surface Plasmon Resonance (LSPR) is a non-propagating electron-density wave that is confined at the surface of a metallic nanoparticle. They can enhance the electromagnetic radiation, concentrating it into sub-wavelength volumes. Its resonance can be tuned by changing the surrounding medium and its geometry. This unique property opens a wide range of applications across various fields of applied research.

Electron Energy Loss Spectroscopy (EELS) within a Scanning Transmission Electron Microscope (STEM) has revealed remarkable capabilities in the analysis of plasmons at nanometric scale, as this technique achieves sub-angstrom spatial resolution and can excite the complete range of LSPR modes supported by the nanostructure. By employing EELS, the plasmonic properties can be correlated with geometric or structural characteristics, enabling a more comprehensive understanding of the plasmonic response.

In this study, based on the analysis of Silicon/Gold nanopillars samples, we demonstrate that clustering techniques can be used for detecting LSPRs in EELS. We propose a novel combination of unsupervised machine learning strategies that detect LSPRs in EELS spectrum images. To demonstrate the effectivity of this methodology, we studied Si/Au nanopillars. The detection of LSPRs is done by reducing the dimensionality of the data, clustering this low-dimensional space, and recuperate the spatial space. We demonstrate that using this methodology, it is possible to recover the LSPRs, among distinct spectra in a large EELS dataset, and easily make a plasmonic spatial map without the need for prior knowledge or labelling of the data.

References

- [1] Ammari H and et al 2016 Mathematical analysis of plasmonic resonances for nanoparticles: the full maxwell equations *Journal of Differential Equations* 261,(6) 3615-3669
- [2] Yu H and et al 2019 Plasmon-enhanced light-matter interactions and applications *npj Computational Materials* 5,(45) 2057-3960
- [3] Koh A L, Fernandez-Domínguez A I, McComb D W, Maier S A and Yang J K W 2011 High-Resolution Mapping of Electron-Beam-Excited Plasmon Modes in Lithographically Defined Gold Nanostructures *Nano Letters* 11,(3) 1323-1330
- [4] Ryu J and et al 2021 Dimensionality reduction and unsupervised clustering for EELS-SI *Ultramicroscopy* 231 113314

04

SCANLESS AND CAMERA-FREE FD-FLIM WITH FREQUENCY ENCODED LIGHT

✉ laura.rodriguez.sune@ub.edu

L. Rodríguez-Suné¹, P. Ricci¹, A. Marchese¹, P. Saggau², M. Duocastella¹

¹ Department of Applied Physics, Universitat de Barcelona, C/Martí I Franquès 1, 08028 Barcelona, Spain

² Department of Neuroscience, Baylor College of Medicine, One Baylor Plaza S640, 77030 Houston, TX, USA

Fluorescence lifetime imaging microscopy (FLIM) allows the extraction of quantitative information from biological specimens. Based on measuring fluorescence lifetimes, it allows detecting changes in the molecular environments where fluorophores are located. As a result, information about cell function and behavior can be retrieved that could not be elucidated with traditional intensity measurements. FLIM can be performed in the time domain (TD), where lifetimes are measured directly by observing the fluorescence decay over time after providing an excitation light pulse¹. In this case, a laser beam is scanned across the sample point by point, and the information is collected with a single-pixel detector. Such a scanning process can be time-consuming, impeding the characterization of rapidly evolving systems. In frequency-domain (FD), the lifetime is determined by measuring a phase shift between the modulated excitation light source (10 - 100 MHz) and the detected fluorescence signal. Interestingly, FD-FLIM can be implemented using parallelized detection – a camera or detector array – thus helping to reduce the overall acquisition time of life-

time images. Still, traditional cameras feature a low frame rate (

100 fps) compared to the rapid modulation of light, thus requiring specialized instrumentation such as gain-modulated cameras.

Here, we present a scan-less and camera-free technology that allows sub-micrometric imaging at thousands of frames per second and is suitable for rapid FD-FLIM. Our design is based on combining a single photodetector with parallelized encoded illumination². We use two AODs placed in a Mach-Zehnder interferometer and drive them simultaneously with multiple and unique acoustic frequencies. As a result, orthogonal light stripes are obtained that interfere with the sample plane, forming a two-dimensional array of flickering spots at frequencies of the order of tens of MHz. The light from the sample is collected with a single photodiode that, after spectrum analysis, allows for image reconstruction at speeds only limited by the AOD's bandwidth and laser power. Notably, by adding a second photodiode before the sample, we can extract the phase shift between excitation and fluorescent light for each of the flickering spots. Thus, we obtain a phase shift map from which we can calculate a fluorescence lifetime image, as it is schematically shown in Fig. 1. The impressive FD-FLIM speed of FREMIC, coupled with the flexibility in the selection of the number of pixels, can pave the way to understanding the dynamics of living processes at high spatio-temporal resolution.

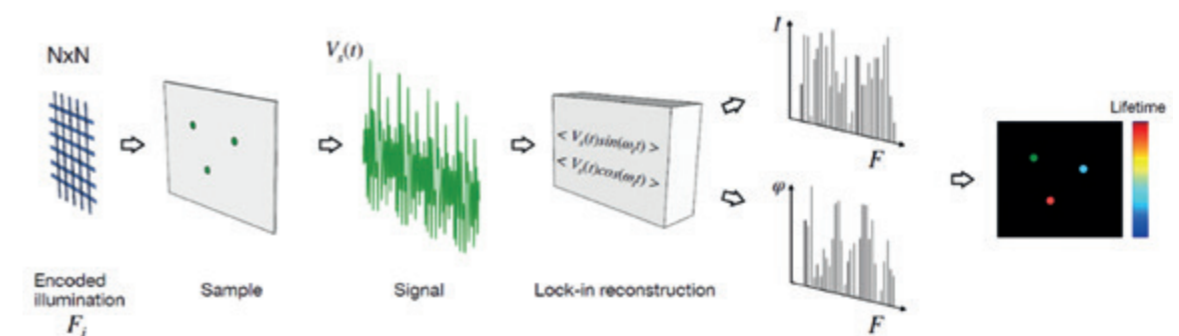


Figure 1. Schematic representation showing the operation principle of the scan-less and camera-free FD-FLIM with frequency encoded light.

References

- [1] R. Datta, et al., *Journal of biomedical optics* 25.7 (2020): 071203-071203.
- [2] A. Marchese, et al., *Nanophotonics* 13.1 (2024): 63-73.

05

MATHEMATICAL MODEL OF FLUID FRONT DYNAMICS DRIVEN BY POROUS MEDIA PUMPS

✉ abenavent@ub.edu

A. Benavent-Claró^{1,2}, Y. Alvarez-Braña^{3,4},
F. Benito-Lopez⁴, L. Basabe-Desmonts^{3,5},
A. Hernandez-Machado^{1,2}

¹ Condensed Matter Physics Department, Physics Faculty, University of Barcelona, Spain

² Institute of Nanoscience and Nanotechnology (IN²UB), University of Barcelona, Spain

³ Microfluidics Cluster UPV/EHU, BIOMiCs Microfluidics Group, University of the Basque Country UPV/EHU, Vitoria-Gasteiz, Spain

⁴ Microfluidics Cluster UPV/EHU, Analytical Microsystems & Materials for Lab-on-a-Chip (AMMa-LOAC) Group, University of the Basque Country UPV/EHU, Vitoria-Gasteiz, Spain

⁵ Basque Foundation of Science, IKERBASQUE, Spain

Air-permeable porous media hosts air in their pores. When air is removed from the interior of the material, the porous media tends to recover it, acting as a suction pump. The technique used to convert a porous media into a pump, consists of degassing the material to remove the air inside. The suction function when recovering the air, can be used to move a liquid through a microfluidic channel, studying the dynamics of the liquid-air front. We have developed a theoretical mathematical model that precisely characterizes the behavior of this kind of pumps and the dynamics of the liquid-air front. Using PDMS as a pore material we have developed and tested the mathematical method, creating a PDMS micropump able to provide self-powered flow control for long periods of time. This type of pump has the interest to have small size and to operate without any external power source.

References

- [1] A. Benavent-Claró, Y. Alvarez-Braña, F. Benito-Lopez, L. Basabe-Desmonts, and A. Hernandez-Machado. "Mathematical model of fluid front dynamics driven by porous media pumps". (Preprint)
- [2] Y. Alvarez-Braña, A. Benavent-Claró, F. Benito-Lopez, A. Hernandez-Machado, and L. Basabe-Desmonts, "Microfluidic front dynamic experiments for the characterization of pumps for long-term autonomous microsystems". (Preprint)
- [3] S. O. Woo, M. Oh, K. Nietfeld, B. Boehler, and Y. Choi, "Molecular diffusion analysis of dynamic blood flow and plasma separation driven by self-powered microfluidic devices," *Biomicrofluidics* 15, 034106 (2021).
- [4] J. Etxebarria-Elezgarai, Y. Alvarez-Braña, R. Garoz-Sanchez, F. Benito-Lopez, and L. Basabe-Desmonts, "Large-volume self-powered disposable microfluidics by the integration of modular polymer micropumps with plastic microfluidic cartridges," *Industrial & Engineering Chemistry Research* 59, 22485–22491 (2020).

06

MOTION AND CONTROL OF VIRTUAL COLLOIDAL PARTICLES IN CONFINED CHIRAL LIQUID CRYSTALS

✉ joel.torres@ub.edu

J. Torres-Andrés^{1,2}, J. Ingés-Mullol^{1,2}, F. Sagués^{1,2}

¹ University of Barcelona, Barcelona, Spain.

² Institute of Nanoscience and Nanotechnology of the University of Barcelona, Barcelona, Spain.

Cholesteric phases are liquid crystals in which a helical twist can be induced by the presence of a chiral agent. This twist, with a periodicity or pitch (p), can be frustrated under geometrical confinement (d) comparable to p . Under those conditions, skyrmions can be formed if the material undergoes an instability. Skyrmions are topologically protected solitonic-like structures [1-3], formed by the spatial discordance in the orientation of the molecules of the liquid crystal, forming a torus in which the principal axis of the molecules turns 180° . Skyrmions behave as quasi-particles and can be driven by the action of a modulated AC

electric field[1-3]. However, the directionality of their motion has, so far, only been in-situ controlled using complex optical systems[3]. In our work, we study the propulsion of skyrmions under modulated AC electric fields of different amplitude, carrier, and modulation frequencies. Moreover, we also study the collective behaviour of skyrmions, showing different self-assembly regimes in high areal density configurations. We also demonstrate the capability of an external fixed magnetic field to steer driven skyrmions (figure 1 (a)), which can be inserted and controlled within microfluidic channels. Experimental suggest an acceleration when skyrmions are introduced in micro-channels due to distortions in the LC molecular alignment generated by the presence of homeotropic walls (figure 1 (b)). We also show that skyrmions can act as micro-cargo transporters, with a slight modification of their velocity of displacement when loaded.

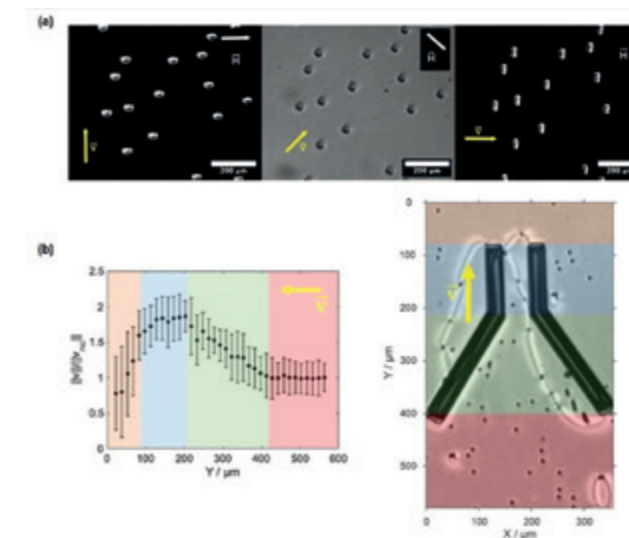


Figure 1. (a) Motion control of skyrmions ($p=23.5 \pm 1.2\mu$ and $d/p= 0.79 \pm 0.06$) under the application of a 0.4 T magnetic fields. Skyrmions are generated with a non-modulated AC field with a $f_c= 30$ Hz and a $V_p= 10$ V. The movement is triggered by the application of an AC electric field ($V_p= 12$ V, $f_c=1$ kHz, $f_m= 20$ Hz). The yellow arrow indicated the direction of motion of the skyrmions. (b) Skyrmions' ($p=7.7 \pm 0.4\mu$ and $d/p = 1.14 \pm 0.11$) acceleration due to the presence of homeotropic walls that provoke a distortion in the alignment of the LC molecules. Skyrmions are propelled by the action of a modulated AC electric field ($V_p=29$ V, $f_c=6$ kHz, $f_m= 20$ Hz) and directed by the application of a fixed external magnetic field (0.4 T). Yellow arrows indicate the direction of motion of the skyrmions.

References

- [1] Shon, et. al., *Nat. Commun*, **2019**, 10:14744, 1-11.
- [2] Ackerman, et. al., *Nat. Commun*, **2017**, 6:673, 1-13.
- [3] Shon, et. al., *Opt. Express*, **2020**, 28:5, 6306-6319.

07

MAGNETIC NANOCOMPOSITES FOR RADAR SHIELDING APPLICATIONS

✉ jaumecalvo@ub.edu

J. Calvo-de la Rosa^{1,2}, A. García-Santiago^{1,2}, J. M. Hernández^{1,2}, M. Vazquez-Aige¹, J. M. Lopez-Villegas^{2,3}, J. Tejada^{1,2}

¹ Departament de Física de la Matèria Condensada, Facultat de Física, Universitat de Barcelona, c. Martí i Franquès 1, 08028 Barcelona, Spain

² Institut de Nanociència i Nanotecnologia (IN²UB), Universitat de Barcelona, 08028 Barcelona, Spain

³ Departament d'Enginyeria Electrònica i Biomèdica, Facultat de Física, Universitat de Barcelona, c. Martí i Franquès 1, 08028 Barcelona, Spain.

There is an increasing interest paid on the development of novel materials for stealth applications, due to their direct impact in fields such as communications, aviation, or military, for instance. In this scenario, nanomaterials emerge as a powerful approach to design materials with new properties, which improve current systems. In this presentation, we report our recent advances on the development of multilayered radar absorbing system based on the use of magnetic nanocomposites.

Materials & Methods

We synthesize, by a common co-precipitation approach, pure and modified barium hexaferrites (Ba-Fe12O19). In modified hexaferrites, we incorporate additional divalent cations, leading to the formation of a magnetic nanocomposite. These powder materials are later mixed with paint and deposited into layers.

The electromagnetic properties (complex permeability and permittivity) of the powder ferrites are measured by using a coaxial system connected to a VNA. The electromagnetic response of the single- or multi-layered systems are also measured by using a two-antenna system. Finally, the layered samples are tested under real far field radar conditions inside an anechoic chamber.

Results and Discussion

The structural and magnetic characterization shows that the modified hexaferrite can be understood as a system of nanometric independent grains with randomly oriented anisotropy axes. These materials behave as random magnets [1], which were recently predicted to be an excellent candidate for radar absorption [2]. Our experimental results support these theories. When these powdered materials are incorporated into layered samples, it results in systems with enhanced microwave absorption [3].

Acknowledgements

The authors would like to thank the Air Force Office of Scientific Research (AFOSR) for their financial support through grant No. FA8655-22-1-7049. The authors also acknowledge Prof. Pilar Marin for her collaboration.

References

- [1] J. Calvo-De La Rosa et al., doi: <https://doi.org/10.48550/arXiv.2402.14324>.
 [2] D. A. Garanin and E. M. Chudnovsky, doi: <https://doi.org/10.1103/PhysRevB.103.214414>.
 [3] J. Calvo-de la Rosa et al., doi: <https://doi.org/10.1002/adfm.202308819>.

08

USAGE OF POLYPURINE REVERSE HOOGSTEN HAIRPINS FOR THERAPEUTIC INTERVENTION AGAINST SARS-CoV-2

✉ vnoe@ub.edu

C. J. Ciudad¹, S. Valiuska¹, J. M. Rojas², P. Nogales-Altozano², A. Aviñó³, R. Eritja³, M. Chillón⁴, N. Sevilla², V. Noé¹

¹ Department of Biochemistry & Physiology, School Pharmacy and Food Sciences & IN²UB, Universitat de Barcelona

² Centro de Investigación en Sanidad Animal-CISA, INIA, CSIC, Madrid

³ Institute for Advanced Chemistry of Catalonia (IQAC), CSIC, Barcelona

⁴ Institute of Neurosciences, Universitat Autònoma de Barcelona, UAB

The severe Acute Respiratory Syndrome Coronavirus 2 (SARS-CoV-2) is a member of the coronavirus family, responsible for the COVID-19 pandemic. Its RNA encodes various proteins, including spike (S), membrane (M), envelope (E), nucleocapsid (N), and non-structural proteins such as polyproteins pp1a and pp1ab. In this study, we employed Polypurine Reverse Hoogsteen (PPRH) hairpins to target specific regions of SARS-CoV-2 for therapeutic and protective purposes. PPRHs are unmodified single-stranded DNA molecules composed of two polypurine strands linked by Hoogsteen bonds and a four-thymidine loop, designed to bind to DNA or RNA sequences rich in polypyrimidines, forming a triplex structure via Watson-Crick bonds. We investigated the effects of two PPRHs, CC1 and CC3, targeting replicase and spike polypyrimidine sequences, respectively. Both PPRHs exhibited strong and highly specific interactions with their targets, with nanomolar K_d values. Optimal internalization of PPRH in VERO-E6 cells (95%) was achieved upon transfection of 300 nM PPRH with 30 μM DOTAP, resulting in sig-

nificant reductions in SARS-CoV-2 expression. In vivo experiments involved intranasal delivery of CC1, CC3, and a scramble PPRH to K18-hACE2 transgenic mice prior to SARS-CoV-2 infection with the MAD6 strain. Mice treated with CC1 showed survival without significant weight loss or clinical signs, while those treated with the scramble PPRH exhibited severe symptoms. These findings highlight the potential of PPRHs as a promising approach to enhance the use of oligonucleotides for viral disease treatment.

Work supported by Ministerio de Ciencia e Innovación, PID2021-122271OB-I00, and La Marató de TV3 Foundation, 202110-30-31.

09

CARBIDES, MAX AND MXENES AS CO-CATALYSTS IN NANOCOMPOSITES FOR THE H₂ PHOTOPRODUCTION FROM BIOETANOL

✉ adria.sanchez@qi.ub.edu

A. Sánchez^{1,2}, M. Gil¹, J. Serafin¹, P. Ramírez de la Piscina¹, N. Homs^{1,2}

¹ Departament de Química Inorgànica i Orgànica, secció de Química Inorgànica & Institut de Nanociència i Nanotecnologia (IN²UB), Universitat de Barcelona, Martí i Franquès 1, 08028 Barcelona, Spain

² Catalonia Institute for Energy Research (IREC), Jardins de les Dones de Negre 1, 08930 Barcelona, Spain

The advances in the photo-production of H₂ is of actual interest to acquire new routes and methods for the renewable H₂ production. In this context, the search of new improved photocatalysts is of great importance. The addition of co-catalysts onto appropriate semiconductors contributes to the suppression of the recombination between photo-generated charges, h⁺ and e⁻, thus enhancing their photo-activity. Different transition metal carbides (TMCs) have been investigated as co-catalysts because they display catalytic properties similar to Pt-group elements, being cheaper [1-4]. Nowadays, besides 3D TMCs, the so-called MAX and MXene compounds, attract much attention because their specific properties related with their structure [5,6]. MAX phases are ternary layered carbides (or nitrides) of general formula M_{n+1}AX_n. MXenes are a new class of 2D carbides (or nitrides), M_{n+1}X_n, which can be obtained from the corresponding MAX

phase by etching the A element using different strategies and methods [7]. The electronic properties of these materials make them good candidates to be explored as co-catalysts for appropriate semiconductors.

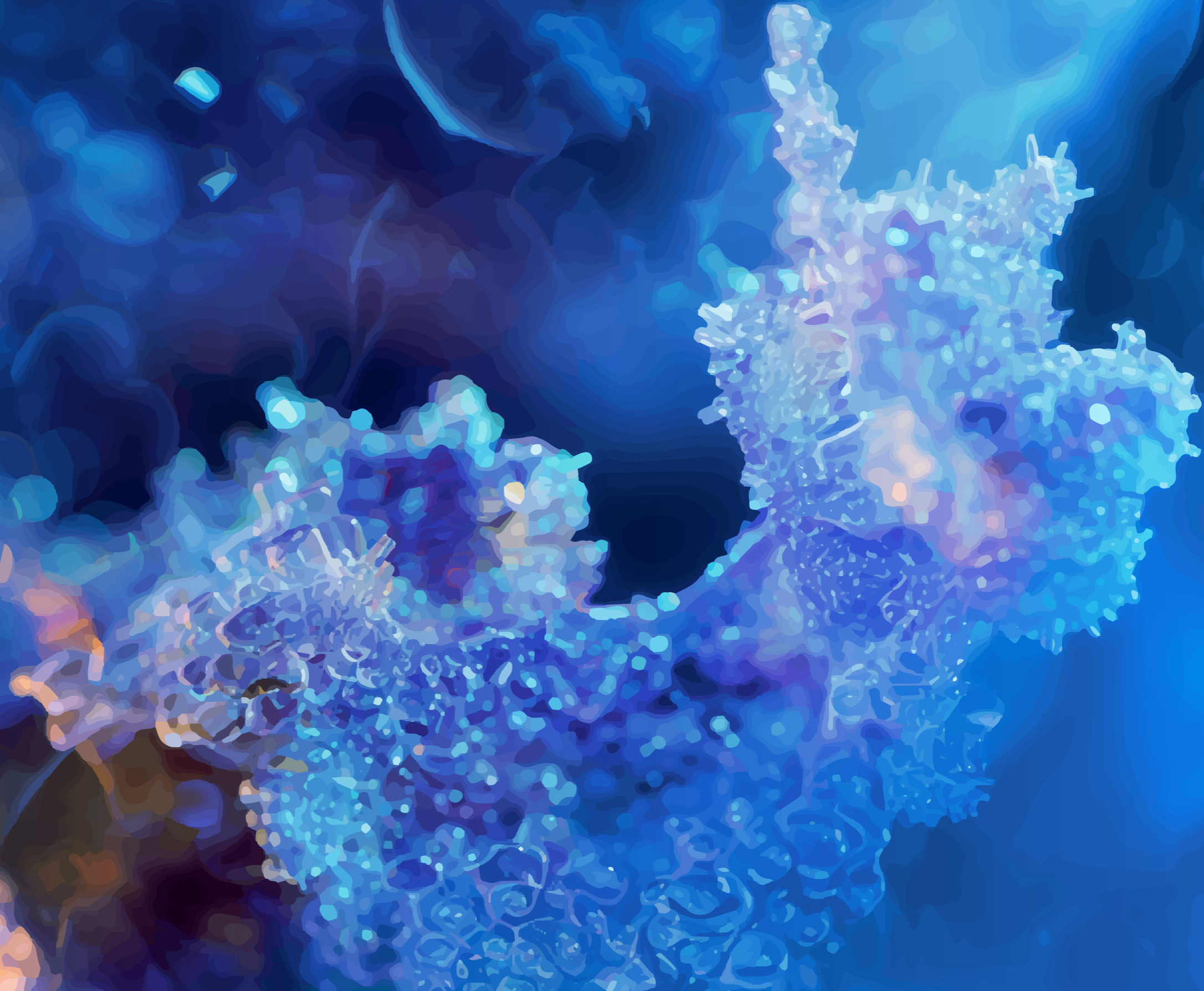
In our group, we are developing new nanocomposites based on semiconductors, such as TiO₂ and C₃N₄, and carbides; their photocatalytic properties in the H₂ production from ethanol solutions are determined and related with their characteristics [1-3]. The co-catalysts, which are 3D-carbides, MAX and MXene phases of groups 4, 5 and 6, are ultrasonically incorporated. The textural, morphological and structural characteristics of all the prepared materials, as well as their photo-electrochemical properties, are determined using different techniques such as N₂ physisorption measurements, scanning electron microscopy with energy dispersive X-ray analysis, X-ray diffraction, temperature-programed reduction, Raman spectroscopy, photoluminescence and electrochemical impedance spectroscopy, and photocurrent measurements.

We will present the preparation, characterization and the photocatalytic behavior of different nanocomposites in the production of H₂ under UV-visible irradiation, using aqueous solutions of ethanol (25% v/v) and continuous flow. The performance of the photocatalysts is related with their characteristics and photo-electrochemical properties in terms of recombination rate of the photo-generated charges, resistance to the electron transport and ability to transfer electrons for the H⁺ reduction

References

- [1] Y. Wang, A. Pajares, J. Serafin, X. Alcobé, F. Güell, N. Homs, P. Ramírez de la Piscina, ACS Sustainable Chem&Eng, 12, 11 (2024) 4365–4374
- [2] Y. Wang, L. Mino, F. Pellegrino, N. Homs, P. Ramírez de la Piscina, Appl. Catal. B Environ., 318 (2022) 121783
- [3] A. Pajares, Y. Wang, M.J. Kronenberg, P. Ramírez de la Piscina, N. Homs, Int. J. Hydrogen Energy, 45 (2020) 20558-20567
- [4] L. Tian, S. Min, F. Wang, Z. Zhang, Int. J. Hydrogen Energy, 45 (2020) 1878-1889.
- [5] K. P. Akshay Kumar, O. Alduhaish, M. Pumera, Electrochem. Commun., 125 (2021) 106977.
- [6] Y. R. Kumar, K. Deshmukh, M. M. Naseer-Ali, J. R. Rajabathar, J. Theerthagiri, M. Pandey, S.K. K. Pasha in: MXenes and their Composites, Synthesis, Properties and Potential Applications, K. K. Sadasivuni, K. Deshmukh, S. K. K. Pasha, T. Kovarik (Eds.), Elsevier, 2022, pp. 91-129.
- [7] E. Rems, M. Anayee, E. Fajardo, R.L. Lord, D. Bugallo, Y. Gogotsi, Y.-J. Hu, Advanced Materials, 35 (2023) 2305200.

POSTTEACHERS BY RESEARCH AREAS



NanoMet

P1 UNSUPERVISED MACHINE LEARNING FOR NANOPARTICLES IN BIOLOGICAL SOLUTIONS

✉ gfranzese@ub.edu

G. Franzese^{1,2}, G. Marchetti^{1,2}, A. Martinez-Serra³,
F. D'Amico⁴, I. Fenoglio⁵, B. Rossi⁴, M. P. Monopoli³

¹ Institut de Nanociència i Nanotecnologia (IN²UB),
Universitat de Barcelona, Barcelona, Spain

² Departament de Física de la Matèria Condensada,
Universitat de Barcelona, Barcelona, Spain

³ Department of Chemistry, Royal College of Surgeons
in Ireland, University of Medicine and Health
Sciences, Dublin, Ireland

⁴ Elettra Sincrotrone Trieste, Trieste, Italy

⁵ Department of Chemistry, University of Turin, Turin,
Italy

Introduction

Numerous commercial products, such as textiles, cosmetics, paints, electronics, foods, and medical treatments, contain nanoparticles (NPs) due to their high chemical reactivity. However, the interactions of NPs with biological systems are still not fully understood. We know that NPs absorb proteins, lipids, sugars, and other biomolecules from the environment, creating a corona that affects the cellular response. However, directly examining the molecular conformations within the corona is difficult. To address this issue, we developed an unsupervised machine learning (ML) protocol that can analyze noisy high-dimensional Ultra Violet Resonance Raman (UVRR) data, along with Circular Dichroism (CD) and UV absorbance (UVA) spectra. Our method is effective at high protein concentration even with limited data, and it works in a high-dimensional space of approximately 900 dimensions. We tested our protocol on a simplified in vitro experiment to demonstrate its ability to quantify changes in protein conformation after adsorption.

Materials & Methods

We prepare and characterize carbon and silica nanoparticles (CNP, SiNP) using Transmission Electron Microscopy (TEM). Then, we mix them with fibrinogen solution and examine the protein corona using Dynamic Light Scattering (DLS) and Differential Centrifugal Sedimentation (DCS). We collect UVRR, CD, and UVA data at different temperatures. We analyze the limited data with our novel ML approach, by combi-

ning physics-informed metrics like the Wasserstein distance and manifold reduction algorithms such as Principal Component Analysis (PCA) and t-distributed Stochastic Neighbor Embedding (t-SNE).

Results and Discussion

At high concentrations, free FIB undergoes unfolding and aggregation at around 50°C. However, addition of CNPs can prevent these changes, whereas SiNPs do not have the same effect. Our ML analysis clarifies the mechanism behind this. We find that CNPs freeze the structure of the FIB, while SiNPs do not. Our ML method is general and can be applied to any NP-corona, making it a valuable tool for studying the structure of highly concentrated proteins adsorbed on nanomaterials for novel applications.

Acknowledgments

G.M. would like to thank Jozsef Kardos for his help in using the BeStSel software. All authors thank Oriol Miro for testing the code. A.M.-S., and M. P.M. gratefully acknowledge the financial support through the H2020 SUNSHINE grant no. 952924. G.F. and G.M. acknowledge the support by MICIU/AEI/10.13039/501100011033 and "ERDF A way of making Europe" grant number PID2021-124297NB-C31 and the support by ICREA Foundation (ICREA Academia prize). G.F. thanks also for the support by "Ministerio de Universidades - Programa Estatal para Desarrollar, Atraer y Retener Talento, subprograma estatal de Movilidad, del Plan Estatal de Investigación Científica, Técnica y de Innovación 2021-2023" grant n. PRX22/00277, the Visitor Program of the Max Planck Institute for The Physics of Complex Systems, Dresden, for a six-month visit in November 2022 and a six-month visit in November 2023, the COST Action CA22143 EuMINe. All authors thank Elettra Sincrotrone Trieste for funding proposal no. 20220499.

P2 IMPACT OF AN INHOMOGENEOUS CONCENTRATION FIELD ON THE TRANSPORT AND SELF-ASSEMBLY OF ACTIVE PARTICLES

✉ jdtorrenegar@unal.edu.co

J. D. Torrenegra-Rico^{1*}, A. Arango-Restrepo¹, M. Rubi¹

¹Departament de física de la materia condensada,
Universitat de Barcelona, Avinguda Diagonal 647,
08028 Barcelona, Spain

Active particles (AP) are known for consuming chemical energy from the medium and converting it into mechanical energy, facilitating their interaction with the environment to perform transport, chemotaxis, self-assembly process [1,2]. Numerous applications involving AP, such as drug delivery in situ medicine and environmental processes, necessitate consideration of fuel consumption to circumvent the need for external forces to propel particles through complex environments [1,3]. Moreover, the self-assembling process of AP could be contingent upon the amount of fuel the system consumes to attain a preferred state [1,4-6]. These observations underscore the necessity, particularly in defining models using the far-field approach, to account for the dependency of AP on the environment and fuel consumption [2,4-6]. This prompts inquiries into how chemical reactions on AP influence their transport through crowded environments and the impact of consumption on the mechanisms underlying the formation of self-assembling structures and potential instabilities.

Our investigations encompass two scenarios involving consumption: (I) the traversal of AP through diverse channels under oscillatory fuel conditions, assisted by environmental noise, to achieve optimal Signal-to-Noise ratio [7].

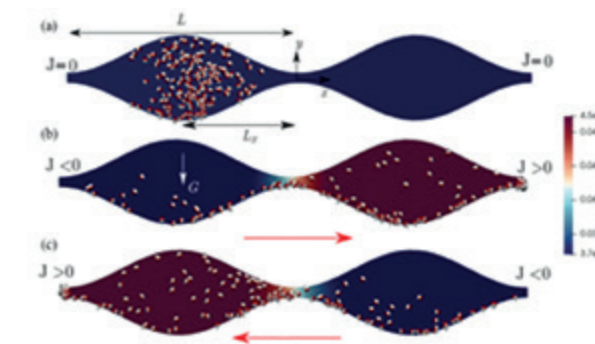


Figure 1. Scheme of the system. APs are driven by a constant force (white arrow) G in the orthogonal direction and by the substrate concentration gradient (color map) $\rho(x, y, t)$ in the longitudinal direction whose flux is J .

We discovered that intermittent substrate injection induces periodic forces Fig. 1 on particles, synchronized with noise, enhancing spectral amplification and optimizing transport, applicable in drug delivery and porous media penetration Fig. 2 [7].

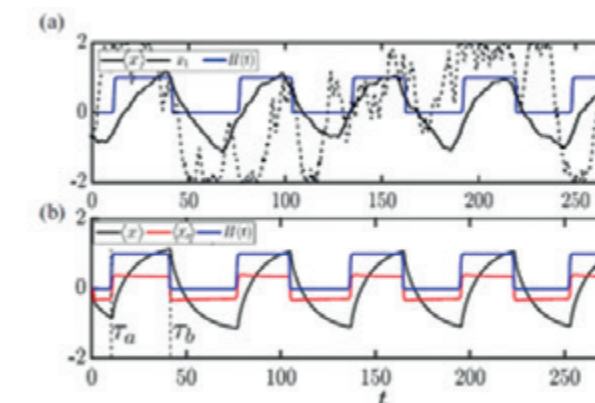


Figure 2. Active particle dynamics. APs mean position $\langle x(t) \rangle$ (black solid line) and periodic signal $H(t)$ (blue solid line) (a) position of a single AP $x_i(t)$ (black dashed line), obtained from Langevin dynamics. (b) Substrate mean position $\langle x_s(t) \rangle$ (red line). The oscillation period is $T = \tau_b - \tau_a$ while the frequency is $\omega = \pi/T$. The values of the parameters used in the simulations are $J_{in} = 3.25D$, $G = 1.0$, $\omega = 0.114$, $kd = 5$, and $kch = 10$.

Finally Utilizing a self-consistent model of catalytic Janus particles, accounting for hydrodynamic interactions and non-uniform fuel concentration, we identified distinct aggregation regimes, elucidating free energy barriers and determining conditions conducive to particle clustering Fig . 3. We posit that the self-organization of active matter remodels the environment, engendering a feedback loop wherein evolving structures modulate environmental conditions to enhance stability.

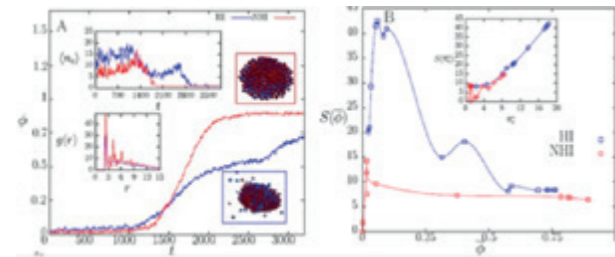


Figure 3. (A) number of clustered particles ϕ_c with Hydrodynamic interaction HI (blue lines) and with out Hydrodynamic interaction NHI (red solid lines). Insets are the number of clusters (n_c) and the radial distribution function. (B) Entropy S as a function of the average number of aggregated particles ϕ , for HI and NHI. The inset depicts the entropy as a function of the averaged number of clusters formed n_c .

References

- [1] D. A. Gregory and S. J. Ebbens, *Langmuir*, vol. 34, no. 14, pp. 4307–4313, 2018
- [2] Bailey, Maximilian R., et al., *Nanoscale* 16.5 (2024): 2444–2451
- [3] Y. Fu, H. Yu, X. Zhang, P. Malgaretti, V. Kishore, and W. Wang, *Micromachines* 13, 295 (2022)
- [4] S. Saha, R. Golestanian, and S. Ramaswamy, *Phys. Rev. E* 89, 062316 (2014)
- [5] A. Laskar, O. E. Shklyaev, and A. Balazs, *Langmuir* 36, 7124 (2020)
- [6] J. Torrenegra-Rico, A. Arango-Restrepo, and J. Rubí, *J. Chem. Phys.* 157, 104103 (2022)
- [7] Torrenegra-Rico, J. D., A. Arango-Restrepo, and J. M. Rubi. *Phys. Rev. E* 108.1 (2023): 014134
- [8] Torrenegra-Rico, J. D., A. Arango-Restrepo, and J. M. Rubi. Pre-Print

P3 NON-EQUILIBRIUM THERMODYNAMICS OF CATALYTIC JANUS PARTICLES SELF-ASSEMBLY

✉ aarangor@ub.edu

A. Arango-Restrepo¹, J. D. Torrenegra-Rico¹, J. M. Rubi^{1,2}

¹ Departamento de Física de la Materia Condensada, Facultad de Física, Universitat de Barcelona

² Instituto de Nanociencia y Nanotecnología, Universitat de Barcelona

The study of the individual and collective behaviour of self-propelled particles, which convert the chemical energy of the surrounding fluid into mechanical energy, is fundamental to understanding the non-equilibrium nature of active matter of which many soft matter and biological systems are composed [1-2]. Being out of equilibrium raises questions such as how fluctuations behave and what are the mechanisms leading to the formation of self-assembling structures and instabilities at large length scales, to name but a few [3-4]. We investigate the energetic cost of Janus particle structure formation and analyse the dynamics of particle assembly to initially inhomogeneous fuel concentrations, revealing several emergent structures. The energy dissipation during structure formation is derived from the entropy production rate, exhibiting a non-monotonic behaviour that depends on the fraction of particles assembled within each self-assembly regime. Furthermore, we establish a thermodynamic criterion for structure formation by analysing the free energy of the particles, focusing on the behaviour of the non-equilibrium chemical potential with respect to the fraction of assembled particles [5].

In a complementary study, we delve into the motion of a catalytic Janus particle, exploring the interplay between self-thermophoresis and self-diffusiophoresis. We illuminate their individual behaviours and the possible coupling resulting from diffusion at the particle-medium interface, a previously neglected factor. Employing an out-of-equilibrium thermodynamic model, we determine crucial parameters such as effective diffusivities, phoretic coefficients and transport properties. By juxtaposing theoretical predictions with experimental data, we discern the conditions for coupled or independent phoretic dynamics. In particular, this work emphasises a detailed examination of particle surface interactions to elucidate the direction and magnitude of phoretic forces as well as their amplification due to collective phenomena, offering valuable information to advance drug delivery and nanomotors in materials science and medicine, promising customised transport properties at the nanoscale [6].

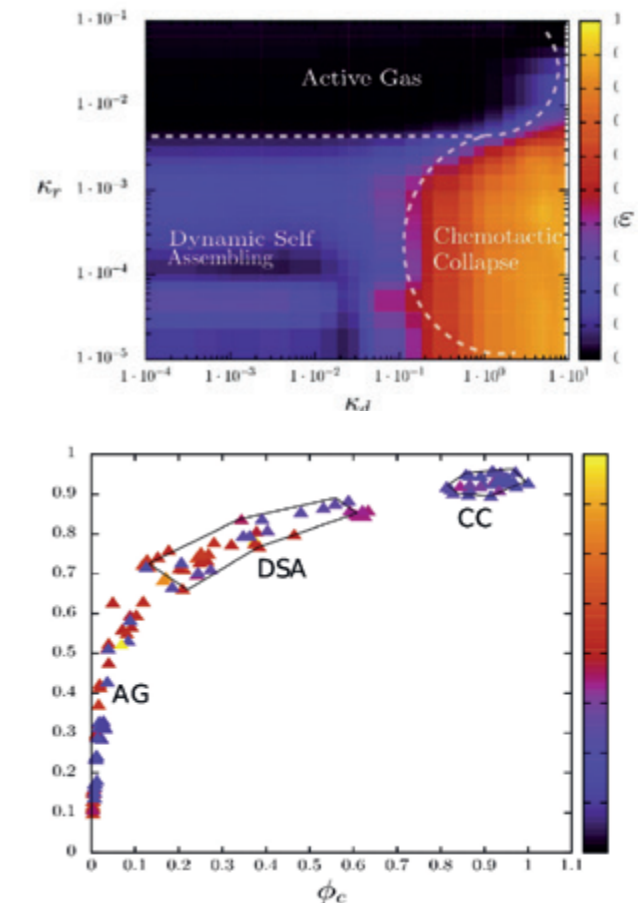


Figure 1. Fraction of assembled particles as a function of the chemophoretic coefficient krk and the diffusiphoretic coefficient kdk . We can identify the presence of three regimes: active gas (AG), dynamic self-assembly (DSA) and chemotactic-collapse (CC). Sphericity ϵ as a function of the fraction of assembled particles ϕ_c . The triangles represent the values of the total entropy produced irreversibly Σ expressed by the colour bar.

References

- [1] M. J. Bowick, N. Fakhri, M. C. Marchetti, and S. Ramaswamy, *Phys. Rev. X* 12, (2022) 010501.
- [2] Y. Fu, H. Yu, X. Zhang, P. Malgaretti, V. Kishore, and W. Wang, *Micromachines* 13, (2022) 295.
- [3] W. Gao, M. D'Agostino, V. Garcia-Gradiella, J. Orozco, and J. Wang, *Small* 9, (2013) 467–471.
- [4] Q.-L. Lei, M. P. Ciamarra, and R. Ni, *Sci. Adv.* 5, (2019) 7423.
- [5] J.D. Torrenegra-Rico, A. Arango-Restrepo, J.M. Rubi, *J. Chem. Phys.*, 157 (2022) 104103.
- [6] A. Arango-Restrepo, J.D. Torrenegra-Rico, J.M. Rubi, *in preparation*.

P4 SOLID-STATE PYROELECTRIC SYSTEM FOR NEAR-FIELD ENERGY CONVERSION

✉ ilatella@ub.edu

I. Latella¹, P. Ben-Abdallah²

¹Department of Condensed Matter Physics and Institute of Nanoscience and Nanotechnology, University of Barcelona, Martí i Franquès 1, 08028 Barcelona, Spain

²Laboratoire Charles Fabry, UMR 8501, Institut d'Optique, CNRS, Université Paris-Saclay, 91127 Palaiseau Cedex, France

Any hot object constitutes a source of thermal energy in the form of heat. Spanning a wide range of scales and situations, the latent potential of most thermal sources is often lost as waste heat. Developing efficient methods for recovering and managing this stream of waste heat is a current challenge for science and technology of notable impact. Among the different mechanisms driving the heat transport, energy exchange between contactless objects through thermal radiation (photons) represents a promising option to take advantage of heat sources in nanoscale applications [1]. Due to a strong dependence on the optical properties of the sources, radiative heat transfer at the nanoscale typically exhibits versatile properties that can be tailored by appropriately selecting materials for the application under consideration [2]. In this talk, we introduce [3] a theoretical mechanism to convert near-field energy using micrometric pyroelectric membranes encapsulated between two graphene field-effect transistors which act as the hot source and cold sink. By modulating the gate voltage in the graphene transistors, the radiative coupling between the pyroelectric membrane and both the source and the sink can be modulated as well. This dynamical modulation can induce controlled temperature variations in the active layer, so useful energy can be obtained thanks to the pyroelectric properties of the layer. We show with an example that these systems can generate a power of 130 mW/cm² using pyroelectric Ericsson cycles, a value which surpasses the current produc-

tion capacity of near-field thermophotovoltaic conversion devices with low-grade heat sources and small temperature differences. In the proposed solid-state device, the temperature of the active layer can be modulated at kHz frequencies, achieving power densities higher than those obtained with mechanical pyroelectric converters [4]. Furthermore, we also show that our graphene-based pyroelectric system is a self-powered conversion device in which the power required to modulate the temperature is much smaller than the delivered power, opening so a new avenue for high-frequency pyroelectric energy harvesting from stationary thermal sources.

References

- [1] I. Latella, S.-A. Biehs and P. Ben-Abdallah. Smart thermal management with near-field thermal radiation, *Optics Express* 29, 24816-24833 (2021).
- [2] M.-J. He, X. Guo, H. Qi, I. Latella, H.-P. Tan. Splitting of temperature distributions due to dual-channel photon heat exchange in many-body systems, *Int. J. Heat Mass Transf.* 216, 124626 (2023).
- [3] I. Latella and P. Ben-Abdallah. Graphene-based autonomous pyroelectric system for near-field energy conversion, *Sci. Rep.* 11, 19489 (2021).
- [4] Fang, J., H. Frederich and L. Pilon, *J. Heat Transf.* 132, 092701 (2010).

P5 INVESTIGATING VACANCIES AND ANISOTROPIC DEFECTS USING STEM AND iDPC IMAGING TECHNIQUES

✉ pnandi@ub.edu

P. Nandi¹, J. Barthel², M. López-Haro³, J. J. Calvino³, F. Chiabrera⁴, F. Baiutti⁴, A. Tarancón^{4,5}, F. Peiró^{1,6}, Ll. Yedra¹, S. Estradé¹

¹Laboratory of Electron Nanoscopies (LENS), Micro-Nanotechnology and Nanoscopies for electrophotonic Devices (MIND), Department of Electronics and Biomedical Engineering and Institute of Nanoscience and Nanotechnology (IN²UB), University of Barcelona, Spain

²Ernst Ruska-Centre (ER-C 2), Forschungszentrum Jülich GmbH, Germany,

³Universidad de Cádiz, Spain

⁴Institut de Recerca en Energia de Catalunya, Spain

⁵Catalan Institution for Research and Advanced Studies, Spain

⁶ICREA Academia, Passeig Lluís Companys 23, Barcelona 08010, Spain

La_{1-x}Sr_xMnO₃ (LSMO) has been widely considered as a promising candidate in fields of mixed ionic-electronic conductors and solid oxide fuel cells. A great amount of effort has been focused on its oxygen mass transport properties[1]. Faster diffusion through dislocations has been generally attributed to higher vacancy concentration or to a higher mobility of oxygen vacancies[2]. It has been reported that oxygen vacancies and antisite defects in LSMO can strongly affect its electronic and magnetic properties[3,4]. We therefore propose a novel method to detect vacancies and antisite defects from scanning transmission electron microscopy (STEM) images by image simulation and analysis software.

LSMO thin films with antisite defects of variable Mn/(La+Sr) ratio were grown by combinatorial pulsed laser deposition on SrTiO₃ and the control of stoichiometry was achieved by using an alternate deposition of Mn-deficient LSM and Mn₃O₄ followed by an in-situ annealing in oxygen[5]. The samples were observed in a FEI Titan3 Themis 60-300 Transmission Electron Microscope operated at 200 KV equipped with segmented STEM detectors.

In this study, we simulated STEM images of LSMO with variable oxygen vacancies from four segmented detectors[6]. The images obtained were then processed to generate integrated differential phase contrast (iDPC) images. Comparing the theoretical iDPC with the experimental images, we could correlate the reduced intensities on O columns with the presence of oxygen vacancies as shown in Fig 1. Further, we introduced antisite defects and simulated the corresponding STEM and iDPC images. The comparison of integrated intensities along the atomic column between different positions in the perovskite and the simulated controlled composition images provide a method to estimate antisite defects supplementary to elemental mapping. Our approach contributes to illustrate the relevance of simulations for analysing STEM images.

Acknowledgements

We acknowledge the funds received from AGAUR FI grants (2021 FI_B 00157) and the support received from the ELECOMI - ICTS Electron Microscopy for Materials Science. L.Y. acknowledges support from the MINECO (Spain) through the IJC2018-037698-I grant. The authors would also like to acknowledge the financial support from the Spanish project PID2019-106165GB-C21, and the Catalan project 2021SGR00242.

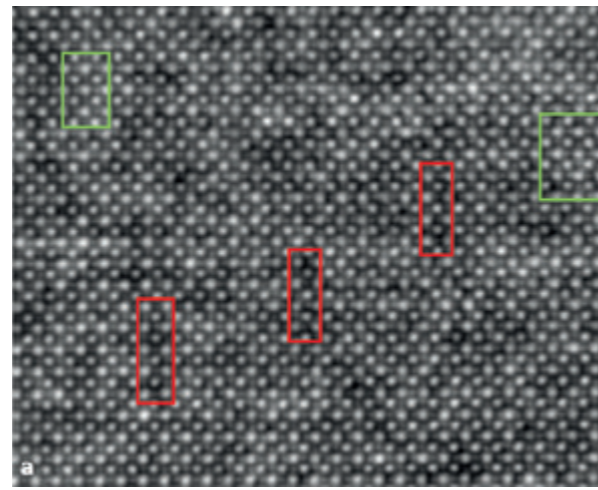
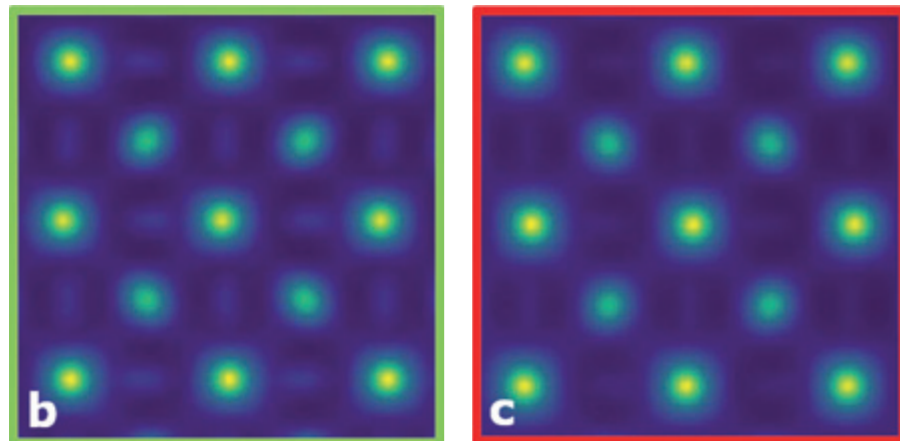


Figure 1. LSMO (a) Experimental iDPC image where regions with oxygen vacancies (in red) and without (in green) are highlighted. (b) Simulated iDPC image with no vacancies. (c) Simulated iDPC image with vacancies.



References

- [1] Saranya, A. M. *et al.* Unveiling the Outstanding Oxygen Mass Transport Properties of Mn-Rich Perovskites in Grain Boundary-Dominated La_{0.8}Sr_{0.2}(Mn_{1-x}Cox)_{0.85}O_{3±δ} Nanostructures. *Chemistry of Materials* **30**, 5621–5629 (2018).
- [2] Navickas, E. *et al.* Dislocations Accelerate Oxygen Ion Diffusion in La_{0.8}Sr_{0.2}MnO₃ Epitaxial Thin Films. *ACS Nano* **11**, 11475–11487 (2017).
- [3] Kumari, S. *et al.* Effects of Oxygen Modification on the Structural and Magnetic Properties of Highly Epitaxial La_{0.7}Sr_{0.3}MnO₃ (LSMO) thin films. *Sci Rep* **10**, (2020).
- [4] Gu, M. *et al.* Antisite defects in La_{0.7}Sr_{0.3}MnO₃ and La_{0.7}Sr_{0.3}FeO₃. *Appl Phys Lett* **102**, (2013).
- [5] Chiabrera, F. M. *et al.* The impact of Mn nonstoichiometry on the oxygen mass transport properties of La_{0.8}Sr_{0.2}Mn_yO_{3±δ} thin films. *JPhys Energy* **4**, (2022).
- [6] Barthel, J. Dr. Probe: A software for high-resolution STEM image simulation. *Ultramicroscopy* **193**, 1–11 (2018).

P6

ANALYSIS OF OPTICAL PROPERTIES OF HfO₂ THIN LAYERS WITH RHOMBOHEDRAL, MONOCLINIC, AND HEXAGONAL STRUCTURES USING EELS

✉ bvargas@ub.edu

B. Vargas¹, D. Nasiou², L. Molina-Luna², C. Coll³, D. del Pozo Bueno¹, P. Nandi¹, S. Estradé¹, LL. Yedra¹, N. Kaiser⁵, L. Alff⁵, L. López-Conesa¹, F. Peiró^{1,4}

¹ LENS, Department of Electronics and Biomedical Engineering and Institute of Nanoscience and Nanotechnology (IN²UB), University of Barcelona (UB), Barcelona, Spain.

² Department of Materials and Earth Sciences, Advanced Electron Microscopy, Technical University of Darmstadt, Darmstadt, Germany.

³ Catalan Institute of Nanoscience and Nanotechnology (ICN2), CSIC and BIST, Campus UAB, Bellaterra, Spain.

⁴ Catalan Institution for Research and Advanced studies, ICREA Academia, Barcelona, Spain.

⁵ Department of Materials Science, Advanced Thin Film Technology, Technical University of Darmstadt, Darmstadt, Germany.

its behaviour in bulk, due to a variety of factors such as defects and surface effects [2].

In this study, we compare the dielectric function and energy loss function of HfO₂ thin layers, with hexagonal and rhombohedral phases. Thin films of 20 nm HfO_{2-x} were grown on a TiN substrate, and each one was extracted from a vacuum atmosphere to an air atmosphere where an oxygen-rich nanolayer was formed at the top of the HfO_{2-x} layer. After this, each sample was deposited in a vacuum atmosphere to sputter a Pt bottom electrode by using molecular beam epitaxy (MBE), obtaining two multilayer devices as shown in Fig. 1. Electron transparent cross-sectional TEM lamellas were fabricated using a JEOL 4600F Focused Ion Beam (FIB), and EELS data were acquired in a JEOL-ARM200F at 200 kV.

The dielectric function and electron energy loss function of HfO₂ have been studied using electron energy loss spectroscopy (EELS) by Kramers-Kronig (KK) analysis, using the algorithm reported by Eljarrat [3]. The effects of crystalline structure on the optical properties of HfO₂ have been observed through the analysis of the dielectric function (see Fig. 2). Additionally, for each sample, the procedure was applied to several regions of the HfO₂ layer with the same size and dimensions, sweeping the area of measurement

Hafnium oxide (HfO₂) is a material with a high dielectric response, making it widely used in the fabrication of advanced semiconductor devices. The dielectric function is an important parameter in the study of its optical and electronic properties [1]. At the nanoscale, the dielectric response of HfO₂ can differ from

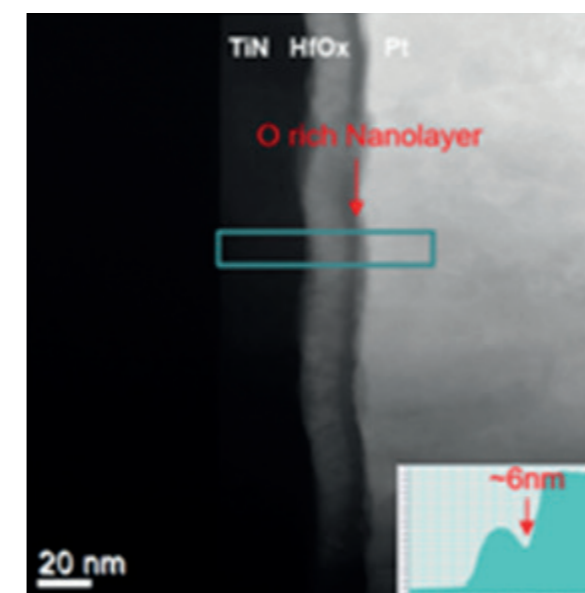


Figure 1. HAADF image indicating the area of HfO₂ layer with a higher oxygen concentration.

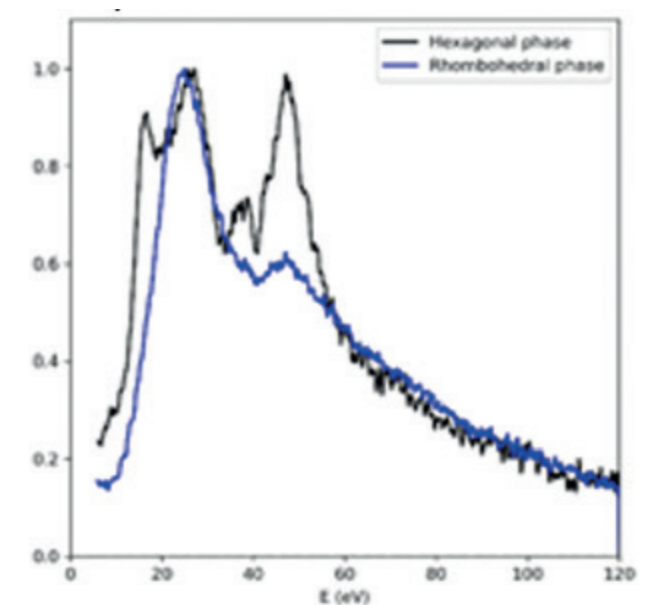


Figure 2. Electron energy loss function of HfO_x: HfO_{a7} with hexagonal phase and HfO_{1.7} with rhombohedral phase.

from one interface to the other, in order to observe how the oxygen variation affects the optical response. KK calculations revealed a shift to higher energies of the ELF, and consequently on the dielectric response of the HfO₂ layer with a hexagonal phase near the oxygen-rich nanolayer. Further, Density Functional Theory (DFT) calculations have been carried out to co-relate with the experimental findings.

Acknowledgements

The authors would like to acknowledge funding from MICIIN under project reference No. PID2019-106165GB-C21, the support received from the ELEC-MI-ICTS Electron Microscopy for Materials Science and funding from Gencat under project reference No. 2021SGR00242. We are also grateful to ATFT group of TU Darmstadt for producing the samples.

References

- [1] E. I. Suvorova, O. V. Uvarov, N. A. Arkharova, A. D. Ibrayeva, V. A. Skuratov, and P. A. Buffat. Structure evolution, bandgap, and dielectric function in La-doped hafnium oxide thin layer subjected to swift Xe ion irradiation. *J Appl Phys*, vol. 128, no. 16, Oct. 2020, doi: 10.1063/5.0025536.
- [2] J. Park and M. Yang, 'Determination of complex dielectric functions at HfO₂/Si interface by using STEM-VEELS', *Micron*, vol. 40, no. 3, pp. 365–369, Apr. 2009, doi: 10.1016/J.MICRON.2008.10.006.
- [3] A. Eljarrat and C. T. Koch. Design and application of a relativistic Kramers–Kronig analysis algorithm. *Ultramicroscopy*, vol. 206, Nov. 2019, doi: 10.1016/j.ultramic.2019.112825.

NanoBio

P7

PROBING ACTIVE NEMATICS WITH IN SITU MICROFABRICATED ELASTIC INCLUSIONS

✉ivelez@ub.edu

I. Vélez-Cerón^{1,2}, P. Cuillamat³, F. Sagués^{1,2}
and J. Ignés-Mullol^{1,2}

¹Department of Materials Science and Physical Chemistry, Universitat de Barcelona, Barcelona 08028, Spain

²Institute of Nanoscience and Nanotechnology, IN²UB, Universitat de Barcelona, Barcelona 08028, Spain

³Institute for Bioengineering of Catalonia, The Barcelona Institute for Science and Technology, Barcelona 08028, Spain

Active nematic dynamics are governed mainly by means of elastic, active and viscous stresses [1], which reveal the elastic constant (k), activity (α) and viscosity (η) as key parameters of the material. However, the values of these parameters are still unclear. Different approaches have been used to determine them. For example, active nematic viscosity has been studied experimentally [2] and theoretically [3], [4] giving out results with different order of magnitude.

In this work, we present a novel method to determine both the activity and viscosity of active nematic based on force measurements using elastic cantilevers. With a custom DMD-based photolithography technique [5], we are able to build polymeric cantilevers in a microtubule-kinesin based active nematic [6], from the bottom to the surface. Measuring the deflection of the cantilevers the force applied by the active material can be determined, and then, the force is correlated to the director and velocity fields to obtain for the first time the values of the activity and the viscosity of active nematics. The results obtained show that the ratio between activity and viscosity is proportional to the mean vorticity as was previously predicted by Giomi [7], and the variation of this ratio with the activity follows the trend that was also predicted [8].

References

- [1] A. Doostmohammadi et al., *Nat. Comms.*, **9**, 3246 (2018).
- [2] D. P. Rivas et al., *Soft Matter*, **16**, 9331 (2020).
- [3] P. Cuillamat et al., *Phys. Rev. E*, **94**, 060602 (2016).
- [4] B. Martínez-Prat et al., *Phys. Rev. X*, **11**, 031065 (2021).
- [5] I. Vélez-Cerón et al., *Proc. of SPIE*, **12435**, 1243507 (2023).
- [6] T. Sanchez et al., *Nature*, **491**, 431 (2012).
- [7] L. Giomi, *Phys. Rev. X*, **5**, 31003 (2015).
- [8] C. Joshi et al., *Phys. Rev. Lett.*, **129**, 2580010 (2022).

P8 LIPOSOMAL ENCAPSULATION AND RELEASE FOR SKIN PROTECTION AND TREATMENT

Botet-Carreras, A.^{1,3}, Calpena-Campmany, A. C.^{2,3}, Mallandrich, M.^{2,3}, Montero, M. T.^{1,3}, Borrell, J. H.¹, Domènech, O.^{1,3}

¹Secció de Físicoquímica, Facultat de Farmàcia i Ciències de l'Alimentació, UB

²Secció de Biofarmàcia, Facultat de Farmàcia i Ciències de l'Alimentació, UB

³Institut de Nanciència i Nanotecnologia (IN²UB)

Introduction

The skin is the first protective barrier of humans against environmental aggressions. When it is damaged by some external factor that produces wounds, during its regeneration it can appear scars and visible pigmentation on the skin as well as infectious agents may enter the body. Therefore, it is of great interest to develop advanced formulations that could improve the current systems of regeneration of the *stratum corneum* to accelerate the healing processes [1]. Knowing the hydrophilic-hydrophobic properties of liposomes, they can be used not only as vehicles for the treatment of different pathologies but to protect the skin from external aggressions. Therefore, in this project, we developed a liposomal formulation with superior properties compared with classic formulations such as ointments with free components. This new formulation is particularly indicated for treating areas with wounds or scars that are permanently exposed, such as wounds derived from lupus, scar regeneration or the treatment of recurrent wounds in patients who spend long periods in bed.

Materials & Methods

Liposome preparation: a chloroform:methanol (2:1, v/v) volume containing the appropriate amount of lipids was placed in a glass balloon flask and dried in a rotary evaporator at room temperature protected from light. Multi-lamellar liposomes were obtained by redispersion of the thin film in buffer.[2]

Atomic Force Microscopy: images were performed with a Nanoscope IV from Digital Instruments (Bruker, AXS Co., Madison, WI, USA) equipped with a 15 µm piezoelectric scanner using V-shaped silicon nitride cantilevers with a nominal spring constant of 80 pN nm⁻¹, in air and in intermittent contact mode.

Ex-vivo permeation and quantification: active principles (AP) release from the liposomes was evaluated by Franz diffusion cells using a human skin at 32°C under sink conditions.

Results and Discussion

The final formulations containing multilamellar liposomes demonstrate the capacity to provide a high re-release through the skin, with a fast delivery of the free AP followed by a delayed release of the AP from the liposomes. This double boost increases dramatically the amount of AP found in the tissue observed during the permeation assays.

Fig. 1A shows an AFM image of clean human skin without any treatment. Different structures related to the intrinsic roughness of the skin can be observed. Figure 1B shows the same skin where liposomes were deposited and left to incubate for 5 minutes before removing the non-adsorbed sample. A decrease in the roughness of the skin is clearly observed due to the adsorption and extension of the liposomes. When liposomes contact the surface of the skin, they break, spread and form what is called a flat bilayer. These flat bilayers will be the reservoir of AP from where the molecules will be released towards more internal regions of the skin while forming an occlusive protective layer that prevents contact with the environment.

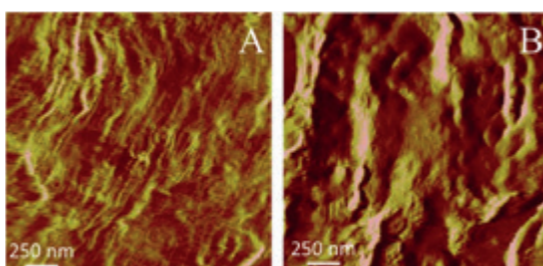


Figure 1. Images of human skin without liposomes (A) and with liposomes (B).

References

- [1] Moniz T, et al. Br J Pharmacol. 177(19):4314-4329 [2] M.L. Vázquez-González, et al. 2019. Int. J. Pharm. 563, 1-8.

P9 TARGETING LNCRNA HOTAIR WITH PPRHS IN THE CONTEXT OF BREAST CANCER AND TAMOXIFEN RESISTANCE

✉vnoe@ub.edu

J. Cullèll¹, C. J. Ciudad¹, V. Noé¹

¹Department of Biochemistry and Physiology, School of Pharmacy and Food Sciences, and Institute of Nanoscience and Nanotechnology of the University of Barcelona (IN²UB)

LncRNA HOTAIR has been described as a driver of breast cancer (BC) and a biomarker of bad prognosis and metastasis in this setting [1], [2]. Since transcription of this lncRNA is induced by estradiol [3], we sought to find a combination therapy by gene silencing of Hotaair using PolyPurine Reverse Hoogsteen hairpins (PPRHs) plus tamoxifen as a selective estrogen receptor (ER) modulator.

Hotaair is also involved in promoting tamoxifen resistance by a ligand-independent activation of the ER and its signaling cascade [4]. For this reason, our combination therapy approach was aimed at treating both tamoxifen-sensitive and -resistant MCF7 cells.

Three PPRHs were designed against the Hotaair lncRNA. Since part of the Hotaair gene overlaps with the sequence HOXC11, which has been described to positively regulate Hotaair and to increase the risk of some types of cancer and endocrine resistance in BC [5], [6], we designed PPRHs that would bind to the overlapping interface of both genes.

Two PPRHs were designed against intron 1 of HOXC11 (HpHotaair-I1a and HpHotaair-I1b) and one against the proximal area of its promoter (HpHotaair-Pr-proxy). Off target effects of the three PPRHs were ruled out using BLAST.

The combinational effect of PPRHs and different concentrations of tamoxifen was evaluated in experiments of cytotoxicity performed by MTT assays in MCF7 cells. HpHotaair-I1a and HpHotaair-I1b produced a significant cytotoxic effect in combination with tamoxifen whereas the effect of HpHotaair-Pr-proxy was much lower. The cytotoxicity of tamoxifen in these cells at the three different concentrations tested was increased by more than 40% with the addition of PPRHs targeting Hotaair. The cationic liposome Dotap was used as a negative control.

The binding specificity of HpHotaair1a and HpHotaair1b to their respective targets was assessed by EMSA (electrophoretic mobility shift assay). FAM-labeled single DNA oligonucleotides corresponding to the predicted binding sequence for each PPRH were used. The specific PPRHs successfully displaced their target sequence, but not a scramble PPRH used as a negative control.

Gene silencing of Hotaair in MCF7 cells was confirmed by RT-PCR, reaching up to 40% decrease of Hotaair RNA expression upon PPRH transfection.

Ongoing experiments will address if gene silencing of Hotaair by PPRHs is also able to decrease the expression of c-Myc which is activated by this lncRNA.

In conclusion, targeting lncRNA HOTAIR may be a potential therapeutic agent in combination with tamoxifen for ER-positive BC.

Acknowledgements

Research supported by grant numbers RTI2018-093901-B-I00 and PID2021-1222710BI00. JC is recipient of a predoctoral fellowship from AGAUR.

References

- [1] G. S. R. Raju et al., "HOTAIR: a potential metastatic, drug-resistant and prognostic regulator of breast cancer," *Mol Cancer*, vol. 22, no. 1, Dec. 2023, doi: 10.1186/S12943-023-01765-3.
- [2] D. Wu, J. Zhu, Y. Fu, C. Li, and B. Wu, "LncRNA HOTAIR promotes breast cancer progression through regulating the miR-129-5p/FZD7 axis," *Cancer Biomark*, vol. 30, no. 2, pp. 203-212, 2021, doi: 10.3233/CBM-190913.
- [3] A. Bhan, I. Hussain, K. I. Ansari, S. Kasiri, A. Bashyal, and S. S. Mandal, "Antisense transcript long non-coding RNA (lncRNA) HOTAIR is transcriptionally induced by estradiol," *J Mol Biol*, vol. 425, no. 19, pp. 3707-3722, Oct. 2013, doi: 10.1016/J.JMB.2013.01.022.
- [4] X. Xue et al., "LncRNA HOTAIR enhances ER signaling and confers tamoxifen resistance in breast cancer," *Oncogene*, vol. 35, no. 21, p. 2746, May 2016, doi: 10.1038/ONC.2015.340.
- [5] X. Peng et al., "HOXC11 drives lung adenocarcinoma progression through transcriptional regulation of SPHK1," *Cell Death Dis*, vol. 14, no. 2, Feb. 2023, doi: 10.1038/S41419-023-05673-8.
- [6] N. Gong et al., "HOXC11 positively regulates the long non-coding RNA HOTAIR and is associated with poor prognosis in colon adenocarcinoma," *Exp Ther Med*, vol. 22, no. 5, Sep. 2021, doi: 10.3892/ETM.2021.10745.

P10

TOWARDS THE REDUCTION OF EXPERIMENTAL COSTS THROUGH THE USE OF META LEARNING

✉ sergio.noe@ub.edu

S. Noé¹, A. Martínez-Blanco¹, L. Carreras-Vidal¹, N. Gavara¹¹ Universitat de Barcelona, Unitat de Biofísica i Bioenginyeria.

In this work we aim reducing the volume of data needed to train a neural network model for a classification task. This reduction helps reducing time spent by the scientists in the lab and consumables used to carry out the experiments. We will use our trained algorithms to the specific task of using fluorescence imaging to differentiate between fibroblasts and tumour activated fibroblasts, the second type promoting cancer cell progression and immune evasion through secretion of immunomodulatory molecules, physical interaction with immune cells, and remodelling of the extracellular matrix. To do so, cancer fibroblasts had been grown on hydrogels [1] to imitate the original environment.

Our computational approach focuses on Meta-Learning, which aims at producing versatile models that can learn to perform different tasks without having to train them from scratch only showing them few examples for the new task.

Here we explore three different strategies to change how a deep learning model learns, and we apply them to classify activated and non-activated fibroblasts. Siamese Neural Networks [2], explore and modify the metric space that they build during training, by studying the distance where a data point is placed in each iteration and updating the weights of the network to modify this distance. The Siamese model yields an accuracy of 62%. Memory-Augmented Neural Networks [3], use an external memory module, where a model can store and retrieve values of data to combine with input data to obtain good performance with few samples. This model yields an accuracy of 48% on the classification of cells. Reptile [4], finds a set of optimized weights to converge faster and achieve good learning. This model yields an accuracy of 87%, being the best model out of the three.

The models show at least a twentyfold reduction in the number of images needed in comparison to the common deep learning algorithms datasets and there is also a two times accuracy increase between the memory augmented model and Reptile. All of this allows us to build entire datasets with a minimal number of images, needing much less experiments in which less materials are being used, reducing the cost of the process.

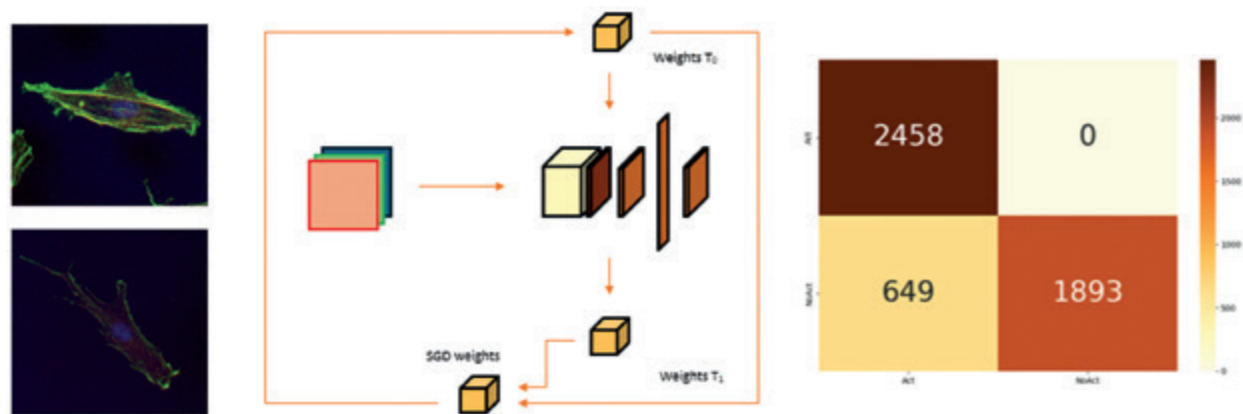


Figure 1. On the left, two different images of cells, the first one activated and the second one not activated. On the center, the structure of Reptile and on the right, a confusion matrix showing a good classification of the cells.

References

- [1] Martínez-Blanco *et al.*, Gels 2023 [2] Dey *et al.*, arxiv 2017 [3] Santoro *et al.*, Int. Conference on ML [4] Nichol *et al.*, arxiv. 2018

P11

3D CULTURING IMMORTALIZED PULMONARY FIBROBLASTS WITHIN EXTRACELLULAR MATRIX HYDROGELS IMPACTS THEIR MECHANICAL PHENOTYPE

✉ rsunyer@ub.edu

M. Moro-López¹, S. Olivé-Palau¹, R. Farré^{1,2,3}, J. Otero^{1,2,4}, R. Sunyer^{1,4,5*}¹ Unit of Biophysics and Bioengineering, School of Medicine and Health Sciences, University of Barcelona, Barcelona, Spain² Centro de Investigación Biomédica en Red de Enfermedades Respiratorias (CIBER-RES), Barcelona, Spain³ Institut Investigacions Biomèdiques August Pi Sunyer (IDIBAPS), Barcelona, Spain⁴ Institute of Nanoscience and Nanotechnology (IN²UB), University of Barcelona, Barcelona, Spain⁵ Centro de investigación Biomédica en Red de Bioingeniería (CIBER-BBN), Barcelona, Spain

Most in vitro studies are based on using cells isolated and expanded on plastic substrates. Nevertheless, the mechanical properties of cells' native tissues are quite different from those from plastic, and new evidence suggests that prolonged exposure to stiff substrates could have altered the mechanical phenotype of those cells so they present an aberrant mechanoreponse [1]. Certain studies showed that freshly isolated primary cells have shown completely different mechanoreponse than the same cells grown extensively in plastic [2], but the use of primary cells in laboratories is often limited. On the other hand, experiments performed with immortalized cancer cell lines [3] suggest that this aberrant mechanoreponse can be reversed, at least to a certain degree, using physiomimetic environments to culture the cells. The goal of this work is

to study to what extent the native mechanical phenotype of pulmonary fibroblasts can be recovered if they are cultured in 3D within lung extracellular matrix hydrogels.

Immortalized rat lung fibroblasts (RFL-6 cells) were cultured on tissue culture plastic, soft polyacrylamide gels, and in 3D lung ECM-derived hydrogels [4] for 4, 7 and 14 days. Then, cells were reseeded on top of type I collagen-coated polyacrylamide gels of different stiffnesses to measure cell area, nuclear to cytosolic YAP protein ratio, and traction forces.

For the three culture periods, cell area increased with stiffness in the plastic and polyacrylamide groups as expected [5], but interestingly it remained constant in the cells cultured within the ECM hydrogels. In addition, cells from hydrogels showed a considerably smaller area even in the higher stiffness (3:1 ratio for the three different culture times). The nuclear to cytosolic YAP ratio remained constant and larger than 1 for all groups and all preconditioning times, meaning that YAP is mostly localized in the nuclei for all groups. Regarding traction forces, an increase in total force with stiffness was observed in plastic and polyacrylamide-primed cells (3-fold increase for both groups) while hydrogel-primed cells showed a constant total force for any preconditioning time. Altogether results showed that culturing immortalized pulmonary fibroblasts within ECM-derived hydrogels affects cell area and total traction force. Further investigation is needed to unravel to what extent these observed differences are related to a reversion in the aberrant mechanobiology of these cells.

References

- [1] Yang C, Tibbitt MW, Basta L, Anseth KS: Mechanical memory and dosing influence stem cell fate. *Nat Mater* 2014, 13:645–652.
 [2] Lerche M, Elosegui-Artola A, Kechagia JZ, Guzmán C, Georgiadou M, Andreu I, Gullberg D, Roca-Cusachs P, Peuhu E, Ivaska J: Integrin Binding Dynamics Modulate Ligand-Specific Mechanosensing in Mammary Gland Fibroblasts. *iScience* 2020, 23:100907.
 [3] Watson AW, Grant AD, Parker SS, Hill S, Whalen MB, Chakrabarti J, Harman MW, Roman MR, Forte BL, Gowan CC, et al.: Breast tumor stiffness instructs bone metastasis via maintenance of mechanical conditioning. *Cell Rep* 2021, 35.
 [4] Falcones B, Sanz-Fraile H, Marhuenda E, Mendizábal I, Cabrera-Aguilera I, Malandain N, Uriarte JJ, Al-mendros I, Navajas D, Weiss DJ, Farré R, Otero J: Bioprintable lung extracellular matrix hydrogel scaffolds for 3D culture of mesenchymal stromal cells. *Polymers* 2021, 13(14):2350.
 [5] Solon J, Levental I, Sengupta K, Georges PC, Janmey PA: Fibroblast adaptation and stiffness matching to soft elastic substrates. *Biophys J* 2007, 93(12):4453–4461.

P12

CRYOSECTIONING OF HYDROGELS AS A RELIABLE APPROACH TO INCREASE YIELD AND FURTHER TUNE MECHANICAL PROPERTIES

✉ ngavara@ub.edu

Á. Martínez-Blanco¹, S. Noé¹, L. Carreras-Vidal¹,
J. Otero^{1,2,3}, N. Gavara^{1,2,*}

¹Unitat de Biofísica i Bioenginyeria, Facultat de Medicina i Ciències de la Salut, Universitat de Barcelona, 08036 Barcelona, Spain

²The Institute for Bioengineering of Catalonia (IBEC), The Barcelona Institute of Science and Technology (BIST), 08028 Barcelona, Spain

³CIBER de Enfermedades Respiratorias, 28029 Madrid, Spain

Introduction

Tissue engineering and the accurate recreation of cellular function in vivo involves the development of culture scaffolds capable of mimicking the physiological and pathological extracellular matrix (ECM). Hydrogels derived from decellularized lungs (L-dECM) are promising materials as they provide a source of specific physicochemical and biomechanical stimuli. However, pathological situations often involve an increase in the mechanical properties of the ECM, which requires the use of crosslinkers so that L-dECM match the stiffness of the tissue they intend to mimic. Among them, genipin has stood out as a natural crosslinker with low cytotoxicity, high biocompatibility, proper diffusion of nutrients and oxygen. In this work, we develop a cryosectioning method for decellularized lung hydrogels crosslinked with genipin which makes it possible to easily obtain lung bioscaffolds that recreate the necessary mechanical properties of different study situations and reliability of samples produced adhered to a glass support.

Materials & Methods

Bulk L-dECM hydrogels (20 mg/mL) were generated and cross-linked with different concentrations of genipin for 72 hours (Figure 1). The cross-linked matrices were frozen in an OCT block and cryosectioned with a cryostat. Cryosectioned slices were characterized by atomic force microscopy (AFM) to verify the effect on their mechanical properties of (1) different genipin concentrations as crosslinker, (2) rehydration time during the thawing steps of the cryosectioning process, and (3) the effect of EtOH-based sterilization. In addition, cryosectioned L-dECM hydrogels were seeded with rat lung fibroblast (RLF-6) to assess their biocompatibility.

Figure 1. Macroscopic images of the structural integrity of the control hydrogel (20 mg/mL) and crosslinked with genipin, and schematic illustration of genipin crosslinking reaction.

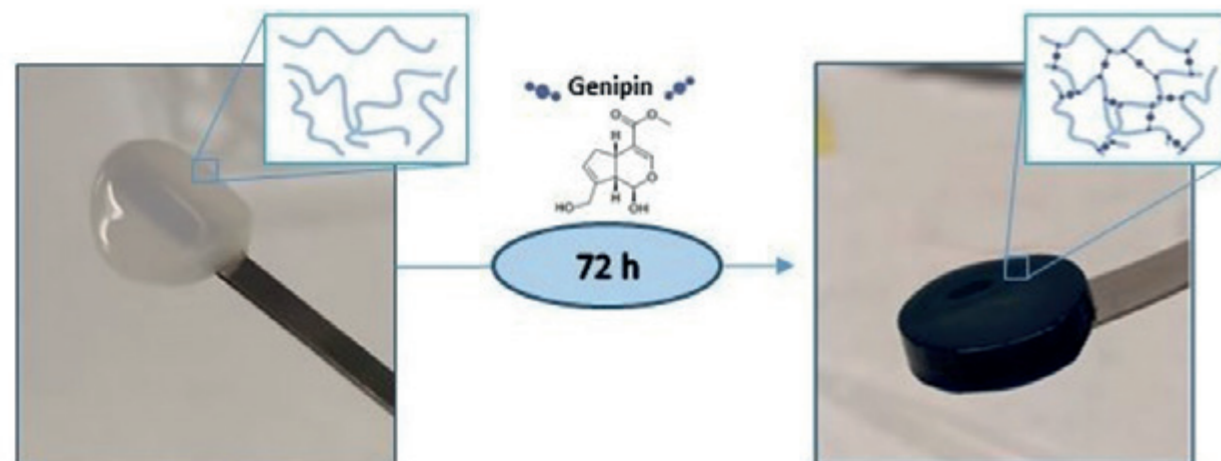
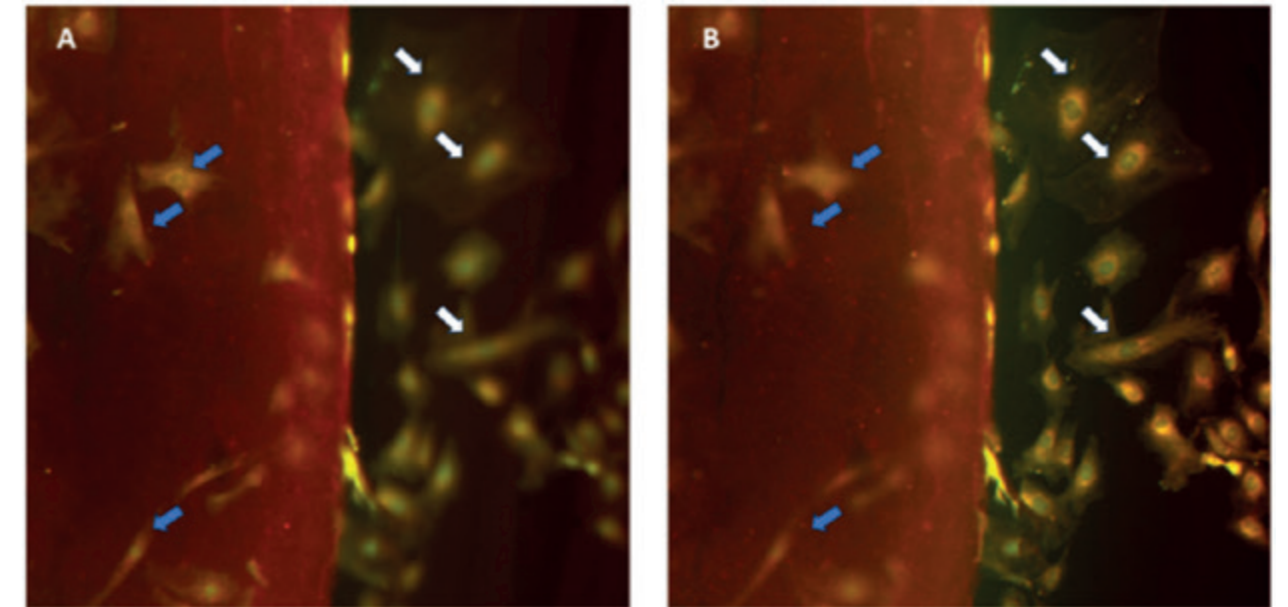


Figure 2. Epifluorescence image with focus on (A) the hydrogel cryosection and (B) the glass



Results & Discussion

L-dECM hydrogels characterized by AFM exhibited 21-fold increase with the addition of 5 mM genipin, 26.3-fold increase at 10 mM genipin and 32.8-fold increase at 20 mM genipin in stiffness compared to non-crosslinked hydrogels. The success of the hydrogel cryosectioning method lies in the rehydration time of the cryosections, which, when varied, modulates the mechanical properties and allows a wide range of stiffness to be simulated. An example of this is the stiffness simulation of the fresh hydrogels homologues with our cryosections, determining a rehydration time at 29 minutes for cryosections crosslinked with 5 mM genipin and at 43 minutes for cryosections crosslinked with 10 and 20 mM genipin. Determination of the sources of variability applied on our cryosections indicated that the major source of variability comes from the starting material as well as their processing, and that our method only contributed 17.47 ± 9.54 % to it. Exploring the effects of ethanol-based sterilization on dECM hydrogels, it may give rise produce significant changes in mechanical properties. Obtaining image stacks using epifluorescence microscopy we were able to confirm that the cells adhered to the hydrogel cryosections without exhibiting desiccated areas or a cell gradient (Figure 2) with high viability of the cells after 72 hours in culture.

Conclusions

The application of this new hydrogel cryosectioning method allows for easy availability and reduction of sample preparation time as well as increasing the yield of the initial sample volume and facilitating their application to multiple techniques and studies.

P13**SUPER-RESOLUTION LASER SCANNING MICROSCOPY WITH PHOTO-SWITCHABLE FLUOROPHORES**

✉ nicktoledogarcia@ub.edu

N. Toledo-García^{1,*}, L. Cambor¹, E. Martín-Badosa^{1,2}, M. Montes-Usategui^{1,2}, J. Tiana-Alsina^{1,2}¹Departament de Física Aplicada, Facultat de Física, Universitat de Barcelona, Martí i Franques 1, 08028 Barcelona, Spain²Institut de Nanociència i Nanotecnologia (IN²UB), 08028, Barcelona, Spain

Advanced optical microscopy technologies are present in a multitude of applications within the field of life sciences being fluorescence microscopy an essential tool for the study of biological processes that occur at the cellular and molecular levels. However, optical microscopy presents limitations in terms of spatial resolution. Owing to the phenomenon of diffraction, structures below the subcellular scale (200 nm) cannot be observed. The development of super-resolution microscopy in the early 21st century managed to overcome the diffraction barrier using only optical means. The early proposals of super-resolution microscopy such as STED [1] or PALM-STORM [2,3], despite demonstrating resolutions in the order of nanometres, are poorly suited for use in live cells. While STED microscopes use high-power pulsed lasers that are harmful to live samples, PALM-STORM microscopes are very slow and therefore incompatible with observations of cellular dynamics in real time. To address these limitations, it is necessary to develop super-resolution technologies compatible with the observation of live cells in real time. In the last 5 years, RESOLFT [4] microscopy has been proposed, being a derivative of STED microscopy, which uses photoactivatable fluorophores and doughnut-shaped illumination beams, allowing the acquisition of super-resolution images (70 nm) with low light intensities. Therefore, RESOLFT

is a promising candidate for obtaining high-resolution images of live cells since the illumination requirements minimize cellular damage. However, image reconstruction from a point-by-point scan of the sample does not allow for obtaining images at video speed. Despite proposals to illuminate the sample with a multi-beam configuration, these present implementation problems due to the complexity of the optical system, and there is still no commercially viable device.

We propose the use of acousto-optic holography techniques to generate large arbitrary arrays of switchable Gaussian and doughnut-shaped beams. We exploit acousto-optic deflectors (AODs) as general spatial light modulators through the computation of driving RF signals obtained with digital holography techniques [5]. This approach enables rapid scanning of the illuminating array without the need of any mechanical moving element, as the illuminating array can be directed rapidly (up to a 150 kHz) by tailored holograms. Importantly, both Gaussian and Laguerre-Gaussian (doughnut-shaped) beams exhibit minimal distortion after crossing AODs, evidencing the promising potential of acousto-optic holography technology to develop live cell super-resolution imaging [6]. To ensure rapid beam switching we suggest employing a multiple path setup that merges all beams, selecting the desired path by triggering different lasers (one for each path) or by polarization means.

In this work we implement in a microscope setup the parallelization of Gaussian and Laguerre-Gaussian beams using acousto-optic holography techniques and beam switching via laser triggering, evaluating and characterizing the quality of the illuminating beams with different architectures of the setup to ensure the best speed and resolution improvement.

References

- [1] S.W. Hell, and M. Kroug, *Applied Physics B* 60, 495 (1995).
- [2] E. Betzig, G. H. Patterson, R. Sougrat, OW Lindwasser, S. Olenych, J. S. Bonifacino, M. W. Davidson, J. Lippincott-Schwartz, and H. F. Hess, *Science* 313, 1642–1645 (2006).
- [3] M. Rust, M. Bates and X. Zhuang, *Nat Methods* 3, 793–796 (2006).
- [4] M. Hofmann, C. Eggeling, S. Jakobs, and S.W. Hell, *PNAS* 102, 17565 (2005).
- [5] M. Montes-Usategui, R. Bola, E. Martín-Badosa, D. Treptow, PCT/EP2019/067517 (2019).
- [6] F. Klingmann, N. Toledo-García, E. Martín-Badosa, M. Montes-Usategui, and J. Tiana-Alsina, Submitted to *JEOS* (2024).

P14**MICROFLUIDIC DEVICE FOR THE STUDY OF ANGIOGENESIS IN CONTROLLED 3D MICROENVIRONMENTS**

✉ adria.noguera@ub.edu

A. Noguera-Monteagudo¹, A. Vilche¹, B. Van Durme³, Y. Dong³, E. Xuriguera¹, R. Rodríguez^{1,2}, S. Van Vlierberghe³, E. Engel², O. Castaño^{1,2}¹ University of Barcelona, 08028, Barcelona, Spain² Institute for Bioengineering of Catalonia, Spain³ Ghent University, Ghent, Belgium

Angiogenesis is the process through which new blood vessels form from pre-existing ones. It holds significant importance as it is implicated in the revascularization of implants, tissue engineering applications, cancer growth, and various diseases [1]. Recent advancements in microfluidics have facilitated the creation of highly representative and controlled microenvironments, enabling the generation of in vitro models of angiogenesis for the study of its mechanisms [2-3]. Additionally, the utilization of the two-photon polymerization technique allows for the printing of 3D hydrogels with desired structures within these microfluidic devices on a micrometer scale [4]. This enables the study of 3D in vitro models with a more controlled microenvironment, thus facilitating the investigation of the effects of different geometries on angiogenesis and blood vessel formation.

Material and Methods

In this study, an angiogenesis-based platform designed in AutoCAD is employed. This platform comprises a central chamber (1300 µm wide, 8800 µm long, 150 µm high) connected to two lateral channels (750 µm wide, 150 µm high), each terminating with deposits (radius 2 mm). Microfluidic devices are fabricated from PDMS using a master mold produced with SU8-350 photoresist (MicroChem) via standard photolithography techniques. Scaffolds composed of gelatin-based ink (HYDROTECH INX U100, Biolnx, Ghent, Belgium)

are processed via two-photon polymerization (2PP) at λ=800 nm and 80 mW using a NanoOne Bio printer (UpNano, Vienna, Austria). These scaffolds, previously designed in Fusion 360 (Autodesk, CA, US) and saved as STL files, are loaded into the device.

Results

By combining microfluidics with the utilization of 2PP, we can print scaffolds composed of gelatin-based ink within the microfluidic device. These scaffolds feature channels of 75 and 100 µm in desired heights and directions, thereby enabling the development of a microfluidic device with precise control over the microenvironment and 3D structuring. This advancement facilitates the study of angiogenesis with enhanced precision and fidelity.

Discussion

In conclusion, microfluidic technology holds the promise of transforming our comprehension of angiogenesis through the provision of a meticulously controlled platform for mechanistic studies. Moreover, the capability to fabricate engineered 3D structures within microfluidic devices via two-photon polymerization opens a multitude of opportunities.

Acknowledgment

We gratefully acknowledge the financial support from the Spanish Ministry of Science and Innovation (MICINN) and the Spanish State Research Agency (AEI) through grants RTI2018-097038-B-C22, PID2021-124575OB-I00 and PDC2022-133918-C22, and the the financial support from the European Union's Horizon Europe research & innovation program (EIC-2021-PATHFINDER-OPEN-01-01-101047099 4DBR). Finally, we also appreciate the support of Research Foundation Flanders (FWO) (1SH3W24N).

References

- [1] A.M.A.O. Pollet and J.M.J. den Toonder, "Recapitulating the vasculature using Organ-on-Chip technology," *Bioengineering*, (2020).
- [2] E. Akbari, G. B. Szychalski, and J. W. Song, "Microfluidic approaches to the study of angiogenesis and the microcirculation," *Microcirculation*, vol. 24, no. 5, pp. 1–8, (2017).
- [3] K. Haase and D. Roger, "Advances in on-chip vascularization," (2017). [4] S. O'Halloran, A. Pandit, A. Heise, A. Kellett, *Two-Photon Polymerization: Fundamentals, Materials, and Chemical Modification Strategies*. *Adv. Sci.* 2022, 2204072.

P15

ON THE TOTAL FIELD CHARACTERIZATION OF HIGHLY FOCUSED BEAMS IN THE FAR FIELD

✉ dmaluenda@ub.edu

D. Maluenda^{1,2}, M. Aviñoá¹, R. Martínez-Herrero³, A. Carnicer¹

¹ Universitat de Barcelona (UB), Departament de Física Aplicada, 08028 Barcelona, Spain

² Institute of Nanoscience and Nanotechnology (IN²UB), Universitat de Barcelona, Spain

³ Departamento de Óptica, Facultad de Ciencias Físicas, Universidad Complutense de Madrid, Spain

The potential of cylindrical vector fields has been demonstrated in many areas, such as optical microscopy, which produces images with sub-lambda resolutions. The management and control of the 3D polarization distribution of the highly focused fields play as relevant a role as the intensity distribution in the focal zone. Likewise, the interaction between light and matter at the nanoscopic level can modify the local distribution of polarization. Therefore, having good measurement and characterization techniques for highly focused vector beams is an essential task. Accurately detecting the three complex components of the electric field remains a challenging task.

Several measurement techniques have been reported directly in the focal zone. These techniques, apart from being invasive, often require specialized equipment that provides poor signal-to-noise ratio [1-3]. An alternative can be found by indirectly inducing the longitudinal component from regular polarimetric measurements in the far field. To achieve this, it is necessary not only to record the amplitude of the transverse field, but also to computationally retrieve the phase. Finally, the longitudinal component in the focal area can be estimated using the Gauss law [4]. Interestingly, after determining the longitudinal component, a complete characterization of the 3D state of polarization can be carried out by using a generalized definition of the Stokes parameters [5].

References

- [1] Novotny, L., Beversluis, M., Youngworth, K. and Brown, T. "Longitudinal field modes probed by single molecules." *Phys. Rev. Lett.* 86, 5251 (2001).
- [2] Wang, J., Wang, Q. and Zhang, M. "Development and prospect of near-field optical measurements and characterizations." *Front. Optoelectron.* 5, 171-181 (2012).
- [3] Alferov, S., Khonina, S. and Karpeev, S. "Study of polarization properties of fiber-optics probes with use of a binary phase plate." *JOSA A* 31, 802-807 (2014).
- [4] Maluenda, D., Aviñoá, M., Ahmadi, K., Martínez-Herrero, R. and Carnicer, A., "Experimental estimation of the longitudinal component of a highly focused electromagnetic field." *Sci Rep* 11, 17992 (2021).
- [5] R. Martínez-Herrero, D. Maluenda, M. Aviñoá, A. Carnicer, I. Juvells, and Á. S. Sanz, "Local characterization of the polarization state of 3D electromagnetic fields: an alternative approach," *Photon. Res.* 11, 1326-1338 (2023).

NanoEnergy

P16

FABRICATION OF AN AUCUIN ALLOY BY APPLYING PULSED CURRENT WITHOUT ADDITIVES FOR DECORATIVE PURPOSES

✉ m.amazian@ub.edu

M. Amazian^{1,2}, J. Boter¹, M. Sarret¹, T. Andreu¹

¹ Sustainable Electrochemical Processes, department of Materials Science and Physical Chemistry and Institute of Nanoscience and Nanotechnology (IN²UB), Faculty of Chemistry, University of Barcelona. Martí i Franquès, 1, 08028-Barcelona, Spain.

² Plating Decor Recubrimientos, S.L. Industria, El Pla, 16, 08980-Sant Feliu de Llobregat, Spain.

Gold coatings are widely used for decorative purposes and are generally based on 18 Karat (kts) AuCuIn alloys. [1] These coatings are manufactured by electro-deposition using direct current (DC) and an electrolyte with additives. The control they have over the deposition mechanism to obtain alloys with the desired physical and mechanical properties is of interest; however, their use compromises the lifespan of the electrolyte and is environmentally unsustainable. As a substitute, the use of pulsed current (PC) is proposed to obtain coatings in a controlled manner.[2] Nevertheless, no work has been reported on the electrodeposition of AuCuIn alloys using this technique, probably due to the complexity of the technique owing to its large number of variables. In this study, we have reported on the behavior of AuCuIn alloys electrodeposited using both DC and PC, analyzing the coatings from compositional, structural, and morphological perspectives.

Materials and Methods

A 100 mL aqueous electrolytic bath was prepared by dissolving CuCN (1.40 g), KCN (2.65 g), and K[Au(CN)₂] (0.76 g) in the solution and heating it to 70 °C. Thereafter, D-glucose (0.045 g) and In₂(SO₄)₃ (0.4 g) were added to the bath. Both DC and PC electrodeposition were carried out using the same working parameters, along with duty cycle (θ) and frequency (ν) parameters in the case of PC, to fabricate the alloys. The crystal structures were analyzed by XRD. The surface morphology of the alloys was processed and analyzed using SEM coupled with an EDX detector for alloy

composition analysis and confocal microscope equipment for surface rugosity determination.

Results and Discussion

By applying DC at different current densities (j), a constant composition of 75% by mass of gold was obtained in the range of 3 - 5 A·dm⁻², following regular deposition. [3] By applying the PC parameters and examining the recovery times (t_{OFF}) of the diffusion layer, the deposition of noble metal ions increased with the reestablishment of the species on the cathode surface. Consequently, the θ and ν were investigated. The highest concentration of Au alloy was achieved at lower θ values, reaching 81%. As θ increased and the j_{ON} decreased, the percentage of Au slightly decreased to 75%. Furthermore, increasing ν also led to a 4% increase in gold content.

According to the XRD analysis, the PC coatings exhibited both the expected AuCuIn alloy phase, and a pure gold phase probably deposited onto the substrate during the t_{OFF} period, explaining the observed increase in the gold content at $\theta < 50\%$. Additionally, the crystallite size of the coating was smaller than that of the DC coatings, in agreement with the application of $j_{ON} > j_A$, and is expected to result in an increase in the hardness of the coating. Morphologically, as depicted in Fig. 1, an increase in both θ and ν (and consequently, a decrease in t_{OFF}) leads to a reduction in the size of the agglomerates, favoring non-agglomerative growth with a smaller size. These findings were corroborated by the Root Mean Square (RMS) surface roughness comparing 190±31 nm in the DC coating (Fig. 1A) and 118±33 nm of the PC coating (Fig. 1B) with θ of 90% and ν of 100 Hz.

Acknowledgments

With the support of the Industrial Doctorate Plan from the SUR of the Government of Catalonia (2021DI20) and the Spanish project PID2019-108136RB-C33 MCIN/AEI/10.13039/501100011033).

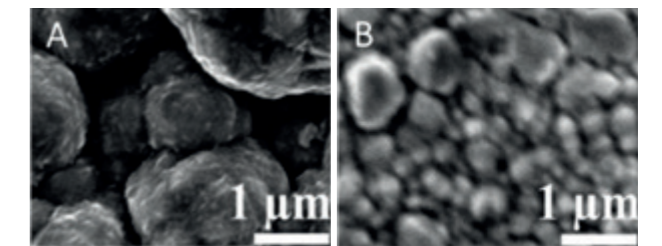


Figure 1. SEM images of AuCuIn DC coating (A) and PC coating (B). j_A was set to 3.5 A·dm⁻² in both cases.

References

- [1] W. Giurlani et al., *Coatings* 2018, Vol. 8, no. 8, pp. 260, Jul. 2018.
- [2] M. S. Chandrasekar and M. Pushpavanam, *Electrochim. Acta*, vol. 53, no. 8, pp. 3313-3322, Mar. 2008.
- [3] I. K. Hong, J. W. Park, and S. B. Lee, *J. Ind. Eng. Chem.*, vol. 20, no. 5, pp. 3068-3074, Sep. 2014.

NanoMagnetism

P17

UNVEILING THE 3D MAGNETIC VORTEX TEXTURE OF IRON OXIDE NANOFLOWERS

✉ carlosmoyaalvarez@ub.edu

C. Moya^{1,2}, M. Escoda-Torroella^{1,2}, J. Rodríguez-Álvarez^{1,2}, A. Figueroa^{1,2}, Í. García¹, I. Batalla Ferrer-Vidal¹, A. Gallo-Cordova³, M. Puerto Morales³, L. Aballe⁴, A. Fraile Rodríguez^{1,2}, A. Labarta^{1,2}, X. Batlle^{1,2}

¹ Departament de Física de la Matèria Condensada, Universitat de Barcelona, Martí i Franquès 1, 08028 Barcelona, Spain

² Institut de Nanociència i Nanotecnologia (IN²UB), Universitat de Barcelona, 08028 Barcelona, Spain

³ Department of Nanoscience and Nanotechnology, Instituto de Ciencia de Materiales de Madrid (ICMM-CSIC), Sor Juana Inés de la Cruz 3, 28049 Madrid, Spain

⁴ ALBA Synchrotron Light Facility, CELLS, 08290 Barcelona, Spain

Magnetic iron oxide Nanoflowers (IONF) have been drawing much attention because of their superior magnetic performance compared to single-core magnetic nanoparticles.[1] Despite the large sizes of IONF, these aggregates show almost zero remanences and nearly vanishing coercivities, while preserving high saturation magnetization. This seemingly effective superparamagnetic behavior has motivated their use in biomedical and environmental applications since the net magnetization can be controlled at will by an external magnetic field so that the particle agglomeration is effectively reduced. Some authors have attributed this phenomenology to the existence of some exchange coupling among the cores, leading to a superferromagnetic state of the whole aggregate. However, the effect of the crystal texture on the nearly demagnetized remnant state of these systems is still unclear. This study reports on how the local magnetic texture, originating from crystalline correlations among the cores, governs the unique magnetic properties of individual IONF in sizes ranging from 40 to 400 nm.[2] Despite size variations, all samples exhibit consistent crystalline correlations extending beyond the IONF cores. A nearly zero remnant magnetization, a persistently blocked state, and temperature-independent

magnetization support the existence of a 3D magnetic texture throughout IONF. Magnetic transmission X-ray microscopy confirms nearly demagnetized states caused by magnetic texture vorticity. Moreover, micromagnetic simulations show vortex-like spin configurations with partial topological protection, stabilized by inter-core exchange coupling and demagnetizing fields at low magnetic fields (see Fig. 1). Overall, this study provides valuable insights into the impact of crystalline texture on the magnetic properties of IONF over a wide size range.

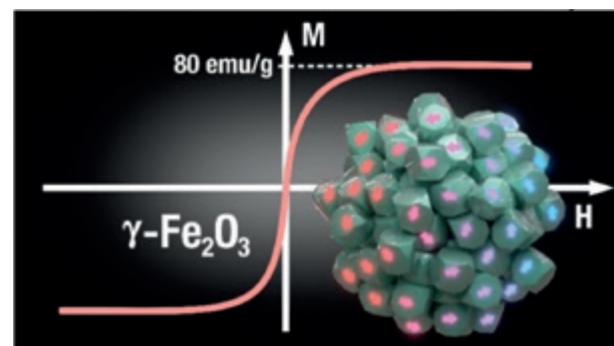


Figure 1. The hysteresis loop shows the effective superparamagnetic behaviour in IONF caused by the near demagnetized state driven by the high vorticity of the core moment texture at low magnetic fields as shown in the inset.

References

- [1] Batlle, X. *et al.* *JMMM*, **543**, (2022), 168594.
[2] Moya, C. *et al.* *Nanoscale*, **16**, (2024), 1942.

P18

A SUPRAMOLECULAR HELICATE WITH TWO INDEPENDENT FE(II) SWITCHABLE CENTRES AND A [Fe(ANILATE)₃]³⁺ GUEST

✉ leoni.barrios@ub.edu

L. A. Barrios^{1,2}, S. J. Teat³, O. Roubeau⁴, G. Aromí^{1,2}

¹ University of Barcelona, Inorganic and Organic Chemistry Department, Barcelona, Spain

² Institute of Nanoscience and Nanotechnology, University of Barcelona, Barcelona, Spain

³ Advanced Light Source, Berkeley Laboratory, 1 Cyclotron Road, Berkeley, California 94720, USA

⁴ Instituto de Nanomateriales de Aragón (INMA), CSIC-Universidad de Zaragoza Zaragoza, Spain

The ability to encapsulate coordination complexes with an octahedral MO6 coordination geometry and extended ligands opens a wide range of possibilities to study the synergy of different properties within such type of supramolecular assemblies, including single ion slow relaxation of the magnetization, quantum coherence, photoluminescence or electron transfer. It also opens an avenue to explore potential metal organic frameworks of host/guest systems, where the guests would act also as connecting nodes.

A biphenyl-spaced bis-pyrazolylpyridine ligand interacts with ferrous ions to engender a dimetallic helical coordination cage that encapsulates an Fe³⁺ tris-anilate complex. The host-guest interaction breaks the symmetry of the Fe²⁺ centers causing a differential spin crossover behavior in them that can be followed in great detail crystallographically.

The presence of [Fe(anilate)₃]³⁺ in a solution of Fe(BF₄)₂ and L2 (Fig. 1) in dry methanol under inert atmosphere, generates crystals after two weeks, of the host-guest supramolecular assembly Fe₂(L₂)₃(BF₄) (1).

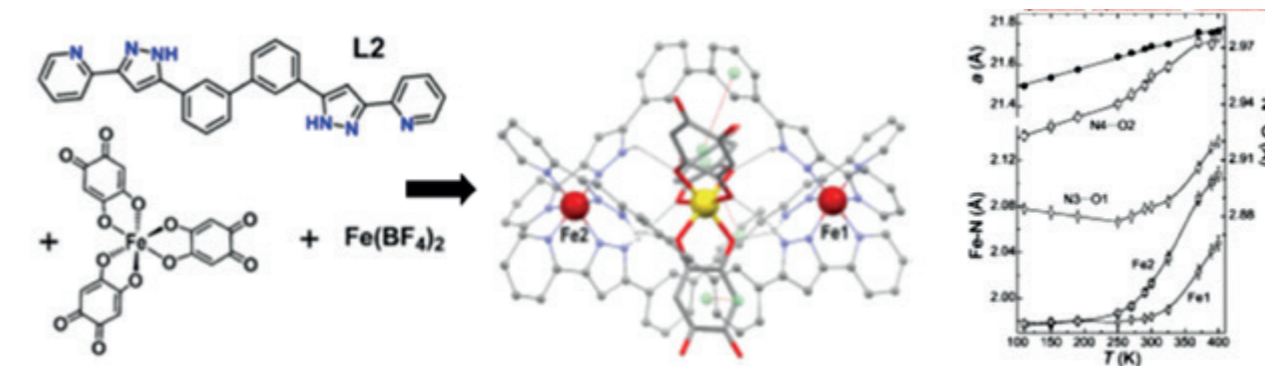


Figure 1. Reaction scheme to produce 1 and the ligand L2 (left). Thermal evolution of the cell parameter *a* (black circles), average Fe-N bond distances (grey symbols) and N...O separations of the pyrazole-anilate hydrogen bonds (empty symbols) of desolvated 1 (right).

References

- [1] Barrios, L. A., *et al.* *Chem. Commun.*, 2023, 59, 10628.
[2] Capó, N., *et al.* *Chem. Commun.*, 2022, 58, 10969.

P19

DESIGN OF H-BONDED SUPRAMOLECULAR Fe(II) SWITCHABLE MATERIALS

✉ david.aguila@ub.edu

D. Aguilà^{1,2}, R. Díaz-Torres^{1,2}, H. H. Nielsen^{1,3},
P. Vilariño¹, G. Rodríguez¹, F. Trepard¹, O. Roubeau⁴,
G. Aromí^{1,2}

¹ Departament de Química Inorgànica i Orgànica,
Universitat de Barcelona, Spain

² Institute of Nanoscience and Nanotechnology,
University of Barcelona (IN²UB), Spain

³ Department of Chemistry, Aarhus University,
Denmark

⁴ Instituto de Nanociencia y Materiales de Aragón
(INMA), CSIC and Universidad de Zaragoza, Spain

Spin-Crossover (SCO) compounds are fascinating magnetic switchable materials with great potential for the development of novel technological devices. Remarkably, their physical properties can be tuned by modifying the weak non-covalent interactions exhibited in between their molecular units. Among them, hydrogen bonds are arguably the most exploited ones for generating those supramolecular motifs. In order to explore the potential of H-bonded SCO materials, we have designed ligands that combine a pyrazolyl-pyridyl chelating unit together with additional H-donor and/or acceptor groups.[1,2] The derived Fe(II) SCO compounds have been exploited to produce novel supramolecular morphologies by encapsulation of ionic species (Figure) or insertion of organic functional co-ligands. The novel magnetic properties of the generated materials have been explored, evidencing the potential of this methodology to produce new supramolecular switchable materials.

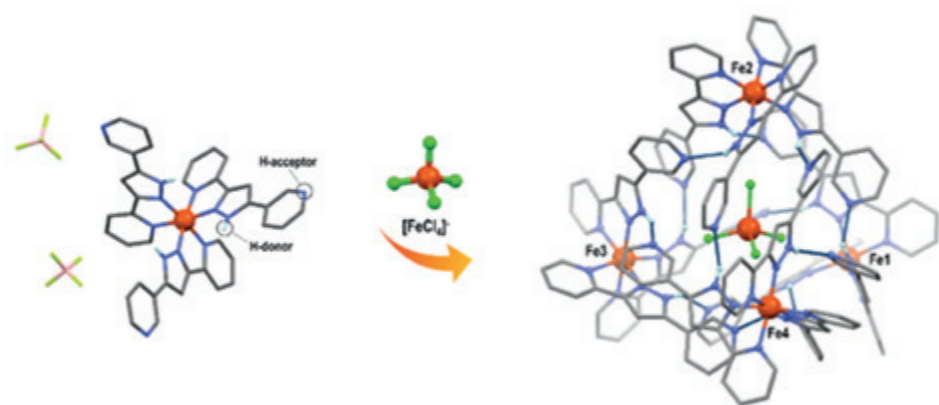


Figure 1. Fe(II) SCO compound featuring H-bonding acceptor and donor groups able to generate a purely supramolecular SCO tetrahedron by encapsulation of $[FeCl_4]^{2-}$.

References

- [1] G. A. Craig, O. Roubeau, G. Aromí. *Coord. Chem. Rev.* **2014**, 269, 13.
[2] M. D. Darawsheh, L. A. Barrios, O. Roubeau, S. J. Teat, G. Aromí. *Chem. Commun.* **2017**, 53, 596.

P20

EXPLORING SIZE-DEPENDENT MAGNETIC PROPERTIES OF NON-STOICHIOMETRIC Ni_{1-δ}O NANOPARTICLES

✉ jaraesca7@alumnes.ub.edu

J. Ara^{1,2*}, C. Moya^{1,2}, M. Xiulan Aribó¹,
A. I. Figueroa^{1,2}, M. García del Muro^{1,2}, A. Fraile
Rodríguez^{1,2}, A. Labarta^{1,2}, X. Batlle^{1,2}

¹ Departament de Física de la Matèria Condensada,
Universitat de Barcelona, Martí i Franquès 1, 08028
Barcelona, Spain

² Institut de Nanociència i Nanotecnologia (IN²UB),
Universitat de Barcelona, 08028 Barcelona, Spain

Non-stoichiometric nickel oxide Ni_{1-δ}O nanoparticles (NP) have been drawing much attention due to their distinctive magnetic properties and p-type semiconductor behavior, which are leveraged in electronics, catalysis, and antimicrobial applications [1],[2]. From a fundamental perspective, the cause of the weakly ferrimagnetism in these systems is still not fully understood [3],[4]. This work sheds some light on this phenomenology by studying the influence of crystal size and Ni composition on the magnetic properties of three samples of Ni_{1-δ}O NPs with sizes of 6, 20, and 30 nm prepared by two-step chemical approaches. Structural analysis confirms the high crystalline quality of the particles, regardless of the particle size. Besides, single particle XAS-PEEM measurements show uniform composition of each sample, revealing the existence of some Ni vacancies caused by the synthesis method. Magnetic properties are size-dependent, including weak superparamagnetism of the smallest NP, while the largest ones show features closer to the bulk counterparts, such as low values of both remnant magnetization and coercivity, with negligible shifts of

the hysteresis loop and minimal coercivity after field cooling (see Figure 1). These size-dependent behavior is due to surface and structural modifications, particularly in the smallest NP. In addition, X-ray magnetic linear dichroism (XMLD) imaging and spectroscopy performed on single 30 nm-Ni_{1-δ}O NPs provided further insights into the antiferromagnetic spin arrangement in these nanostructures. These findings contribute to improve our understanding of size-related phenomena in nanoscale antiferromagnetic materials.

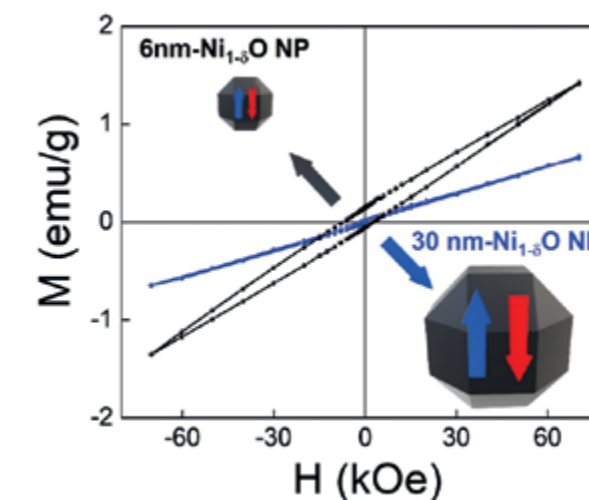


Figure 1. Comparison between hysteresis loops at 5K for Ni_{1-δ}O NP with mean sizes of 6 (gray dots) and 30 nm (blue dots) with a maximum field of H= 70 kOe.

References

- [1] Danjumma, S. et.al. Nickel Oxide (NiO) Devices and Applications: A Review. *International Journal of Engineering Research and 2019*, V8 (04).
[2] Delgado, D., et.al. Support Effects on NiO-Based Catalysts for the Oxidative Dehydrogenation (ODH) of Ethane. *Catal Today* 2019, 333, 10–16.
[3] Kodama, R. H., et.al. Finite Size Effects in Antiferromagnetic NiO Nanoparticles. *Phys. Rev. Lett.* 1997, 79 (7), 1393–1396.
[4] Jafari, A. et. al. Evolution of Structural and Magnetic Properties of Nickel Oxide Nanoparticles: Influence of Annealing Ambient and Temperature. *J. Magn. Magn. Mater.* 2019, 469, 383–390.

P21

ENERGY TRANSFER DYNAMICS IN HETEROMETALLIC [LnLn'Ln] TRINUCLEAR COMPOUNDS

✉ dmaniaki@ub.edu

D. Maniaki,^{1,2} A. Sickinger,³ L. A. Barrios,^{1,2}
D. Aguilà,^{1,2} O. Roubeau,⁴ Y. Guyot,⁵ F. Riobé,³
O. Maury,³ L. Abad Galán,⁶ G. Aromí^{1,2}

¹ Departament de Química Inorgànica i Orgànica, Universitat de Barcelona, Barcelona, Spain.

² Institute of Nanoscience and Nanotechnology of the University of Barcelona (IN²UB), Barcelona, Spain.

³ Université de Lyon, ENS Lyon, CNRS, Laboratoire de Chimie, Lyon, France.

⁴ Instituto de Nanociencia y Materiales de Aragón (INMA), CSIC and Universidad de Zaragoza, Zaragoza, Spain.

⁵ Univ. Lyon, Institut Lumière Matière, CNRS–Université Claude Bernard, Lyon, France.

⁶ Departamento de Química Inorgánica, Universidad Complutense de Madrid, Madrid, Spain.

Efficiently accessing site-selective heteronuclear lanthanide molecules is a significant development into the exploration of unique photophysical phenomena based on Ln-to-Ln' energy transfer (ET). This ET process enables interesting conversion of light energy (up-/down-conversion), making it promising for various applications such as solar energy harvesting, telecommunications, or light-emitting devices. However, addressing this challenge requires effective strategies to incorporate different Ln metal ions within distinct positions of a molecule. Our research group has discovered a coordination scaffold hosting three Ln(III) ions, providing access to a unique family of trinuclear heterometallic complexes with formula [LnLn'Ln(LA)₂(LB)₂(py)(H₂O)₂](NO₃) (Figure 1a). These complexes selectively position the metal ions in a specific [LnLn'Ln] arrangement.^[1,2] Two of our complexes, [YbNdYb] and [ErNdEr], have been investigated through photophysical measurements to assess the ET between the metal centers. While complex [YbNdYb] shows ET from Nd³⁺ to the two Yb³⁺ centers (Figure 1b),^[3] [ErNdEr] exhibits two different types of ET (ET1 from the Nd³⁺ to the Er³⁺, and a second ET2 from the Er³⁺ to the Nd³⁺ center, Figure 1c), evidencing the potential of these molecular platforms to explore Ln-to-Ln' ET.

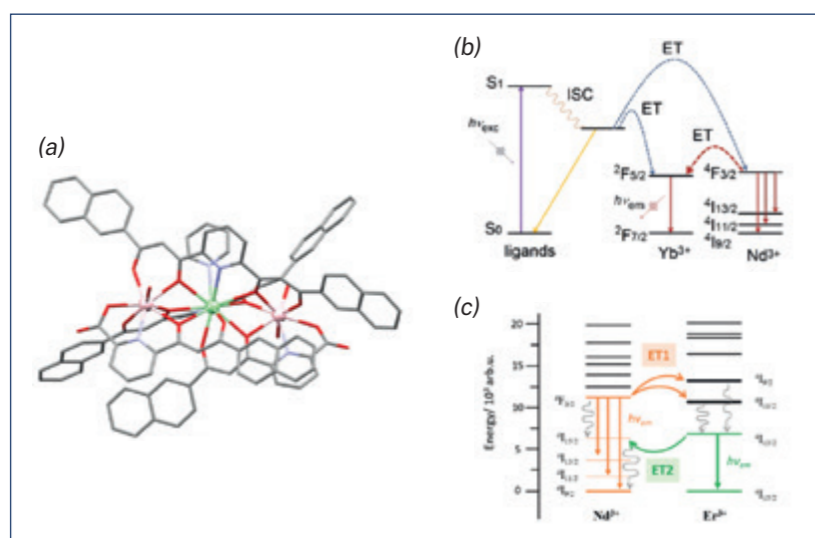


Figure 1. (a) Molecular structure of [LnLn'Ln] complex cation, (b) Energy diagram levels of Nd³⁺ and Yb³⁺ in [YbNdYb], (c) Energy diagram levels of Nd³⁺ and Er³⁺ in [ErNdEr].

References

- [1] V. Velasco et al. *Chem. Eur. J.* **2019**, 25, 15228
[2] E. Macaluso et al. *Chem. Sci.* **2020**, 11, 10337.
[3] D. Maniaki et al. *Inorg. Chem.* **2023**, 62, 3106.

P22

SLOW MAGNETIC RELAXATION AND LUMINESCENCE PROPERTIES IN β-DIKETONATE LANTHANIDE(III) COMPLEXES. PREPARATION OF Eu(III) AND Yb(III) OLED DEVICES

✉ anniatubau@ub.edu

À. Tubau¹, L. Rodríguez¹, P. Pander^{2,3,4}, L. Weatherill⁴,
F. B. Dias⁴, M. Font-Bardía⁵, R. Vicente¹

¹ Departament de Química Inorgànica i Orgànica, Universitat de Barcelona, Martí i Franquès 1-11, E-31321 Barcelona, Spain.

² Faculty of Chemistry, Silesian University of Technology, Strzody 9, 44-100 Gliwice, Poland.

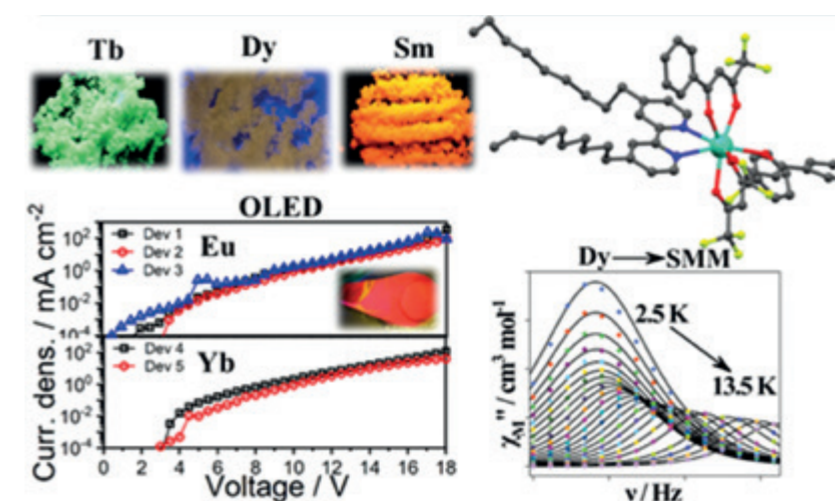
³ Centre for Organic and Nanohybrid Electronics, Silesian University of Technology, Konarskiego 22B, 44-100 Gliwice, Poland.

⁴ Durham University, Physics Department, South Road, Durham, DH1 3LE, UK.

⁵ Departament de Mineralogia, Cristal·lografia i Dipòsits Minerals and Unitat de Difracció de R-X. Centre Científic i Tecnològic de la Universitat de Barcelona (CCiTUB). Universitat de Barcelona. Solé i Sabarís 1-3. 08028 Barcelona, Spain.

The reaction of [Ln(btfa)₃(H₂O)₂] (btfa = 4,4,4-trifluoro-1-phenyl-1,3-butanedionate) with 4,4'-dinonyl-2,2'-bipyridyl (4,4'-dinonylbipy) in ethanol allows isolation of mononuclear complexes [Ln(btfa)₃(4,4'-dinonylbipy)] Ln = Sm (**1-Sm**), Eu (**2-Eu**), Tb (**3-Tb**), Dy (**4-Dy**), Er (**5-Er**) and Yb (**6-Yb**). The solid state luminescence emission in the visible region for

1-Sm, **2-Eu**, **3-Tb** and **4-Dy** and in the NIR region for **1-Sm**, **5-Er** and **6-Yb** shows efficient energy transfer from the 4,4,4-trifluoro-1-phenyl-1,3-butanedionate ligands to the central Ln³⁺ ion for all the compounds. Finally, complexes **2-Eu** and **6-Yb** were successfully used as emitters in multilayer vacuum-deposited OLEDs. The electroluminescence quantum efficiency (EQE) of the corresponding devices reached 2.1% and ~0.1-0.2% for **2-Eu** (λ_{EL} = 614 nm) and **6-Yb** (λ_{EL} = 977 nm), respectively. Maximum radiant emittance recorded for the Ln-associated emission achieved 135 μW cm⁻² for **2-Eu** and 121 μW cm⁻² for **6-Yb**. These values for efficiency and radiant emittance are unusually high for such type of emitters. Moreover, magnetic studies were performed on all compounds. Alternating current (AC) dynamic measurements indicated Single Molecular Magnet (SMM) behaviour for **4-Dy** and field-induced slow relaxation of the magnetization for complexes **3-Tb**, **5-Er** and **6-Yb**. The anisotropy energy barriers and pre-exponential factors are 91.1 cm⁻¹, τ₀ = 7.2 × 10⁻⁹ s (under zero magnetic field) and ΔE = 109.3 cm⁻¹, τ₀ = 9.3 × 10⁻¹⁰ s under 0.1 T magnetic field for **4-Dy** and ΔE = 24.6 cm⁻¹, τ₀ = 8.7 × 10⁻⁸ s (under 0.07 T) for **5-Er**. Besides, we observe that for compounds **3-Tb** and **6-Yb** the relaxation of the magnetization does not occur through the Orbach process.



P23 STRONG SPIN-PHOTON COUPLING IN VAN DER WAALS MAGNETS

✉ pabloces64@gmail.com

**P. Cerrato-Serrano¹, M. I. Sturza², M. Rovirola^{1,3},
F. Macià^{1,3}, A. García-Santiago^{1,3}, H. Kohlmann²,
J. M. Hernández^{1,3}, M. V. Costache^{1,3}**

¹ Departament de Física de la Matèria Condensada, Universitat de Barcelona

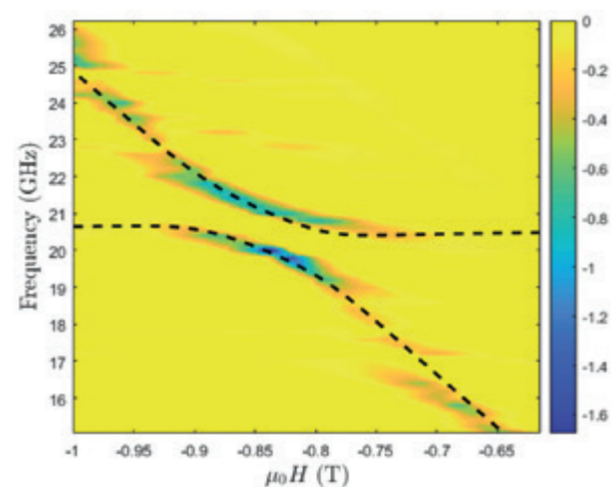
² Leipzig University, Faculty of Chemistry and Mineralogy. Institute of inorganic chemistry and crystallography

³ Institut de Nanociència i Nanotecnologia (IN²UB)

Strong coupling between electromagnetic (EM) field and magnetization is emerging as powerful tool for pursuing coherent information processing owing to their rich quantum engineering functionalities. One prototypical example in hybrid systems is cavity magnonics, which consist of a magnetic material and a 2D/3D microwave cavity [1,2].

Here we report strong EM field-magnetization coupling in Cr₂Ge₂Te₆ (CGT), a van der Waals magnet, and a nearly ideal 2D Heisenberg system, with highly correlated electronic and spin degrees of freedom [3]. The magnetocrystalline anisotropy energy required for long-range ferromagnetic order is generated by covalent bond between ligand Te-p and Cr-e_g orbitals. We experimentally demonstrate the coherent coupling between magnons (collective spin excitations in CGT) and microwaves photons. The microwave absorption spectrum of the cavity shows anti-crossing features at each intersection between the cavity mode and magnetic resonance (figure below). Coupling strength values up to 1 GHz are obtained indicating a strong magnon-photon coupling in this system.

Our work introduces van der Waals magnets to the field of strong EM field-solid state physics and offer prospects for design and control of collective quantum phenomena such as magnetic phase transitions via cavity quantum electrodynamics.



References

- [1] D. D. Awschalom *et al.*, IEEE Trans. Quantum Eng. 2, 5500836 (2021).
- [2] D. Lachance-Quirion *et al.*, App. Phys. Express 12, 070101 (2019).
- [3] C. Gong *et al.*, Nature, 546, 265–269 (2017).

P24 DEEP LEARNING FOR MAGNETIZATION DYNAMICS

✉ jbuchpal22@alumnes.ub.edu

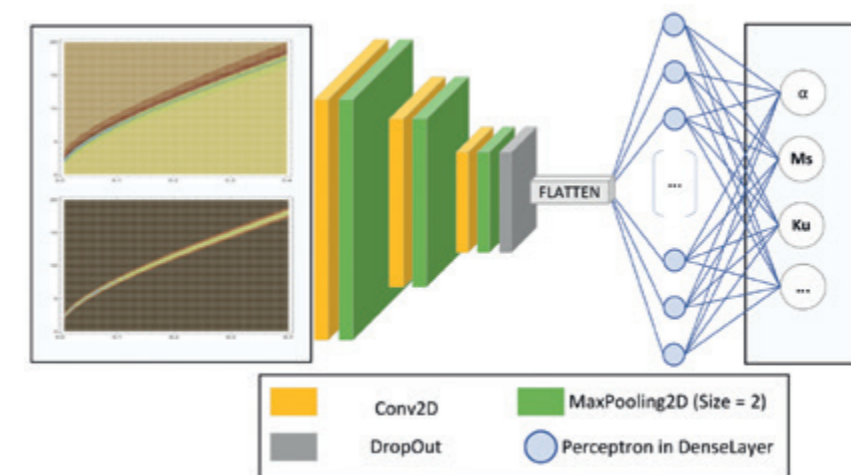
J. Buch-Palasi¹, J. M. Hernández^{1,2}, M. V. Costache^{1,2}

¹ Departament de Física de la Matèria Condensada, Universitat de Barcelona

² Institut de Nanociència i Nanotecnologia (IN²UB)

Building block of magnetic memories and sensors are magnetic thin films materials. In order to calculate the magnetization dynamics of thin magnetic film, the Landau-Lifshitz-Gilbert (LLG) equation is solved numerically. The typical way for solving LLG equations is to first discretize it in space by finite elements or finite differences and then to solve numerically the resulting system in time, and requires a considerable computational effort. To ease this process, by reducing the computational load or assisting in characterizing field measurements, machine learning can be of utility also in the field of magnetism [1-3].

In this work, a deep neural network is used to model the ferromagnetic resonance in magnetic thin films. The data for training the model was obtained by time integration of the LLG equation. To obtain an optimal compression ratio a convolutional autoencoder was used. Consequently, the magnetic dynamics to an external field can be computed quickly.



References

- [1] A. Kovacs *et al.*, J. Magn. Magn. Mater. 491, 165548 (2019).
- [2] S. Pollok *et al.*, “Magnetic Field Prediction Using Generative Adversarial Networks” (2022), arXiv:2203.07897.
- [3] S. Pollok, and R. Bjørk, Europhysics News (2022), DOI: <https://doi.org/10.1051/eprn/2022204>.

P25 ANTIFERROMAGNETIC RESONANCE IN CANTED ANTIFERROMAGNETS

✉ hilman12fikry@gmail.com

H. Fikry¹, J. M. Hernández^{1,2}, M. V. Costache^{1,2}

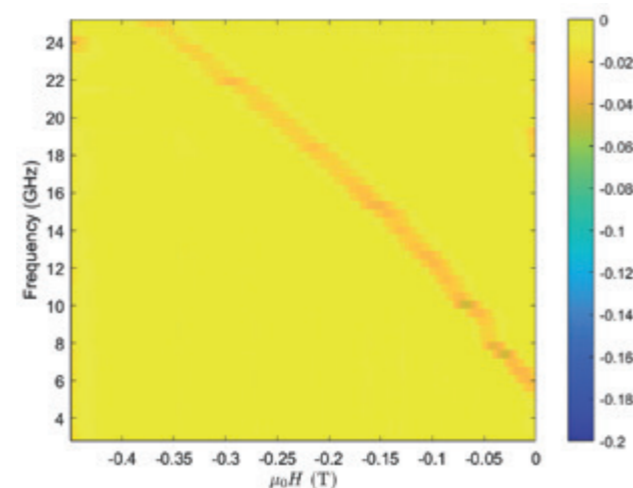
¹ Departament de Física de la Matèria Condensada, Universitat de Barcelona

² Institut de Nanociència i Nanotecnologia (IN2UB)

Existing spintronics devices are based on ferromagnetic materials. However, antiferromagnets have advantages over ferromagnets in that their resonant frequency is enhanced by the exchange coupling of the sublattices, extending into the terahertz regime [1,2].

We experimentally study temperature dependence of antiferromagnetic resonance in a bilayer of polycrystalline hematite/heavy metal (α -Fe₂O₃/Pt) as a model system. This investigation allows us to extract the temperature dependence of the Dzyaloshinskii-Moriya interaction field, exchange field, and damping. Accessing the temperature dependence of these parameters could provide new insights into the spin-relaxation and spin-dynamics processes in antiferromagnets. This understanding represents a step further towards terahertz devices based on antiferromagnetic materials, offering a platform for high-density memory and ultrafast data processing speeds [3].

Figure 1. The magnitude of S_{21} plotted against frequency and static magnetic field in the FMR experiment for the bilayer polycrystalline α -Fe₂O₃/Pt sample at room temperature.



References

- [1] R Lebrun, et al., Nature 561 (7722), 222-225 (2018).
- [2] I Boverter, et al., Physical review letters 126 (18), 187201 (2021).
- [3] V. Baltz, et al., Antiferromagnetic spintronics, Rev. Mod.Phys. 90, 015005 (2018).

P26 MODULATED SPIN DYNAMICS OF [Co₂] COORDINATION HELICATES VIA DIFFERENTIAL STRAND COMPOSITION

✉ ksotirakopoulos@ub.edu, leoni.barrios@ub.edu, aromi@ub.edu

K. A. Sotirakopoulos¹, L. A. Barrios¹, N. Capó¹, H. Boulehour³, D. Reta^{2,3,4}, I. Tejedor⁵, O. Roubeau⁵, G. Aromí¹

¹ Departament de Química Inorgànica i Orgànica and IN²UB, Universitat de Barcelona, Diagonal 645, 08028 Barcelona, Spain.

² Faculty of Chemistry, The University of the Basque Country UPV/EHU, Donostia, 20018, Spain.

³ Donostia International Physics Center (DIPC), Donostia, 20018, Spain.

⁴ IKERBASQUE, Basque Foundation for Science, Bilbao, 48013, Spain.

⁵ Instituto de Nanociencia y Materiales de Aragón (INMA), CSIC and Universidad de Zaragoza, Plaza San Francisco s/n, 50009 Zaragoza, Spain

perature without any cooperative effect, thus behaving as individual magnets. Through synthetic efforts that focused on producing molecules with large S ground state values and axial anisotropy parameters, D, it became clear that the anisotropy of single 3d and lanthanide ions was sufficient to yield large barriers to the magnetic relaxation. At the same time, the emerging prospect of using molecular spins as qubits for the coherent manipulation of quantum information opens new opportunities to explore the implementation of SMMs. These could be considered as potential hardware hosting the permanent memory used by spin-based molecular quantum processors [1].

Coordination supramolecular chemistry provides a versatile entry into materials with functionalities of technological relevance at the nanoscale. Here, we describe how two different bis-pyrazolpyridine ligands assemble with Co(II) ions into dinuclear triple-stranded helicates encapsulating different anionic guests. These constructs are described as (Cl@[Co₂(L1)₃]³⁺), (SiF₆@[Co₂(L1)(L2)₂]²⁺), and (ClO₄@[Co₂(L2)₃]³⁺) (Figure 1).

The discovery of Single-Molecule Magnets (SMMs) has been one of the most fascinating events in the area of molecular magnetism. SMMs are capable of preserving their magnetization below a certain tem-

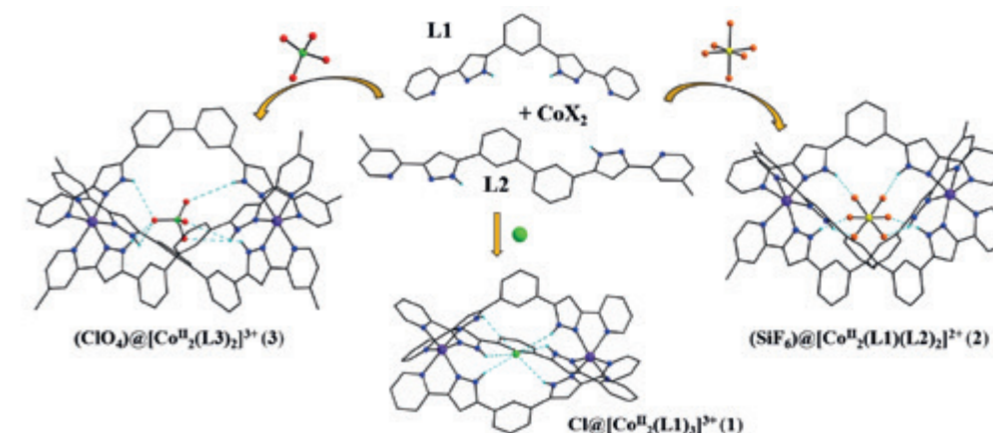


Figure 1. Schematic representation of the role of the anionic guest acting as a template that promotes the formation of the respective helicate.

References

- [1] Leoní A. Barrios, Nuria Capó, Hanae Boulehour, Daniel Reta, Inés Tejedor, Olivier Roubeau, Guillem Aromí, Dalton Trans., 2024, 53, 7611–7618.

P27 SPIN-CROSSOVER AND SUPRAMOLECULAR INTERACTIONS: MODULATING STRUCTURAL CHANGES

✉ rauldiaz@ub.edu

R. Díaz-Torres^{1,2}, O. Martínez¹, G. Aromí^{1,2}, D. Aguilà^{1,2}

¹ Departament de Química Inorgànica i Orgànica, Universitat de Barcelona, Spain

² Institute of Nanoscience and Nanotechnology, University of Barcelona (IN²UB), Spain

Structure and function are intimately associated and nowhere is this more true than in the field of spin crossover (SCO).[1] SCO complexes are versatile materials capable of switching between two electronic configurations: low spin (LS) and high spin (HS), triggered by various external stimuli such as temperature, light, and pressure. In this study, we explore the interplay between spin-crossover behavior and supramolecular interactions. Specifically, we investigate how these properties can be precisely tuned by manipulating weak non-covalent interactions among their molecular components. This is carried out through a crystallographic study of mononuclear Fe(II) complexes, wherein either the ligand or the anion bears H-donor and H-acceptor groups. Furthermore, we explore the impact of modifying the position of these groups within the ligand (ortho, meta, para) on the spin-crossover behavior (Figure)

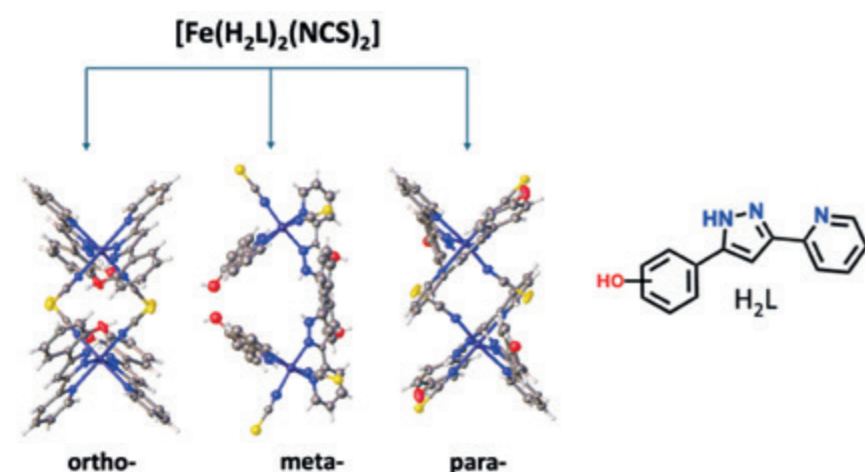


Figure 1. Cross-section view of the 1D chain for the ortho, meta, and para complexes.

References

[1] *Chem. Sci.*, **2022**, 13,3176–3186

P28 STRAIN ASSISTED MAGNETIC DOMAIN WALL MOTION

✉ marc.rovirola@ub.edu

M. Rovirola^{1,2}, B. Casals^{1,2}, J.M. Hernández^{1,2}, F. Macià^{1,2}

¹ Dept. of Condensed Matter Physics, University of Barcelona, 08028 Barcelona, Spain

² Institute of Nanoscience and Nanotechnology (IN²UB), University of Barcelona, 08028 Barcelona, Spain

The domain wall (DW) motion, rather to be continuous, proceeds by avalanches (jumps) with a certain power law distribution giving rise to the well-known Barkhausen noise [1]. This power law can be modified by external perturbations. We explore how the magnetoelastic effect, which describes the coupling between strain and magnetization, can affect the DW motion by studying hybrid devices of piezoelectric and ferromagnetic thin films. It has been found that an oscillating strain, in the form of surface acoustic waves (SAWs), can change the criticality of the switching process, where small avalanches rule the switching. We studied the avalanche distribution by measuring jumps in magnetoresistance during the switching process. We further confirmed the results through magneto-optical Kerr microscopy by tracking the DW position in time with and without the presence of SAWs. Furthermore, we performed micromagnetic simulations to deepen our understanding of the interaction between strain and magnetization and found that DW chirality can impact the dynamics of the switching process, influencing the depinning process and the DW velocity. We found that strain can be used as a tool to control the domain wall position in a more deterministic way.

References

[1] S. Kaappa and L. Laurson, *Phys. Rev. Research* **5**, L022006 (2023)
[2] B. Casals, et al. *Phys. Rev. Lett.* **124**, 137202 (2020).

NanoPharmaMed

P29

CHANGES IN THE AGGREGATION PATHWAYS AND FINAL CONFORMATION OF α -SYNUCLEIN INDUCED BY LIPID ENVIRONMENT

✉ mabusquetsvinas@ub.edu

I. Álvarez-Berbel¹, R. Sabaté^{1,2}, G. Putriūtė¹,
A. Espargaró^{1,2}, M. A. Busquets^{1,2}

¹ Physical-Chemistry section, Pharmacy, Pharmaceutical Technology, and Physical Chemistry Department. Faculty of Pharmacy and Food Sciences. University of Barcelona. Av. Joan XXIII, 27-31. 08028 Barcelona.

² Institute of Nanoscience and Nanotechnology. University of Barcelona. Av. Diagonal 645. 08028 Barcelona

α -synuclein is the main hallmark in Parkinson disease. It is known that the presence of lipids could represent a key factor in the aggregation of PrP^{Sc} and other prion-like proteins. Liposomes (lipid bilayers) represent the simplest model to mimic cell membranes. With the goal to decrypt the effect of lipid presence in the amyloid aggregation of α -synuclein, we assayed the effect of liposomes with different lipid composition in the aggregation of α -synuclein under physiological conditions.

Liposomes were prepared by hydration of a thin layer film of the selected lipid (Fig. 1) with PBS, pH 7.4, and subsequent extrusion through polycarbonate filters of 200 nm of pore size. The final lipid concentration was adjusted to 20 mM. Aggregation kinetics of α -synuclein was followed by recording the fluorescence of Thioflavin T in absence (control) and presence of liposomes with a 96-well plates in a FLUOStar Omega plate reader (BMG Lab tech). Lipids differing in acyl chain lengths and charge were chosen to study the influence of charge and fluidity in the aggregation process.

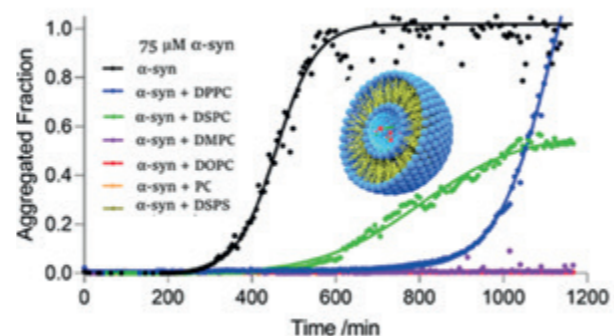


Figure 1. *In vitro* aggregation kinetics of 75 μ M α -synuclein in presence of liposomes.

Inhibitor	Control	+DPPC	+DSPC
k_n (min^{-1})	1.06E-06	1.14E-08	5.39E-06
k_c ($\text{M}^{-1}\cdot\text{min}^{-1}$)	290.0	155.2	127.5
t_0 (min)	344.4	986.3	511.6
$t_{1/2}$ (min)	455.5	1194.7	789.3
t_1 (min)	566.6	1403.0	1067.1
Aggregation (%)	100	287.3	53.1

Table 1. Kinetic parameters of amyloid aggregation.

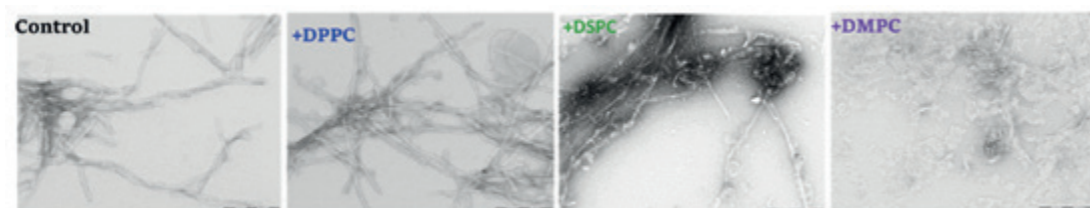


Figure 2. TEM images of α -synuclein alone (control) and in presence of DPPC, DSPC and DMPC liposomes.

P30

INTRACELLULAR GLUTATHIONE (GSH) DETECTION USING BODIPY-FUNCTIONALIZED SILICON OXIDE MICROCHIPS

✉ mlperez@ub.edu

S. Bagherpour^{1,2}, M. Duch³, J. A. Plaza³, P. Vázquez⁴,
T. Suárez⁴, LL. Pérez-García^{1,2}

¹ Departament de Farmacologia, Toxicologia i Química Terapèutica, Universitat de Barcelona, Av. Joan XXIII 27-31, Barcelona, 08028 Spain

² Institut de Nanociència i Nanotecnologia IN²UB, Universitat de Barcelona, Barcelona, 08028 Spain

³ Instituto de Microelectrónica de Barcelona, IMB-CNM (CSIC), Campus UAB, Cerdanyola del Vallès, Barcelona, 08193 Spain

⁴ Centro de Investigaciones Biológicas Margarita Salas, CIB (CSIC), Madrid, 28040 Spain

Biological thiols, including glutathione (GSH), play crucial roles in maintaining the appropriate redox status of biological systems. Despite notable advancements in the creation of fluorescent probes, some limitations, such as aggregation leading to quenching in the biological environment, restricts the capacity of probes to offer long-term monitoring of intracellular GSH levels [1].

Self-assembled monolayers (SAMs) are considered a key tool in the surface design of nanolayers for the bioactive coating of biomedical devices [2]. In the current work, two types of glutathione probes based on BODIPY derivatives were synthesized and conjugated to the surface of silicon oxide microchips, which had been functionalized with a linker using self-assembled silane-based monolayers. The sensitivity of functionalized microchips was studied in GSH solution. Functionalized microchips were finally released in suspension from the wafer by using a mounting medium and characterized by confocal microscopy. The cell internalization of functionalized microchips and their sensitivity to intracellular GSH were also investigated in HeLa cells.

Acknowledgment

Project PID2020-115663GB-C3 was funded by MCIN/AEI/10.13039/501100011033. We also thank AGAUR (Generalitat de Catalunya) for a grant to consolidated research groups 2021 SGR 01085. S. B. thanks Generalitat de Catalunya for a predoctoral FIDUR scholarship.

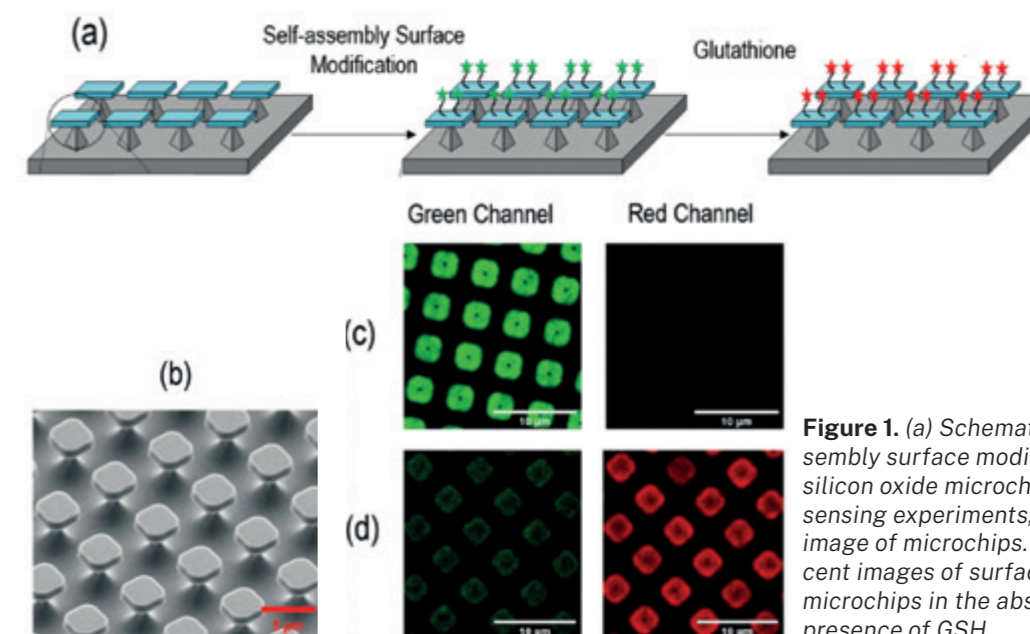


Figure 1. (a) Schematic of self-assembly surface modification of silicon oxide microchips and GSH sensing experiments, (b) SEM image of microchips. (c) Fluorescent images of surface modified microchips in the absence and (d) presence of GSH.

References

- [1] Zhang, J.; Wang, N.; Ji, X.; Tao, Y.; Wang, J.; Zhao, W. BODIPY-Based Fluorescent Probes for Biothiols. *Chem. - A Eur. J.* 2020, 26 (19), 4172–4192.
- [2] Aguil, J. P.; Torras, N.; Duch, M.; Esteve, J.; Pérez-García, L.; Samitier, J.; Plaza, J. A. Highly Anisotropic Suspended Planar-Array Chips with Multidimensional Sub-Micrometric Biomolecular Patterns. *Adv. Funct. Mater.* 2017, 27 (13), 1605912.

P31

CHARACTERIZATION OF POLY(ϵ -CAPROLACTONE) NANOPARTICLES FOR ENHANCED OCULAR DRUG DELIVERY

✉ nbeirabe7@alumnes.ub.edu

N. Beirampour¹, M. J. Rodríguez-Lagunas²,
M. Mallandrich^{1,3}, N. Garrós¹, R. Mohammadi^{1,3},
A. C. Calpena^{1,3}

¹ Universidad de Barcelona, Departamento de Farmacia y Tecnología Farmacéutica y Físicoquímica. Facultad de Farmacia y Ciencias de la Alimentación, Avda. Joan XXIII 27-31. Edificio A. Escalera A. Tercer piso, 08028 Barcelona, España.

² Universidad de Barcelona, Departamento de Bioquímica y Fisiología. Facultad de Farmacia y Ciencias de la Alimentación, Avda. Joan XXIII 27-31. Edificio B. Escalera A. Tercer piso, 08028 Barcelona, España

³ Universidad de Barcelona, Instituto de Nanociencia y Nanotecnología, Avenida Diagonal 645, 08028 Barcelona, España.

Polymeric nanoparticles, particularly those crafted from polycaprolactone (PCL), have emerged as a focal point in drug delivery systems due to their auspicious potential [1]. In this study, we synthesized and characterized PCL nanoparticles to elucidate their physicochemical attributes and explore their application in enhancing ocular drug delivery. The cornea, as the outermost layer of the eye, presents a formidable barrier to effective drug delivery [2][3]. However, PCL nanoparticles, with their diminutive size and favorable surface charge, hold promise in surmounting this barrier, thereby facilitating targeted delivery for a spectrum of ocular maladies, including corneal infections, inflammation, and neovascularization.

Our methodology involved the creation of nanoparticles from an organic solution comprising 50 mg of PCL and 10 mg of baricitinib dissolved in 10 ml of acetone, followed by dropwise addition into water under moderate magnetic stirring. Subsequently, a solution containing P188 (200 mg) at a pH of 6.8 was added as a stabilizer; then, the organic solvent was evaporated overnight under continuous stirring. The resulting PCL nanoparticles were physicochemical characterized, including the assessment of zeta potential, pH, size distribution, and rheological properties, alongside the investigation of their capacity to permeate through the corneal tissue.

Our results indicate that the synthesized PCL nanoparticles exhibited a zeta potential of -20.55 mV, maintaining stability for 1 month at a pH of 6.8, with an average diameter of 138.36 nm. Rheological characterization demonstrated favorable flow behavior crucial for administration, while ex vivo permeation studies underscored their efficient penetration capacity, with a flux (J) value of $14.66 \pm 0.70 \mu\text{g}/\text{h}$. Furthermore, the sustained release potential of these nanoparticles was evidenced by an amount retained in the tissue (Q_{ret}) of $6.09 \pm 0.58 \mu\text{g}/\text{cm}^2$.

In summary, our findings underscore the promising attributes of synthesized PCL nanoparticles, signifying their potential for transformative applications in biomedical fields, particularly in drug delivery systems and targeted ocular therapy.

References

- [1] Gratton, S. E. A., Ropp, P. A., Pohlhaus, P. D., Luft, J. C., Madden, V. J., & Napier, M. E., et al. (2008). The effect of particle design on cellular internalization pathways. *Proceedings of the National Academy of Sciences*, 105(33), 11613–11618. <https://doi.org/10.1073/pnas.0801763105>
- [2] Gaudana, R., Jwala, J., Boddu, S. H. S., Mitra, A. K. (2010). Recent Perspectives in Ocular Drug Delivery. *Pharmaceutical Research*, 27(6), 1192–1203. <https://doi.org/10.1007/s11095-010-0093-4>
- [3] Gote, V., Sikder, S., Sicotte, J., Pal, D., Othman, M., Ganapathy, V., & Mitra, A. K. (2014). Transporter-Targeted Nanoparticles for Enhanced Delivery to the Ocular Epithelium. *Investigative Ophthalmology & Visual Science*, 55(3), 2147–2156. <https://doi.org/10.1167/iovs.13-13198>

P32

FORMULATION, CHARACTERIZATION AND EVALUATION OF THE ANTI-INFLAMMATORY EFFICACY OF A CHRYSABOROL-LOADED NANOEMULSION FOR THE TREATMENT OF ATOPIC DERMATITIS

✉ mireia.mallandrich@ub.edu

L. C. Espinoza^{1,5}, P. Sarango-Granda^{1,5}, L. Sosa²,
M. Rincón³, A. Calpena^{4,5}, M. Mallandrich^{4,5}

¹ Departamento de Química, Universidad Técnica Particular de Loja, 1101608 Loja, Ecuador

² Pharmaceutical Technology Research Group. Faculty of Chemical Sciences and Pharmacy, National Autonomous University of Honduras, 11101 Tegucigalpa, Honduras.

³ Department of Materials Science and Physical Chemistry, Faculty of Chemistry, University of Barcelona, 08028 Barcelona, Spain

⁴ Department of Pharmacy, Pharmaceutical Technology and Physical Chemistry, Faculty of Pharmacy and Food Sciences, University of Barcelona, 08028 Barcelona, Spain.

⁵ Institute of Nanoscience and Nanotechnology (IN²UB), University of Barcelona, 08028 Barcelona, Spain.

Atopic dermatitis (AD) represents the most prevalent inflammatory dermatological disorder affecting both adults and children, significantly diminishing patient quality of life. To date, AD remains without a definitive cure, prompting the exploration of new therapeutic modalities that are both efficacious and safe. Crisaborole emerges as a pioneering non-steroidal anti-inflammatory pharmaceutical, exerting its effects through the selective inhibition of phosphodiesterase 4, thereby modulating cAMP levels. The objective of this study was to formulate a crisaborole nanoemulsion (CR-NE) aimed at enhancing the penetration, absorption, and bioavailability of the active compound. The solubility of crisaborole was assessed across various oils, surfactants, and co-surfactants.

Subsequently, four pseudo-ternary phase diagrams were constructed to determine the optimal composition of CR-NE, which underwent comprehensive physicochemical, chemical, and biopharmaceutical characterizations. These evaluations encompassed measurements of pH, rheological properties, droplet size, polydispersity index, and morphological features. The in vivo efficacy was validated using a mouse ear inflammation model, where inflammation was elicited via topical xylene application to the right ear. The CR-NE formula comprised Lauriglicol 90, Tween 80, Transcutol P, and water, exhibiting a pH of 5.02 ± 0.003 , mean droplet size of $109.4 \pm 3.97 \text{ nm}$, polydispersity index (PI) of 0.27 ± 0.014 , spherical droplets, a viscosity of $48.76 \pm 0.01 \text{ mPa}\cdot\text{s}$, and Newtonian flow behavior. The release kinetics were characterized by a hyperbolic profile. Efficacy assessments indicated that while xylene exposure induced vasodilation and erythema, subsequent treatment with CR-NE significantly attenuated these inflammatory responses, as confirmed by detailed histological analysis. Therefore, these findings advocate for the topical application of CR-NE as a non-irritating, skin-compatible therapeutic alternative for the management of inflammatory dermatoses such as atopic dermatitis.

References

- [1] Maliyar, K., & Sibbald, C. Diagnosis and Management of Atopic Dermatitis: A Review. *Advances in Skin & Wound Care*, 31(12), 538–550 (2012).
- [2] Zane, L., Chanda, S., Jarnagin, K., Nelson, D., Spelman, L., & Gold, L. Crisaborole and its potential role in treating atopic dermatitis: overview of early clinical studies. *Immunotherapy*, 8(8) (2016).
- [3] Zane, L. T., Kircik, L., Call, R., Tschen, E., Draelos, Z. D., Chanda, S., Ph, D., Syoc, M. Van, & Hebert, A. A. Crisaborole Topical Ointment, 2 % in Patients Ages 2 to 17 Years with Atopic Dermatitis: A Phase 1b, Open-Label, Maximal-Use Systemic Exposure Study. *Pediatric Dermatology*, 33(4), 380–387 (2016).
- [4] Azeem, A., Rizwan, M., Ahmad, F. J., Iqbal, Z., Khar, R. K., Aqil, M., & Talegaonkar, S. Nanoemulsion components screening and selection: A technical note. In *AAPS PharmSciTech*, 10, 69–76. (2009).

P33

EXPLORING THE IMPACT OF TITANIUM OXIDE NANOPARTICLES: UNVEILING THEIR PHOTOTOXIC BEHAVIOUR IN A KERATINOCYTE CELL LINE

✉ adrianamaddaleno@ub.edu

A. S. Maddaleno^{1,2}, L. Bescós¹, M. P. Vinardell^{1,2}, M. Mitjans^{1,2}¹ Physiology, Dpt. Biochemistry and Physiology, Universitat de Barcelona² Institute of Nanoscience and Nanotechnology, Universitat de Barcelona

Introduction

Detrimental effects of ultraviolet (UV) radiation exposure include skin cancer and photoaging. Skin cancers are the most diagnosed group of cancers worldwide, with an estimation of more than 1.5 million new cases for 2020 being malignant melanoma the 20% of them [1]. Thankfully, the risk to develop such pathological entities can be reduced by the use of sunscreens. Titanium oxide (TiO₂) is an inorganic compound widely used in a variety of products and is the most frequently used UV filter [2]. In this sense, the use of micro-sized particles of TiO₂ in cosmetic formulations presents the disadvantage of leaving a visible white residue on the skin (white cast) but this effect can be solved by the use of nanoparticles (NPs) that reflect less visible light, therefore appearing nearly transparent. However, the photoreactivity of TiO₂ NPs is higher and, consequently, an increase in Reactive Oxygen Species (ROS) can lead to potential cellular damage [3]. For this reason, the main goal of the present work is to study the potential phototoxic behaviour of TiO₂ micro and nano-sized particles.

Material and Methods

Commercially TiO₂ nano (21 nm) and micro sized NPs were purchased at Sigma-Aldrich (St. Louis, MO, USA). NPs size and morphology of TiO₂ were further characterized by Transmission Electron Microscopy (TEM) and by Dynamic Light Scattering (DLS) when suspended in phosphate buffer saline (PBS, pH 7.4) and/or in culture media (DMEM containing 5% of FBS). Phototoxicity of TiO₂ micro and nano-sized particles were assessed in the human keratinocyte cell line Ha-CaT following the OECD TG 432 [4]. Cell viability was

determined by the colorimetric reduction of the dye 2,5 diphenyl-3-(4,5-dimethyl-2-thiazolyl) tetrazolium bromide (MTT) and Neutral red Uptake (NRU) assays. Potential interferences and/or interactions caused by TiO₂ particles with the cytotoxic assays was previously evaluated. According to OECD TG 432 [4], we can predict the potential phototoxic behaviour of TiO₂ by calculating the photoirritation factor or PIF, which represents the ratio between the concentration of the test chemical by which the cell viability is reduced by 50% (IC50) in the absence and presence of UV radiation. Thus, a test chemical with a PIF < 2 predicts “no phototoxicity”; A PIF >2 and < 5 predicts “equivocal” phototoxicity and a PIF > 5 predicts: “phototoxicity”.

Results and Discussion

Technical information provided by the commercial supplier was confirmed by TEM observation and thus, that nano-TiO₂ is a mixture of 80% anatase (spherical shape) and 20% rutile (spherical and rod shape) with a particle size of 21 nm. DLS revealed that TiO₂ NPs agglomerate when in presence of physiological solutions as the hydrodynamic diameter obtained is 479 ± 355 nm and 281 ± 21.5 nm in PBS or DMEM 5% FBS, respectively. No chemical interactions of TiO₂ particles with the reagents of MTT or NRU were found. Nevertheless, the insolubility of TiO₂ particles could interfere with the absorbance measurement. Therefore, cytotoxicity assays should utilise low particle concentrations to minimize TiO₂ traces and transfer the supernatant to another plate for the readings. In the case of phototoxicity assay, average PIF obtained with the NRU is < 1 for micro-sized TiO₂ and 3.0 for TiO₂ NPs; whereas in the case of MTT PIF is 5.1 independently of the particle size. In conclusion, TiO₂ shows some potential ability to induce phototoxic reactions in the conditions assessed here and further investigations needs to be conducted.

Acknowledgement: This work is part of the grant PID2020 funded by MICIU/AEI/10.13039/501100011033.

References

- [1] Arnold M., Singh D., Laversanne M. et al., *JAMA Dermatol*, 158(5): 495-503, **2022**; doi: 10.1001/jamadermatol.2022.0160.
- [2] Chaiyabutr C., Sukakul T., Kumpangsin T. et al., *Contact Dermatitis*, 85(1): 63-65, **2021**, doi: 10.1111/cod.13777.
- [3] Smijs T. G. and Pavel S., *Nanotechnol Sci Appl*, 4(1): 95-112, **2011**. doi: 10.2147/nsa.s19419.
- [4] OECD, Test No. 432: In Vitro 3T3 NRU Phototoxicity Test, **2019**. <https://doi.org/10.1787/9789264071162-en>

P34

SUPRAMOLECULAR GELS FOR PHOTODYNAMIC THERAPY

✉ mlperez@ub.edu

N. V. Lakshmi Kavya Anguluri¹, S. Bagherpour^{1,2}, L. I. Pérez-García^{1,2}¹ Departament de Farmacologia, Toxicologia i Química Terapèutica, Universitat de Barcelona, Spain² Institut de Nanociència i Nanotecnologia UB (IN²UB), Universitat de Barcelona, Spain

The application of Photodynamic Therapy (PDT) has spurred interest in improving photosensitizer delivery, with gel formulations. Research has shown that incorporating porphyrin into a bis-imidazolium gelator matrix increases the generation of reactive oxygen species (ROS) compared to the photosensitizer in solution[1]. Our study investigated how varying porphyrin chemical structures affect their photosensitizing abilities within a supramolecular hydrogel based on gemini imidazolium amphiphiles. Our findings revealed increased singlet oxygen (¹O₂) generation within the hydrogel matrix compared to the solution, validated through antimicrobial studies. Rheological measurements confirmed favourable viscoelastic properties, suggesting the potential of porphyrin hydrogels as effective PDT delivery systems.

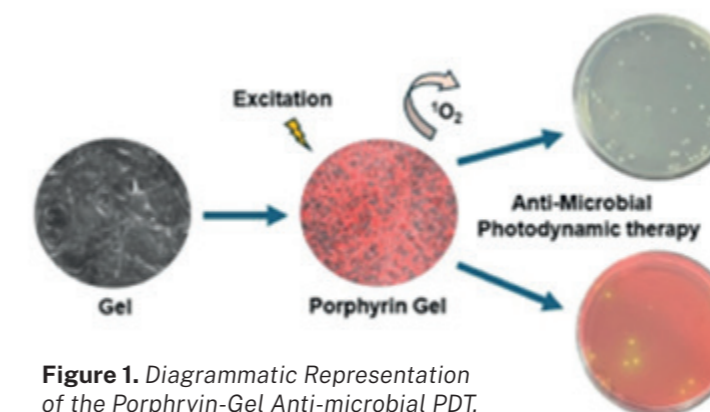


Figure 1. Diagrammatic Representation of the Porphyrin-Gel Anti-microbial PDT.

References

- [1] [Samperi, M.; Limón, D.; Amabilino, D. B.; Pérez-García, L. Enhancing Singlet Oxygen Generation by Self-Assembly of a Porphyrin Entrapped in Supramolecular Fibers. *Cell Reports Physical Science* **2020**, 1, 100030.

P35 NOVEL RILUZOLE LOADED NANOSTRUCTURED LIPID CARRIERS FOR THE TREATMENT OF PSORIASIS

✉ xavier.llorente@ub.edu

X. Llorente¹, G. Esteruelas^{1,2}, L. Bonilla-Vidal^{1,2},
I. Filgaira³, D. Lopez-Ramajo³, R. C. Gong³, C. Soler³,
M. Espina^{1,2}, M. L. García^{1,2}, J. Manils³, M. Pujol^{1,2},
E. Sánchez López^{1,2}

¹ Department of Pharmacy, Pharmaceutical
Technology and Physical Chemistry, Faculty of
Pharmacy, University of Barcelona, 08028 Barcelona,
Spain

² Institute of Nanoscience and Nanotechnology
(IN²UB), University of Barcelona, Barcelona, Spain

³ Departament de Patologia i Terapèutica Experimental
and Hospital Universitari de Bellvitge-Bellvitge
Institute for Biomedical Research, Barcelona, Spain

Introduction

Chronic inflammatory dermatoses such as psoriasis are complex diseases with no fully effective treatment [1]. In this area, Riluzole (RLZ) is a glutamate release inhibitor with anti-proliferative effects potentially beneficial for diseases such as psoriasis. However, RLZ possess low water solubility and light-sensibility [2]. To overcome these drawbacks, nanostructured lipid carriers (NLC), represent one of the most effective systems for topical drug administration. Therefore, the aim of this study is to develop and optimize NLCs loaded with RLZ (RLZ-NLCs) as topical treatment for psoriasis.

Material & methods

RLZ-NLCs were prepared using the hot-pressure homogenization method and optimized employing the design of experiments approach. RLZ-NLCs release was studied by direct dialysis technique against free RLZ. RLZ-NLCs safety and anti-hyperproliferative activity were assessed in HaCat cells.

Results and discussion

The optimized formulation showed suitable physico-chemical parameters for dermal applications (average size < 200 nm, PI < 0.2, negative zeta potential and entrapment efficiency around 87 %) [3]. Furthermore, *in vitro* release studies demonstrate that RLZ-NLCs deliver RLZ in a sustained manner (Figure 1). At a cellular level, RLZ-NLC were safe and able to inhibit HaCaT keratinocyte growth. Therefore, RLZ-NLCs constitute a promising system for the treatment of psoriasis.

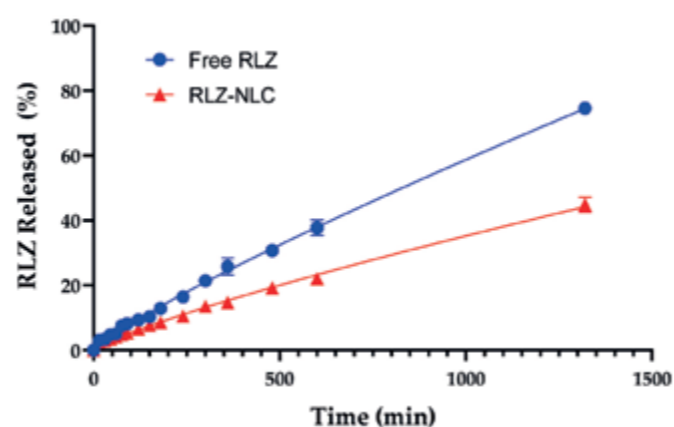


Figure 1. *In vitro* release of free RLZ and RLZ-NLC [3].

References

- [1] C. E. M. Griffiths et al., 'The global state of psoriasis disease epidemiology: a workshop report', *Br. J. Dermatol.*, vol. 177, no. 1, p. e4, Jul. 2017, doi: 10.1111/BJD.15610.
- [2] G. Esteruelas et al., 'Development and optimization of Riluzole-loaded biodegradable nanoparticles incorporated in a mucoadhesive in situ gel for the posterior eye segment', *Int. J. Pharm.*, vol. 612, p. 121379, Jan. 2022, doi: 10.1016/J.IJPHARM.2021.121379.
- [3] X. Llorente et al., 'Riluzole-Loaded Nanostructured Lipid Carriers for Hyperproliferative Skin Diseases', *Int. J. Mol. Sci.*, vol. 24, no. 9, 2023, doi: 10.3390/ijms24098053.

P36 CRUCIAL ROLE OF PrP^{Sc} IN TRIGGERING OLIGOMERIZATION OF A β PEPTIDES

✉ rsabate@ub.edu

I. Álvarez-Berbel¹, G. Putriūtė¹, M. A. Busquets^{1,2},
A. Espargaró^{1,2}, R. Sabate^{1,2}

¹ Physical-Chemistry section, Pharmacy,
Pharmaceutical Technology, and Physical Chemistry
Department, Faculty of Pharmacy and Food Sciences,
University of Barcelona, Av. Joan XXIII, 27-31. 08028
Barcelona.

² Institute of Nanoscience and Nanotechnology,
University of Barcelona.

In recent years, there have been several pieces of evidence suggesting potential interactions between PrP and amyloid-beta peptide. With this in mind, we conducted experiments to test the effect of preformed PrP^{Sc} fibrils on the aggregation of A β peptide, the main hallmark of Alzheimer's disease.

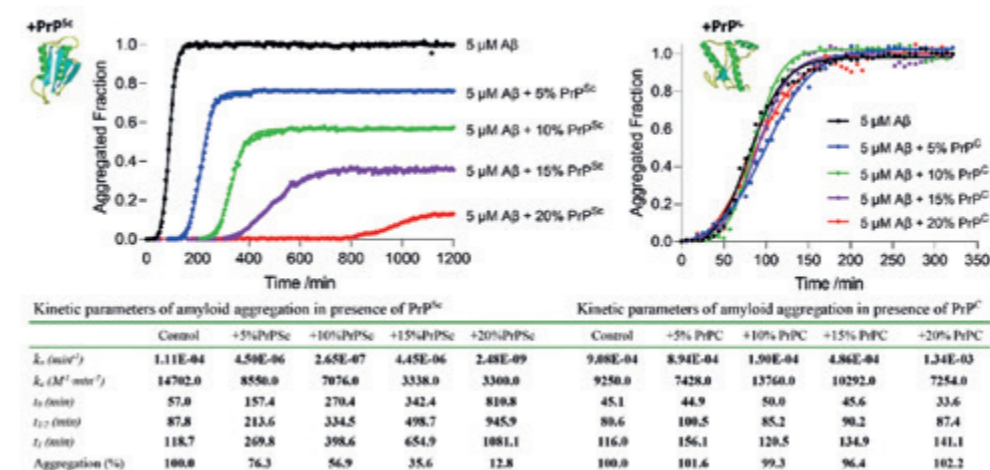
Our assays revealed that the presence of PrP^{Sc} fibrils increased the lag time and nucleation constant of A β aggregation, while reducing the fibril growth ratio. The data obtained suggest a potential direct binding between PrP^{Sc} seeds and A β monomers, leading to the formation of larger aggregates and a reduction in the concentration of mature fibers. Interestingly, we also observed an increase in the formation of oligomeric

species with potential toxicity and spreading capacity.

The compiled data confirm that PrP has a potential effect on the aggregation of A β 40 peptide. It appears that while PrP^{Sc} acts to reduce both nucleation and elongation constants in a concentration-dependent manner, and apparently reduces the final amount of A β 40 fibrils, PrP^C has minimal effect on the aggregation of A β 40 (see Figure 1). We checked the fibril structure and stability using TEM and chemical denaturation, respectively. The TEM images showed apparently similar structural features for A β 40 fibrils in the absence and presence of PrP^{Sc}. However, as expected, we observed a higher concentration of aggregates in the absence of PrP^{Sc}.

To investigate the potential structural differences between A β 40 fibrils formed in the absence of PrP^{Sc}, we determined their stability using guanidine HCl as a chaotropic agent. Importantly, we observed that the presence of PrP^{Sc} resulted in the formation of more stable A β 40 fibrils, suggesting that the amyloid aggregation of A β 40 could follow an alternative pathway.

In light of these findings, we decided to explore the possibility that PrP^{Sc} favored the formation of oligomeric species of A β 40. Importantly, preliminary data suggest an increase in the formation of multimeric soluble species in the presence of PrP^{Sc}.



P37

3D SPHEROIDS INDUCED BY SUPERHYDROPHOBICITY AS CELL-DERIVED STRATEGIES FOR THERAPEUTICAL TARGETS

✉ mcmoranb@ub.edu and ✉ michele.ferrari@ge.imate.cnr.it

M. C. Morán^{1,2}, F. Cirisano³, M. Ferrari^{2,3}¹ Departament de Bioquímica i Fisiologia, Secció de Fisiologia – Facultat de Farmàcia i Ciències de l'Alimentació, Universitat de Barcelona, Avda. Joan XXIII, 27-31, 08028 Barcelona, Spain² Institut de Nanociència i Nanotecnologia – IN²UB, Universitat de Barcelona, Avda. Diagonal, 645, 08028 Barcelona, Spain³ CNR-ICMATE Istituto di Chimica della Materia Condensata e di Tecnologia per l'Energia, Via De Marini, 6, 16149 Genova, Italy

density. Moreover, the effectiveness of the spheroids to be recovered and grown under 2D culture conditions was evaluated. The morphology of the migrated cells from the 3D spheroids was characterized at the nano-microscale through 3D profilometry. Results demonstrated improved adhesion and proliferation in the migrated cells of representative skin cell lines, both advanced properties for regenerative applications [4]. When considering macrophage-derived spheroids, changes in polarization and activation of migrated cells exhibited promising properties to be used in immunotherapy [5].

Cell therapies commonly pursue tissue stimulation by replacing cell numbers or supplying functional deficiencies. To this aim, monodispersed cells are usually transplanted for incorporation by local injection. The limitations of this strategy include poor success associated with cell death, insufficient retention, or cell damage due to shear forces associated with the injection. Spheroids have recently emerged as a model that mimics an in vivo environment with more representative cell-to-cell interactions and better intercellular communication [1]. Nevertheless, cost-effective and lab-friendly fabrication and effectively performed recovery are challenges that restrict the broad application of spheroids [2]. In this work, surfaces were modified with environmentally friendly superhydrophobic coatings. The superhydrophobic surfaces were used for the 3D spheroid preparation from different cell lines ranging from tumoral and non-tumoral cell lines [3]. The resulting 3D spheroids were characterized in terms of size distribution and circularity as well as cell viability in the 3D environment as a function of cell

References

- [1] M. C. Decarli, R. Amaral, D.P.D. Santos, L. B. Tofani, E., Katayama, R.A. Rezende et al. Cell Spheroids as a Versatile Research Platform: Formation Mechanisms, High throughput Production, Characterization and Applications. *Biofabrication* **2021**, 13, 032002.
- [2] M. Ferrari, F. Cirisano, M. C. Morán, Super Liquid-repellent Surfaces and 3D Spheroids Growth. *Front. Biosci. (Landmark Ed)* **2022**, 27, 144.
- [3] M. Ferrari, F. Cirisano, M. C. Morán, Mammalian Cell Spheroids on Mixed Organic-Inorganic Superhydrophobic Coating, *Molecules* **2022**, 27, 1247.
- [4] M. C. Morán, F. Cirisano, M. Ferrari, Spheroid Formation and Recovery Using Superhydrophobic Coating for Regenerative Purposes. *Pharmaceutics* **2023**, 15, 2226.
- [5] M. C. Morán, F. Cirisano, M. Ferrari, Macrophage Polarization on Spheroids induced by Superhydrophobic Coatings. *Pharmaceutics* **2024**, submitted.

P38

IN-VITRO PrP^{Sc} AGGREGATES ALTER α -SYNUCLEIN AGGREGATION PATTERN

✉ aespargaro@ub.edu

I. Álvarez-Berbel¹, G. Putriütè¹, M. A. Busquets^{1,2}, R. Sabaté^{1,2}, A. Espargaró^{1,2}¹ Physical-Chemistry section, Pharmacy, Pharmaceutical Technology, and Physical Chemistry Department. Faculty of Pharmacy and Food Sciences. University of Barcelona. Av. Joan XXIII, 27-31. 08028 Barcelona.² Institute of Nanoscience and Nanotechnology. University of Barcelona. Av. Diagonal 645. 08028 Barcelona

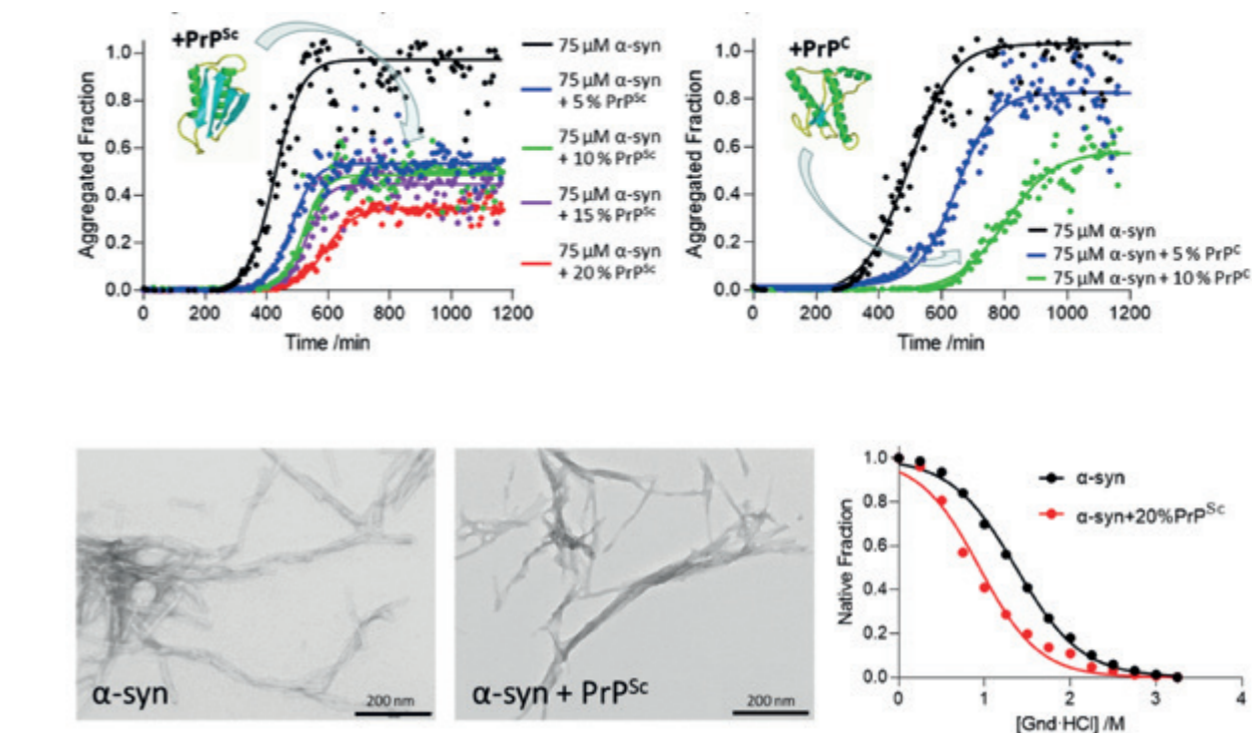
of α -synuclein protein, linked to Parkinson disease. Interestingly, our results show that in-vitro PrP^{Sc} aggregates alter α -syn aggregation pattern. Thus, whereas nucleation constant is practically unaltered in presence of PrP^{Sc} seed, the elongation constant is drastically reduced, lowering concomitantly the concentration of α -syn mature fibers.

Aggregation kinetics

Both PrP^{Sc} and PrP^C affect the kinetic of α -syn aggregation by increasing the time required for nucleation in a concentration-dependent manner and by increasing the elongation constant.

Fibril structure and stability

Although the final structure of the aggregates (observed by TEM) shows small differences, their stability against chaotropic agents exhibits significant structural differences.



P39

DUALY ACTIVE APIGENIN-LOADED NANOSTRUCTURED LIPID CARRIERS WITH ROSEHIP OIL FOR CANCER TREATMENT

✉ lbonilla95@ub.edu

L. Bonilla-Vidal^{1,2}, M. Espina^{1,2}, G. Esteruelas^{1,2}, M. L. García^{1,2}, A. Gliszczynska³, E. Sánchez-López^{1,2}¹ Department of Pharmacy, Pharmaceutical Technology and Physical Chemistry, Faculty of Pharmacy and Food Sciences, University of Barcelona, Barcelona 08028, Spain² Institute of Nanoscience and Nanotechnology (IN²UB), University of Barcelona, Barcelona 08028, Spain³ Department of Chemistry, Wrocław University of Environmental and Life Sciences, Norwida25, 50-375 Wrocław, Poland

Cancer remains a significant global health burden, and conventional therapies often suffer from adverse effects and limited efficacy (1). Natural products such as apigenin (APG) exhibit promising antitumor properties but are hampered by low water solubility. Nanostructured lipid carriers (NLC) offer a strategy to address this limitation. This study aimed to develop and evaluate a novel dual NLC system encapsulating APG (APG-NLC) incorporating rosehip oil, recognized for its anti-inflammatory and antioxidant properties, which in the last years has showed a potential antitumoral properties (2).

We optimized the composition of the formulation to achieve optimal physicochemical characteristics, including particle size, surface charge, and encapsulation efficiency. Stability studies were carried out by the analysis of the backscattering profile and physicochemical properties of APG-NLC stored at 3

different temperatures (4 °C, 25 °C and 37 °C). The biopharmaceutical behaviour of the formulations was studied throughout Franz-diffusion cells at 37 °C. The therapeutic efficacy of APG-NLC was assessed using *in ovo* and *in vitro* models, focusing on antiangiogenic activity and antiproliferative effects on different cancer cells while ensuring minimal cytotoxicity towards healthy cells (3).

The optimized APG-NLC formulation exhibited suitable particle size below 200 nm, negative surface charge of -20 mV, and exceptionally high encapsulation efficiency exceeding 99 %. The system displayed sustained APG release and exceptional stability for over 10 months when stored at 4 °C. APG released from APG-NLC in a slow and sustained manner in comparison to free APG. *In ovo* and *in vitro* studies demonstrated significant antiangiogenic activity (Figure 1) and a selective antiproliferative effects against various cancer cell lines, with minimal toxicity observed in healthy cells.

We successfully optimized APG-NLC containing rosehip oil. These NLC possessed favourable physicochemical properties, extended storage stability, and sustained APG release. Furthermore, APG-NLC demonstrated antiangiogenic activity in an *in ovo* model inhibiting all the new blood vessels formed. *In vitro* studies confirmed that APG-NLC were cytotoxic against all the tested cancer cell lines, thus confirming the dual effect of APG with rosehip oil in the lipid matrix. These findings suggest the potential of APG-NLC as a promising nanomedicine approach for cancer treatment.

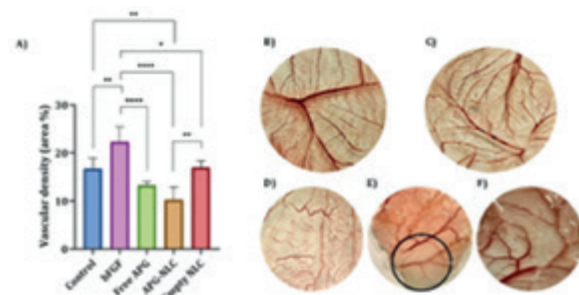


Figure 1. *In ovo* antiangiogenic activity. Membranes after the incorporation of 48 h of product: (A) bFGF, (B) NaCl, (C) Free APG, (D) APG-NLC with a black circle highlighting its effect, (E) Empty NLC.

References

- [1] Sung H, Ferlay J, Siegel RL, Laversanne M, Soerjomataram I, Jemal A, et al. Global cancer statistics 2020: GLOBOCAN estimates of incidence and mortality worldwide for 36 cancers in 185 countries. *A Cancer J Clin.* 2021;71(3):209–49.
- [2] Salehi B, Venditti A, Sharifi-Rad M, Kręgiel D, Sharifi-Rad J, Durazzo A, et al. The therapeutic potential of apigenin. *Int J Mol Sci.* 2019;20(6):1305.
- [3] Bonilla-Vidal L, Świtalska M, Espina M, Wietrzyk J, García ML, Souto EB, et al. Dually active apigenin-loaded nanostructured lipid carriers for cancer treatment. *Int J Nanomedicine.* 2023;18:6979–97.

P40

DEVELOPMENT AND CHARACTERIZATION OF PLGA NANOPARTICLES LOADED WITH *PHLOMIS CRINITA* EXTRACT: PROMISING POTENTIAL FOR ENHANCED SKIN TREATMENTS

✉ tahsine223@gmail.com

T. Kosksi¹, P. Bustos Salgado^{2,3}, A. C. Calpena^{2,3}, L. G. Chekir¹¹ Unity of Bioactive Natural Substances and Biotechnology, Faculty of Dental Medicine–University of Monastir, Monastir, Tunisia.² Department of Pharmacy, Pharmaceutical Technology, and Physical-Chemistry, Faculty of Pharmacy and Food Sciences, University of Barcelona, 08028 Barcelona, Spain³ Institut de Nanociència i Nanotecnologia IN²UB, Universitat de Barcelona, 08028 Barcelona, Spain

Nanoparticles have emerged as effective carriers for encapsulating plant extracts. This approach improves the stability, bioavailability, and controlled release of bioactive compounds. Nanoparticles, which protect plant extract components from degradation, provide intriguing opportunities for improving the delivery and efficacy of plant-based therapies [1].

In this study, we aimed to develop and characterize PLGA nanoparticles loaded with *Phlomis crinita* plant extract for potential applications in skin treatments. The nanoparticles were synthesized using the solvent displacement method. Initially, the plant extract was dissolved in ethanol, and PLGA (poly(lactic-co-glycolic acid)) was dissolved in an organic solution comprising acetone. The resulting organic phase was then added drop by drop, with moderate stirring, to an aqueous phase at pH 3.5, containing P188 as a stabilizer. After evaporating the solvents (ethanol and acetone), the dispersions of nanoparticles were concentrated. Subsequently, the physicochemical properties of the nanoparticles were determined, including size distribution, zeta potential, polydispersity index (PDI), and extensibility. Additionally, scanning electron microscopy (SEM) was employed to analyze the morphology of the nanoparticles.

Our results indicate that the synthesized PLGA nanoparticles loaded with *Phlomis crinita* plant extract exhibited a zeta potential of -38.5 ± 0.379 mV. The average diameter of the nanoparticles was measured to be 59.5 ± 2.876 nm, with a polydispersity index (PDI) of 0.439. The nanoparticles demonstrated moderate extension and significant stretchability, indicating their flexibility and ability to undergo considerable deformation. These findings make them promising for skin treatments. The surface morphology revealed that they were uniformly distributed and had a spherical morphology with no aggregation process observed.

In conclusion, these findings highlight the potential of PLGA nanoparticles loaded with *Phlomis crinita* plant extract as promising candidates for innovative solutions in fields such as biomedical engineering, drug delivery systems, and for enhancing the efficacy of skin treatments.

References

- [1] S. Yang, L. Liu, J. Han, et Y. Tang, « Encapsulating plant ingredients for dermocosmetic application: an updated review of delivery systems and characterization techniques », *Intern J of Cosmetic Sci*, vol. 42, no 1, p. 16 28, févr. 2020, doi: 10.1111/ics.12592.

P41

CUBIC LIQUID CRYSTALLINE-BASED EMULSIONS FOR BAKUCHIOL TOPICAL DELIVERY

✉ mjgarcia@ub.edu

M. J. García Celma^{1,2,3,4}, T. Kakabadze¹, L. C. Rosales Rivera¹, G. Morral Ruiz^{1,3}, A. del Pozo Carrascosa¹, C. Rodríguez Abreu^{3,4,5}, E. Escribano Ferrer^{1,2,4,6}

¹ Department of Pharmacy and Pharmaceutical Technology and Physical Chemistry, Pharmacy and Food Sciences School, University of Barcelona (UB), Joan XXIII 27-31, 08028, Barcelona, Spain.

² Institute of Nanoscience and Nanotechnology (IN²UB), University of Barcelona, Spain.

³ CIBER-BBN, Institute of Health Carlos III, Madrid, Spain.

⁴ Pharmaceutical Nanotechnology Group, Associated Unit to CSIC through the IQAC, Barcelona, Spain

⁵ Institute of Advanced Chemistry of Catalonia (IQAC), CSIC, Barcelona, Spain.

⁶ CIBER-OBN, Institute of Health Carlos III, Madrid, Spain

The development of innovative topical dosage forms to facilitate actives penetration through the stratum corneum and avoiding reaching the systemic circulation is a challenge [1]. Lyotropic liquid crystals consist of amphiphilic molecules and are formed in presence of solvents being the most common types lamellar, hexagonal, and cubic mesophases. They offer promising prospects for encapsulation of a wide range of target molecules. Formulations containing liquid crystalline structures show merits over other vehicles in terms of high payload, long-term stability, high solubilization capacity, sustained release, and ease of scale-up [2]. Bakuchiol (BAK) is a natural product obtained from the *Psoralea corylifolia* seeds with anti-inflammatory, antiproliferative, and antiacne properties that constitutes a retinol alternative with anti-aging properties and less side effects. The high lipophilicity of BAK is a drawback for its formulation in conventional pharmaceutical excipients and its diffusion through the skin [3]. In this context, the aim of the present work is the development of topical emulsions based on cubic liquid crystalline structures for BAK solubilization and the study of their rheological properties and in-vitro skin permeation.

References

- [1] Arias EM, Guiró P, Rodríguez-Abreu C, Solans C, Escribano-Ferrer E, García-Celma MJ (2019). *International Journal of Pharmaceutics* 569: 118531.
- [2] Teeranachaiideekul V, Soontaranon S, Sukhasem S, Chantasart D, Wongrakpanich A (2023). *Sci Rep* 13: 4185-4199.
- [3] Inmuangkham N, Sukjarernchaikul P, Thepwatee S, Iemsam-Arng J (2024). *Industrial Crops & Products* 209: 118052.

Materials & Methods

Materials: Bakuchiol (BAK, DKSH); PEG-40 Hydrogenated Castor Oil (RH40, BASF); Polysorbate 80 (T80, Sigma Aldrich); Miglyol 812 (M812, Acofarma); Polyethylene glycol 200 (PEG-200, Fluka); Ethanol (Et, Carlo Erba); Phosphate buffer solution pH=7.4 (PBS); Deionized and filtered water (W).

Methods: The phase diagram of the W/RH40/M812 system was determined at 25 and 32 °C by the stepwise addition method, as described previously [1]. Formulations nanostructure was characterized by Small-Angle X-Ray scattering (SAXS), with a S3 MICRO instrument (Hecus X-ray Systems) equipped with a GENIX micro-focus X-ray source ($\lambda=1.54$ Å). Spreadability determinations were performed with a TA.X-PlusC 650 Texture Analyser (Stable Micro Systems). The permeation studies of BAK from emulsions were carried out by using a Microette Plus equipment (Hanson Research) containing 6 amber Franz diffusion cells with a diffusion area of 1.77 cm². A synthetic lipophilic membrane (Strat-M®, Millipore, Merck) was used, as an attempt to emulate the structure and composition of the skin. Quantification of BAK was carried out by HPLC (Shimadzu HPLC equipment) and UV detection (262 nm).

Results and Discussion

BAK (1 wt%) has been successfully incorporated to diluted, concentrated, and highly concentrated emulsions based on cubic liquid crystalline structures, in the system W/RH40/M812. The emulsions presented suitable spreadability and cosmetic properties. Liquid crystalline nanostructures formed in formulations with and without BAK were identified by SAXS. The in-vitro permeation studies showed that less than 2% of the dose of BAK in the donor compartment was found in the receptor solution after 24h. The developed emulsions can be considered as promising formulations for sustained release of BAK for skin delivery, with minimal permeation across the Strat-M membrane, leading to efficacious topical application, avoiding possible systemic effects.

P42

NOVEL OPTIMIZED CLOBETASOL-LOADED LIPID NANOPARTICLES FOR DERMAL APPLICATIONS

✉ jmadariaga@ub.edu

J. Madariaga Burgos¹, M. Espina^{1,2}, M. L. García^{1,2}, M. Pujol^{1,2}, E. Sánchez López^{1,2}

¹ Departament de Pharmacy, Pharmaceutical Technology and Physical Chemistry, Faculty of Pharmacy and Food Sciences, University of Barcelona, Barcelona, 08028, Spain

² Institute of of Nanoscience and Nanotechnology (IN²UB)

Clobetasol propionate (CP) is one of the most widely used drugs for the management of skin diseases such as psoriasis, although it has limitations due to its poor solubility and its erratic penetration into the deeper layers of the skin. Moreover, long-term treatment leads to serious adverse effects [1]. To enhance drug permeation and retention and obtain a prolonged effect, nanostructured lipid carriers (NLC) have aroused as suitable candidates. Therefore, the aim of this work is the development, optimization and characterization of NLC encapsulating CP (CP-NLC) for dermal administration.

Materials and Methods

CP-NLC were obtained using high-pressure hot homogenization method [2]. Formulation was optimized by a central composite factorial design and characterized in terms of size, polydispersity index, zeta potential and encapsulation efficiency. Morphologic characterization was carried out using transmission electron microscopy (TEM) and interaction studies between components were performed by X-ray diffraction (XRD), differential calorimetry scanning (DSC) and Fourier-transformed infrared spectroscopy (FTIR). Moreover, in vitro irritation potential was evaluated using the HET-CAM test.

Results and Discussion

Optimization of CP-NLC showed that size decreases as surfactant percentage increases and increases as lipid phase percentage in a direct manner (Figure 1A). Optimized CP loaded NLC possess an average size below 200 nm (confirmed by TEM), polydispersity index below 0,2, zeta potential around -30 mV and an encapsulation efficiency over 90%. XRD and DSC (Figure 1B) profiles shows that CP is dissolved in the lipidic matrix and FTIR confirms that there is no formation of new covalent bonds. HET-CAM assay shows no evidence of vascular lysis, haemorrhage or coagulation, thereby classifying this formulation as non-irritant.

Conclusion

A CP loaded NLC system has been developed. The optimized formulation shows suitable physicochemical characteristics confirmed by different techniques being safe for dermal application.

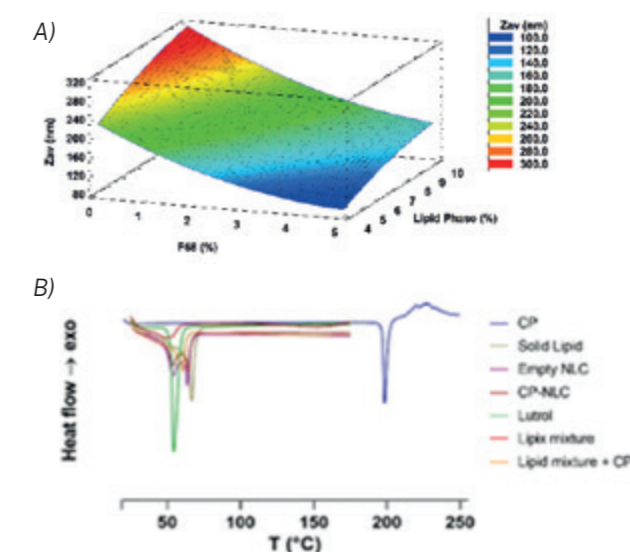


Figure 1. A) Surface response chart of average size, B) DSC profiles of CP-NLC and its components.

References

- [1] Rosso, J.Q. Del; Rosso, D. Topical Corticosteroid Therapy for Psoriasis — A Review of Clobetasol Propionate 0.025% Cream and the Clinical Relevance of Penetration Modification. *J Clin Aesthet Dermatol* 2020, 13, 22.
- [2] Carvajal-Vidal, P.; Fábrega, M.J.; Espina, M.; Calpena, A.C.; García, M.L. Development of Halobetasol-Loaded Nanostructured Lipid Carrier for Dermal Administration: Optimization, Physicochemical and Biopharmaceutical Behavior, and Therapeutic Efficacy. *Nanomedicine* 2019, 20, 102026, doi:10.1016/J.NANO.2019.102026.

P43

RUTHENIUM (II) THIOCYANATE COMPLEXES: MOVING FROM DYE-SENSITIZED SOLAR CELLS TO PHOTODYNAMIC THERAPY FOR CANCER TREATMENT

✉ gspinesp8@alumnes.ub.edu

G. Spinelli^{1,3}, A. Ferchichi², A. B. Caballero^{1,3}, D. Aguilà^{1,3}, P. Gamez^{1,3}¹ Departament de Química Inorgànica i Orgànica, Facultat de Química, Secció de Química Inorgànica, Universitat de Barcelona, Martí i Franquès, 1-11, 08028 Barcelona, Spain² Laboratory of Material Chemistry, Faculty of Sciences of Bizerte, University of Carthage, Bizerte Zarzouna, Tunisia³ Institute of Nanoscience and Nanotechnology (IN²UB), Universitat de Barcelona, Barcelona, Spain

Ruthenium polypyridyl complexes have gained vast attention in the last twenty years in photodynamic therapy (PDT) as potential photosensitizer agents due to their ability to kill cancer cells under light irradiation. [1] A Ru (II) polypyridyl complex synthesized by McFarland and co-workers is currently in phase II as PDT photosensitizer for the treatment of bladder cancer. [2] Strikingly, and to the best of our knowledge, thiocyanate-based Ru(II) polypyridyl complexes, which are used in dye-sensitized solar cells (DSSCs), have not been investigated as possible candidates in PDT. This type of compounds is well known to display electron-transfer reactions in photo-induced oxidation/reduction processes. [3]

Herein we describe the synthesis and characterization of [Ru(bipy)₂(NCS)(DMSO)]NCS, including its X-ray structure. This water-soluble compound is highly photounstable and able to produce photo-oxidative damage to DNA at low micromolar concentrations.

References

- [1] Luca Conti, Eleonora Macedi, Claudia Giorgi, Barbara Valtancoli, Vieri Fusi. *Coord. Chem. Rev.* 2022, 469, 214656.
 [2] Intravesical Photodynamic Therapy ("PDT") in BCG-Unresponsive/Intolerant Non-Muscle Invasive Bladder Cancer ("NMIBC") Patients. Available from: <https://clinicaltrials.gov/study/NCT03945162>
 [3] Md. K. Nazeeruddin, P. Péchy, M. Grätzel. *Chem. Commun.*, 1997, 1705.

P44

APPLICATION OF NANOMEDICINE FOR THE DEVELOPMENT OF A NOVEL DICLOFENAC FORMULATION FOR PROLIFERATIVE DISEASES

✉ gesteruelas@ub.edu

G. Esteruelas^{1,2}, L. Bonilla^{1,2}, M. Espina^{1,2}, A. Gliszczynska³, M. L. García^{1,2}, E. Sánchez-López^{1,2}¹ Department of Pharmacy, and Pharmaceutical Technology and Physical Chemistry. Faculty of Pharmacy and Food Science. University of Barcelona, 08028 Barcelona, Spain.² Institute of Nanoscience and Nanotechnology (IN²UB). University of Barcelona; 08028 Barcelona, Spain.³ Department of Food Chemistry and Biocatalysis, Faculty of Biotechnology and Food Science, Wrocław University of Environmental and Life Sciences, Norwida 25, 50-375 Wrocław, Poland

Proliferative diseases are identified as one of worldwide leading causes of mortality. Proliferative pathologies include cancer, which is associated to an enormous societal and economic burden [1]. Despite these facts, there is still a pressing need to develop effective treatments. In this area, drugs such as Diclofenac, a non-steroidal anti-inflammatory drug (NSAID) [2] widely known and studied for its anti-inflammatory properties, have shown promising anti-proliferative properties that may be enhanced by combining it with

biodegradable nanoparticulated systems offering a prolonged release.

Therefore, in this study, we optimized and characterized a PLGA-based biodegradable polymeric nanoparticles able to encapsulate Diclofenac (DCF NP) and release it in a prolonged manner. DCF NP formulation was optimized using a rational approach based on factorial design of experiments. A negatively charged monodisperse formulation with an average size below 200 nm, and high loading efficiency was obtained. Moreover, in vitro release was performed by direct dialysis technique obtaining a prolonged release profile and stability of DCF NP, measured monthly, revealed that they were stable for 60 days at 4 °C. Furthermore, in vitro studies, based on DCF NP, demonstrated their ability to enhance antiangiogenic capacity and provide anti-tumoral properties towards leukaemia MV4-11, lung cancer A549 and breast cancer MCF-7 cells without causing cytotoxicity to non-tumoral cells [3].

As a conclusion, a promising nanotechnological formulation with suitable therapeutic properties to be used in the treatment of proliferative diseases has been developed.

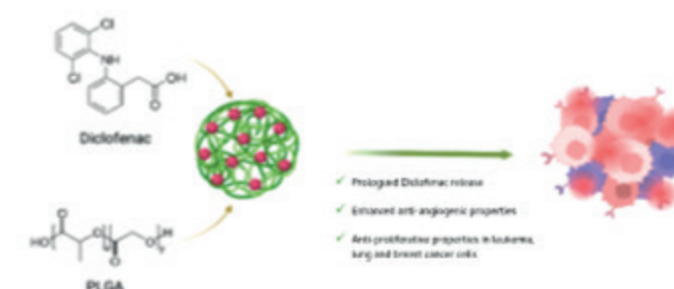


Figure 1. Diclofenac loading into PLGA nanoparticles were able to improve drug release, stability and enhance anti-angiogenic an anti-proliferative property.

References

- [1] Almutairi, M.S.; Hassan, E.S.; Keeton, A.B.; Piazza, G.A.; Abdelhameed, A.S.; Attia, M.I. Antiproliferative activity and possible mechanism of action of certain 5-methoxyindole tethered C-5 functionalized isatins. *Drug Des. Devel. Ther.* 2019, 13, 3069–3078, doi:10.2147/DDDT.S208241.
 [2] Öztürk, A.A.; Namlı, İ.; Güleç, K.; Kıyan, H.T. Diclofenac sodium loaded PLGA nanoparticles for inflammatory diseases with high anti-inflammatory properties at low dose: Formulation, characterization and in vivo HET-CAM analysis. *Microvasc. Res.* 2020, 130.
 [3] Esteruelas, G.; Souto, E.B.; Espina, M.; García, M.L.; Świtalska, M.; Wietrzyk, J.; Gliszczynska, A.; Sánchez-López, E. Diclofenac Loaded Biodegradable Nanoparticles as Antitumoral and Antiangiogenic Therapy. *Pharmaceutics* 2023, 15.

NanoPhotoElectro

P45

UNLOCKING THE POTENTIAL OF METAL OXIDE NANOWIRES: TAILORED SYNTHESIS AND INTEGRATION FOR ADVANCED APPLICATIONS

✉ guillemdomenech@ub.edu ✉ pellegrino@ub.edu ✉ albert.romano@ub.edu

G. Domènech-Gil^{1,2}, A. Estany Macià^{1,2},
R. Pieres Termes², M. López^{1,2}, M. Moreno-Sereno^{1,2},
P. Pellegrino^{1,2}, A. Romano-Rodríguez^{1,2}

¹ Institute of Nanoscience and Nanotechnology,
Universitat de Barcelona, 08028 Barcelona, Spain

² Dept. of Electronic and Biomedical Engineering,
Universitat de Barcelona, 08028 Barcelona, Spain

Introduction

Metal oxide nanowires (NWs) are semiconducting nanomaterials. Their diameter lies below 100 nanometers while their length ranges from few micrometers up to tens of micrometers. Their wire-like morphology exhibits unique properties, and compared to their micro- and macroscopic counterparts, NWs offer improved efficiency in different aspects such as high surface-to-volume, shorter diffusion paths, or less electron scattering. These properties make them suitable for a wide range of applications, including energy storage, optoelectronic devices, and gas sensors.

Materials & Methods

By means of chemical vapor deposition and the vapor-liquid-solid process, our research group fabricates different types of single-crystal NWs of several metal oxides, such as In₂O₃, SnO₂, ZnO or Ga₂O₃. Later, we either fabricate gas sensors based on individual NWs using techniques such as Focused Ion Beam Induced Deposition or Electron Beam Lithography, or we fabricate sensors based on micrometer-sized forests of NWs by growing them directly onto specific locations of gas sensors. We attain a huge versatility in tailoring active regions of the devices, while at the same time improves their cost and simplicity by skipping several fabrication steps.

Results and Discussion

In the last years we have successfully fabricated a series of gas sensor prototypes based on NWs for monitoring toxic and greenhouse gases. The grown nanostructured materials have been structurally characterized confirming their crystalline nature, and their gas sensing properties tested and reported in a series of publication [1-7] that we will summarize. Furthermore, these materials and techniques hold promise for a wider range of applications, and we are open to exploring them further.

References

- [1] G. Domènech-Gil, J. Samà, C. Fàbrega, I. Gràcia, C. Cané, S. Barth, A. Romano-Rodríguez, *Sensors and Actuators B Chemical* 383, 133545 (2023).
- [2] E. Lopez-Aymerich, G. Domènech-Gil, M. Moreno, P. Pellegrino, A. Romano-Rodríguez, *Sensors* 21, 3342 (2021).
- [3] J. Samà, G. Domènech-Gil, I. Gràcia, X. Borrís, C. Cané, S. Barth, F. Steib, A. Waag, J.D. Prades, A. Romano-Rodríguez, *Sensors and Actuators B Chemical* 286, 616-623 (2019)
- [4] L. Hrachowina, G. Domènech-Gil, A. Pardo, M.S. Seifner, I. Gràcia, C. Cané, A. Romano-Rodríguez, S. Barth, *ACS Sensors* 3, 727-734 (2018)
- [5] O. Chmela, J. Sadílek, G. Domènech-Gil, J. Samà, J. Somer, R. Mohan, A. Romano-Rodríguez, J. Hubalek, S. Vallejos, *Nanoscale* 10, 9087-9096 (2018)
- [6] J. Samà, M.S. Seifner, G. Domènech-Gil, J. Santander, C. Calaza, M. Moreno-Sereno, I. Gràcia, C. Cané, S. Barth, A. Romano-Rodríguez, *Sensors and Actuators B Chemical* 243, 669-677 (2017)
- [7] G. Domènech-Gil, S. Barth, J. Samà, P. Pellegrino, I. Gràcia, C. Cané, A. Romano-Rodríguez, *Sensors and Actuators B Chemical* 238, 447-454 (2017).

P46

ZIF-8 BASED SURFACE PLASMON RESONANCE SENSORS FOR CHEMICAL VAPOR OPTICAL DETECTION

✉ anna_estany@ub.edu

A. Estany-Macià^{1,2}, G. Domènech-Gil^{1,2},
I. Fort-Grandas^{1,2}, W. E. Svendsen³,
M. Dimaki³, A. Romano-Rodríguez^{1,2},
M. Moreno-Sereno^{1,2}

¹ Department of Electronics and Biomedical Engineering, University of Barcelona, 08028 Barcelona, Spain

² Institute of Nanoscience and Nanotechnology (IN²UB), University of Barcelona, 08028 Barcelona, Spain

³ Group NABIS, Nanotech Department, Technical University of Denmark, 2800 Kongens Lyngby, Denmark

Introduction

The use of sorption coatings to functionalize samples is a frequent strategy to enhance the sensitivity and selectivity of some gas sensors. In this regard, the nanometer-sized pores of metal-organic frameworks (MOFs) allow the molecular adsorption of gases into their structure, which modulates the refractive index (RI) of this material depending on the amount of adsorbed gas molecules. This research explores their use in surface plasmon resonance sensors (SPR) for volatile organic compound (VOC) optical detection and the further miniaturization of the sensing device to achieve smaller and portable gas sensors.

Materials and methods

A ZIF-8 film (Fig. 1a), which is the MOF that has been used as sorptive coating, is grown via the layer-by-layer deposition method reported by Hupp et. al. [1] on top of SPR substrates containing diffraction gratings (DG) with periods of $\Delta=400$ nm and $\Delta=500$ nm. Gas sensing measurements are then conducted via spectral interrogation at room temperature by placing the samples inside a home-built aluminum chamber with a quartz window which is connected to two mass flow controllers (MFC) that command the gas flux entering the gas chamber. The reflectivity spectra are currently being obtained by a spectrometer and the data is processed with a home-developed MATLAB software.

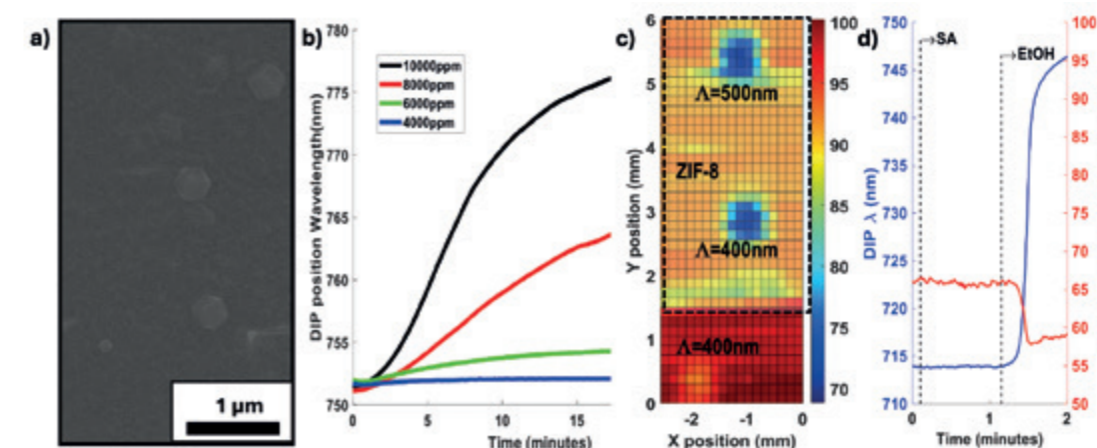


Figure 1. (a) SEM image of a ZIF-8 film (b) Response towards 4000-10000ppm EtOH with $\Delta=500$ nm (c) Simulated reflectivity acquired by a PD using a 660nm-LED to scan the chip (d) red-shift of the $\Delta=400$ nm SPR dip under SA and saturated EtOH atmospheres (blue curve) when illuminating with a 680nm-LED and simulated PD response (red curve).

Results and discussion

The bulk sensitivity of the sensor was measured with liquids and was determined around 387nm/RIU and 527nm/RIU for $\Delta=400$ nm and $\Delta=500$ nm, respectively. Room temperature gas sensing measurements on the ZIF-8 covered DG have been performed by flowing ethanol (EtOH) diluted in dry synthetic air (SA) into the gas chamber, and the estimated RI value change of ZIF-8 under a saturated EtOH atmosphere is $\Delta n = 35\text{nm}/[400\text{nm}/\text{RIU}] = 0.08\text{RIU}$, which is in accordance with the reported values [2]. In Fig.1b, the response towards 4000 to 10000 ppm is shown as example. To further miniaturize our device, measurements are now being conducted by illuminating the sample with LEDs instead of white light (Fig. 1c and 1d), for which the LED needs to be adjusted to the period of the DG and the thickness of the deposited ZIF-8 film to obtain the maximum sensitivity of our sensors. Preliminary simulations (Fig. 1d) suggest that further miniaturization can be done using a photodetector (instead of a spectrometer, which will be the next step.

References

- [1] Lü, G., & Hupp, J. T. (2010). Metal–Organic frameworks as sensors: A ZIF-8 based Fabry–Pérot device as a selective sensor for chemical vapors and gases. *Journal of the American Chemical Society*, 132(23), 7832–7833. DOI: <https://doi.org/10.1021/ja101415b>
- [2] Keppler, N., Hindricks, K. D. J., & Behrens, P. (2022). Large refractive index changes in ZIF-8 thin films of optical quality. *RSC Advances*, 12(10), 5807–5815. DOI: <https://doi.org/10.1039/d1ra08531j>

P47

COUPLED OPTICAL MODES IN TWISTED TRISKELIA NANOSTRUCTURES

✉javier.rodriguez@ub.edu

Rodríguez-Álvarez, J.^{1,2}, García-Martín, A.³, Fraile Rodríguez, A.^{1,2}, Batlle, X.^{1,2}, Labarta, A.^{1,2}

¹ Departament de Física de la Matèria Condensada, Universitat de Barcelona, 08028 Barcelona, Spain

² Institut de Nanociència i Nanotecnologia (IN²UB), Barcelona, 08028, Spain

³ Instituto de Micro y Nanotecnología IMN-CNM, CSIC, CEI UAM+CSIC, Isaac Newton 8, E28760 Tres Cantos, Madrid, Spain

Our work is focused on the design, simulation, and the manufacture of a simple 3D structure that presents large circular dichroism (CD) and polarization-selective near-field distributions in the optical range, which can be easily tuned by adjusting its geometrical parameters [1]. The building block used in this work, so-called “triskelion”, shows three-fold rotational symmetry and has chiral nature (Figure 1a). Our simulations reveal that a stacking of two twisted triskelia presents

a strong dichroic signal in the extinction. The arising dichroism is mainly due to two extra excitations, exhibited by the absorption at wavelengths greater than 0.7 and 1.1 μm , respectively (Figure 1b), which are not present in the single triskelion case. These extra excitations are found only for one of the light circular polarizations (Figure 1c and 1d) and show strong near field distributions between the stacked elements.

The spectral position of these two peaks can be tuned by changing either the edge-to-edge distance between the triskelia or their relative angle of rotation. This enables an accurate control of both the wavelength ranges at which the CD appears and the associated field excitations, providing a simple platform to finely control the chiral response of the system by adjusting two parameters that can be easily modified in the manufacturing process. Such a fine control of the chiral response paves the way for highly specific enantiomer detection through polarization-selective near field interaction.

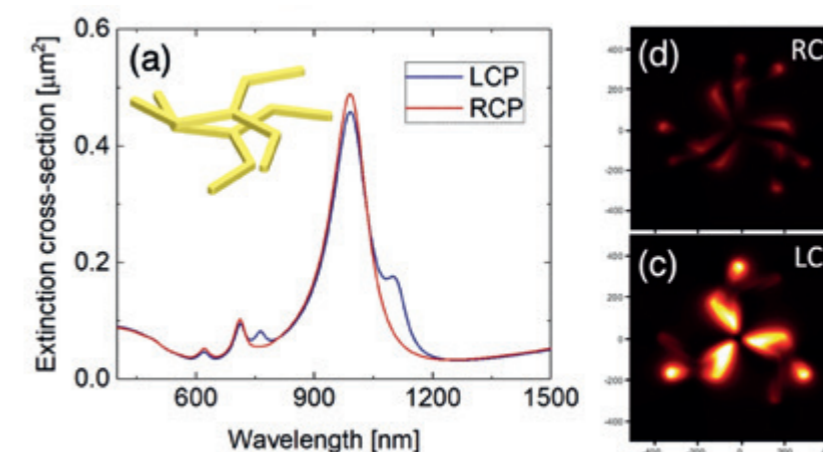


Figure 1. (a) Extinction cross-section for right circular polarization (RCP) and left circular polarization (LCP) with a schematic depiction of the system in the inset. (b) and (c) panels show near field distributions in the plane at the middle between the two triskelia for the extra resonance at 1100 nm for RCP and LCP, respectively

References

- [1] J. Rodríguez-Álvarez, et al., *Scientific reports*, 2022, 12, 1-10.

P48 LEAD-FREE PEROVSKITE-BASED OPTOELECTRONIC DEVICES: ADVANCEMENTS IN FLEXIBLE INKJET PRINTING

✉ gvescio@el.ub.edu

G. Vescio,¹ D. Dirin,² S. González-Torres,¹
J. Sanchez-Díaz,³ V. Chirvony,⁴ J. Pastor,⁴ I. Suarez,⁴
S. Öz,⁵ I. Mora-Seró,³ S. Hernández,¹ A. Cirera,¹
M. Kovalenko,² B. Garrido,¹

¹ MIND-IN²UB, Department of Electronics and Biomedical Engineering, Universitat de Barcelona, 08028 Barcelona (Spain)

² Department of Chemistry and Applied Biosciences, ETH Zürich, Zürich CH-8093, Switzerland; Laboratory for Thin Films and Photovoltaics, Empa-Swiss Federal Laboratories for Materials Science and Technology, Dübendorf CH-8600, Switzerland

³ Institute of Advanced Materials (INAM), Universitat Jaume I (UJI), Avenida de Vicent Sos Baynat, Castelló la Plana 12071, Spain.

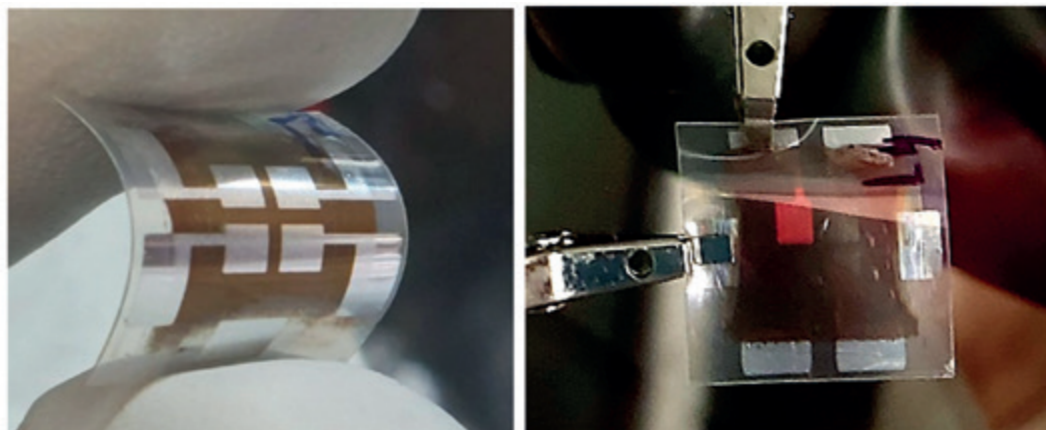
⁴ UMDO, Instituto de Ciencia de los Materiales, Universidad de Valencia, Valencia 46980, Spain

⁵ Saule Technologies, Wroclaw, Poland

Perovskite materials, particularly lead-free tin halide variants, hold significant potential for the development of efficient optoelectronic and electronic microsystems, including image sensors. These advancements can be achieved through accessible fabrication methods such as inkjet printing. Within our research, we have explored innovative avenues with 2D and 2D/3D tin halide perovskites, envisioning their transition into commercially viable products.

Materials & Methods

Throughout our investigations, we have synthesized and experimentally examined various perovskite and perovskite-like materials. Among these, our focus has centered on developing 2D/3D perovskite compounds such as $(R_{0.5}BA_{0.5})_2FA_9Sn_{10}I_{31}$, where R represents PEA, TEA, DIP cations. These compounds facilitate crystallization and stabilize the tin-perovskite phase, crucial for inkjet printing deposition techniques. Additionally, we explored FASn₃ with additives and light soaking for spin-coated films, particularly optimizing vertical lasing structures. Furthermore, we investigated materials like PEA₂SnI₄ and TEA₂SnI₄ for applications in red-emitting LEDs and photonics, along with Cs₃Cu₂Cl₅ and Rb₃InCl₆:Sb for blue and green LEDs.

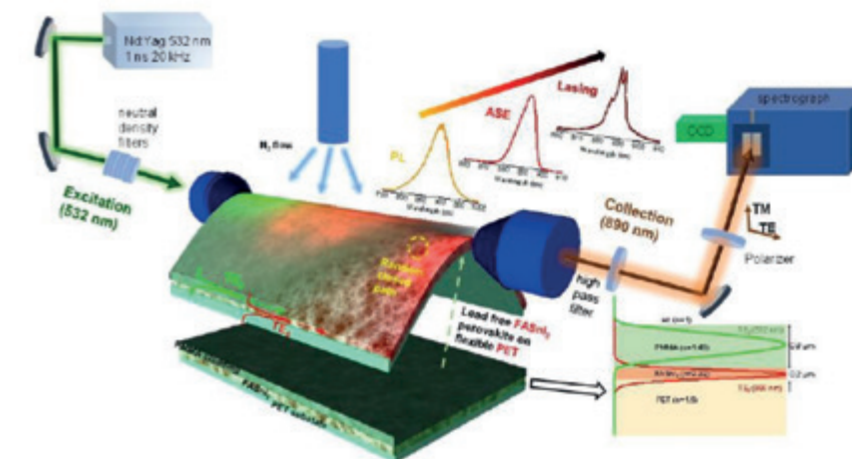
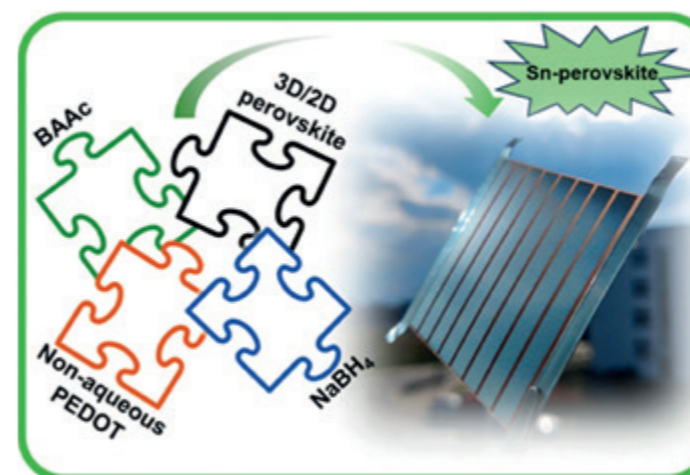


Results and Discussion

Significant progress has been made in photovoltaic devices, including achieving a world-record efficiency for flexible lead-free perovskite solar modules, demonstrating their suitability for indoor applications. This was made possible through the in-situ synthesis of SnI₂ from metallic tin and iodine in a DMF:DMSO solvent. Furthermore, in the realm of lead-free LEDs, we have developed the first inkjet-printed Pb-free perovskite LED emitting at red wavelengths, along with the first on a flexible substrate utilizing common DMF and sustainable DMSO solvents.

In photonics applications, notable advancements include observing ASE/lasing action and near sin-

gle-mode operation in inkjet-printed films of 2D/3D G-LFPs, showcasing their comparable performance to devices implemented with 3D FASn₃ film deposited by spin-coating. Additionally, we have demonstrated the efficacy of 2D/3D G-LFPs in low-level light photodetection, with responsivity as high as 50 A/W measured after one month at 450 nm in encapsulated devices. Flexible photodetectors also exhibited similar performance. Finally, we have established efficient two-photon absorption mechanisms at room temperature in inkjet-printed films of 2D tin-perovskites (including TEA₂SnI₄), leading to effective photodetectors on glass and PET substrates with minimal dark currents.



References

- [1] HP Adl, J Sánchez-Díaz, **G Vescio**, A Cirera et al.; *Tailoring single-mode random lasing of tin halide perovskites integrated in a vertical cavity*, Advanced Materials, **2024**
- [2] **Vescio G.**, J. Sanchez-Diaz, J.L. Friero, et al.; *2D PEA₂SnI₄ Inkjet-Printed Halide Perovskite LEDs on Rigid and Flexible Substrates*, ACS Energy Letters **2022**
- [3] W. Żuraw, F. Vinocour Pacheco, **G. Vescio** et al., *Large-Area, Flexible, Lead-Free Sn-Perovskite Solar Modules* ACS Energy Letters **2023**
- [4] **Vescio G.**, G. Mathiazhagan, S. González-Torres, et al., *Fully Inkjet-Printed Green-Emitting PEDOT:PSS/NiO/Colloidal CsPbBr₃/SnO₂ Perovskite Light-Emitting Diode on Rigid and Flexible Substrates*; Adv. Engineering Mat., **2023**

P49

NON-INVASIVE LIGHT GUIDING IN UNIFORM AND SCATTERING MEDIA VIA PHOTOACOUSTIC EXCITATION

✉ pietro.ricci@ub.edu

P. Ricci^{1,2}, M. Colom¹, B. Mestre-Torà¹, M. Duocastella^{1,2}¹ Department of Applied Physics, Universitat de Barcelona, Barcelona, Spain² Institut de Nanociència i Nanotecnologia, Universitat de Barcelona, Barcelona, Spain

Guiding, focusing, and deflecting light within a medium are pivotal tasks for various light-based applications. Typically, these tasks are performed using bulky optical components, such as lenses or deflectors, that must be positioned external to the sample. Therefore, light control is always managed remotely, which imposes restrictive geometries and constrains the ability to select specific light trajectories. Such a problem is further aggravated in non-uniform media, where scattering can erase the photon directionality provided by external optical elements. As a result, controlled illumination is normally lost at depths of only a few hundred microns, which proves insufficient for imaging, characterizing, or treating organoids or similar tissue-like constructs.

A straightforward solution to this problem is using miniaturized optical elements like microlenses, and micro-endoscopes, which can be directly inserted into the medium of interest. While deep light control has been demonstrated in areas such as photodynamic therapy, two-photon microscopy, and optogenetics, these elements are intrinsically invasive. A promising

alternative is to use ultrasound waves directly inside a sample. In this case, the refractive index gradients generated by ultrasound act as embedded and non-invasive lenses or waveguides. Unfortunately, generating shaped ultrasound waves presents challenges, often involving acoustic resonant cavities driven by piezoelectric transducers. In such configurations, the geometry of the piezoelectric remains fixed, limiting flexibility. Additionally, external transducers optimized for continuous high-intensity ultrasound emission can risk tissue damage.

Here, we exploit the photoacoustic effect to generate localized ultrasound waves, enabling precise light guidance inside homogeneous and scattering media without external acoustic elements. As shown in Figure 1, we send laser pulses (pump) into a light-absorbing layer consisting of a mixture of polydimethylsiloxane and candle soot nanoparticles (CSNPs), to launch ultrasound waves into the medium. A second laser beam (probe), orthogonal to the pressure wave, is then sent to interact with the sound-perturbed region. As a result, guiding of the probe beam is achieved, which properties can be adjusted by simply tuning the parameters of the pump laser. Experimental and simulation studies validate this method for guiding light over millimeter ranges within various scattering phantoms. Our approach is a step forward toward the real-time and non-invasive control of light directly within a sample of interest.

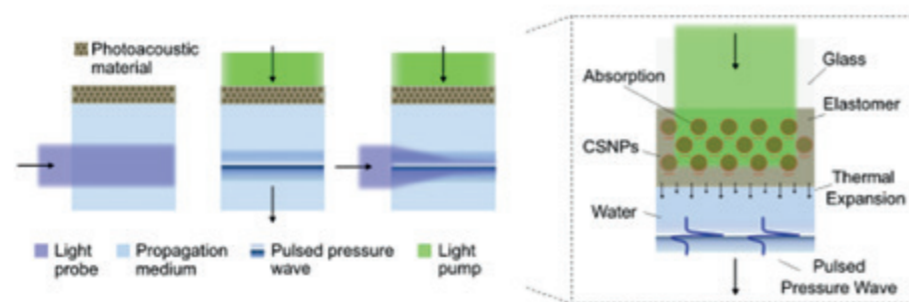


Figure 1. Schematic of the principle of photoacoustically generated waveguide and light confinement. Without sound wave generation, a probe light beam enters a low-scattering medium, without being affected (left). A short light pulse excitation of the photoacoustic material generates a pressure wave (center). The pressure wave focuses and guides the light probe inside the material (right). Zoomed panel: detail of the photoacoustic generation using candle-soot nanoparticles (CSNPs).

P50

MUELLER MATRIX POLARIZATION SPATIAL FREQUENCY DOMAIN IMAGING SYSTEM (pSFDI) FOR MAPPING BIOLOGICAL TISSUES

✉ iago.pardo@ub.edu

I. Pardo, E. Pascual, O. Arteaga

Dep. Física Aplicada, PLAT group, Universitat de Barcelona, IN²UB

Several optical imaging modalities based on the anisotropic scattering and fluorescence of incident light have been used to investigate the biological tissues microstructure. Common polarization microscopy techniques such as polarization sensitive coherence tomography or small angle light scattering have high sensitivity to fiber structures [1] and can finely resolve tissue samples in 2D and 3D volumes but also present limitations. Some techniques are confined to measurements across relatively small regions of interest (<1cm²) or require extensive scanning times. Due to this, there is a clear need for a rapid, non-destructive, wide-field imaging technique to quantify the microstructure of different biological tissues.

A large volume of work exists in polarized light imaging and Mueller matrix polarimetry of biological tissues [2]. These techniques allow characterization of the polarimetric properties of tissues, and have been

used to relate polarization dependent optical properties to various underlying structural and physiological features [3]. Importantly, polarized light imaging can be performed in wide-field with adjustable fields-of-view, allowing large sample areas to be imaged rapidly. However, polarization imaging systems have some inherent challenges as the not capability of distinguish distinct tissue layers within the sample. Transmissive polarization systems measure average optical anisotropy through the entire sample thickness, while reflective polarization systems average through a sampling depth up to several millimeters in biological samples.

The main objective of this work is to implement a full functional Mueller Matrix polarization Spatial Frequency Domain Imaging system which provides sensitivity to tissue structure. The use of structured illumination allows reduction of the effective imaging depth to distinguish superficial tissue layers, on the order of several hundred microns thick and also, is able to separate the effect of optical absorption and scattering by observing how a sample alters a 2-D sinusoidal illumination pattern.

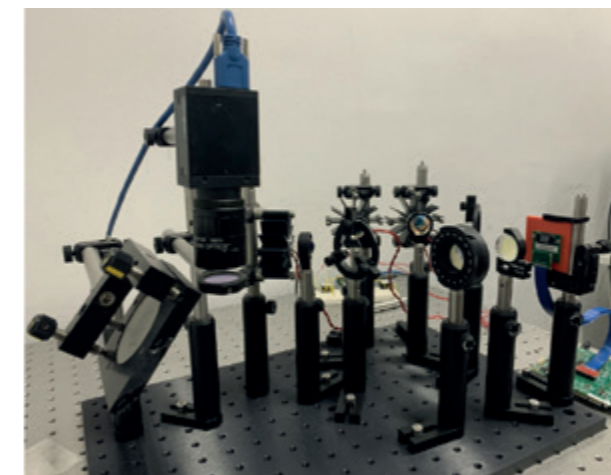


Figure 1. Our pSFDI System consist mainly in three LEDs as light sources (all emit in the red or near-infrared spectrum), different lenses to collimate light and image the sinusoidal patterns, polarizers and retarders to generate and analyze the polarization states and a digital micromirror device (DMD) to generate the patterns. This system has been used to analyze the effect of the the optical absorption and scattering of several biological tissues in order to mapping different polarimetric properties of the samples.

References

- [1] Allen, A. C., et. al. Electrospun poly(*N*-isopropyl acrylamide)/poly(caprolactone) fibers for the generation of anisotropic cell sheets. *Biomater. Sci.* 5:1661-1669, 2017.
- [2] Qi, J., and D. S. Elson. Mueller polarimetric imaging for surgical and diagnostic applications: a review. *J. Biophotonics* 10:950-982, 2017.
- [3] Sun, M., et. al. Characterizing the microstructures of biological tissues using Mueller matrix and transformed polarization parameters. *Biomed. Opt. Express* 5:4223-4234, 2014.

P51

3D SHAPE CONTROL OF LASER-PRINTED PARTS WITH SUBSTRATE RESHAPING

✉ emartije7@alumnes.ub.edu

E. Martí Jerez^{1,2}, J. M. Fernández-Pradas^{1,2}, P. Serra^{1,2}, M. Duocastella^{1,2}

¹ Department of Applied Physics, Universitat de Barcelona, C. Martí i Franquès 1, 08028 Barcelona, Spain

² Institute of Nanoscience and Nanotechnology (IN²UB), Universitat de Barcelona, 08028, Barcelona, Spain

Additive manufacturing (AM) is becoming the gold standard for the customized fabrication of entire multilayered devices directly from digital layouts. Among AM techniques, laser-induced forward transfer (LIFT) offers a unique combination of design selection, speed, and compatibility with a wide range of materials. For instance, highly viscous liquids and high particle-content inks can be printed with LIFT beyond the possibilities of ink-jet printing. However, when operating with liquid inks – which is of high interest in optoelectronics – the three-dimensional (3D) shape of the LIFT-printed structures is out of the manufacturer's control – it is determined by the wettability between liquid and substrate. Consequently, structures

such as microlenses or electronic circuit lines exhibit a fixed geometry in terms of contact angle and aspect ratio, respectively.

Here we introduce a novel approach for printing structures beyond the limits imposed by the liquid-substrate wettability. Termed print-n-release, our method consists of LIFT-printing structures on top of mechanically pre-stretched substrates.[1] Provided pinning of the contact line, a contraction on the liquid printed structures can be induced upon relaxation of the substrate stress, all while their 3D shape is modified according to the substrate miniaturization. Thus, by adjusting the initial elongation of the substrate, we can achieve an on-demand control of the contact angle of drops and the aspect ratio of lines. As shown in Figure 1(a), print-n-release allows for microlens printing with an increased contact angle of up to 400% and a decreased focal length down to 90% compared to traditional LIFT-printing. Similarly, conductive silver tracks can be fabricated with an increased aspect ratio of up to 800% (Figure 1(b)). Our results are a promising step toward the rapid printing of materials with customized 3D shapes.

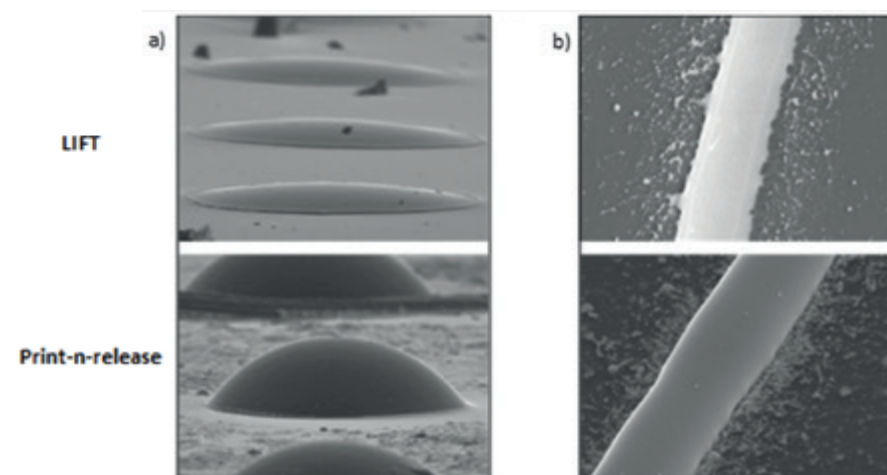


Figure 1. Examples of additively manufactured structures using print-n-release. a) SEM images of polymeric microlenses fabricated with traditional LIFT (up) and with print-n-release (down). b) Conductive tracks containing silver nanoparticles printed with traditional LIFT (up) and print-n-release (down). Scale bars are 10 μm in all images.

References

- [1] E. Martí Jerez, J. M. Fernández Pradas, P. Serra, M. Duocastella, *Substrate reshaping for optically tuned liquid-printed microlenses beyond their wetting properties*, Adv. Mater. Technol. 2023, 2300564, 1

P52

INSIGHTS INTO INKJET-PRINTED 2D TIN IODIDE PEROVSKITE: OPTICAL AND OPTOELECTRONIC ANALYSES

✉ gvescio@el.ub.edu

G. Vescio¹, D. Dirin², S. V. Chirvony³, J. Pastor³, I. Suarez³, S. Öz⁴, S. Hernández¹, A. Cirera¹, M. Kovalenko², B. Garrido¹

¹ MIND-IN²UB, Department of Electronics and Biomedical Engineering, Universitat de Barcelona, 08028 Barcelona (Spain)

² Department of Chemistry and Applied Biosciences, ETH Zürich, Zürich CH-8093, Switzerland; Laboratory for Thin Films and Photovoltaics, Empa - Swiss Federal Laboratories for Materials Science and Technology, Dübendorf CH-8600, Switzerland

³ UMDO, Instituto de Ciencia de los Materiales, Universidad de Valencia, Valencia 46980, Spain

⁴ Saule Technologies, Wroclaw, Poland

In recent years, metal halide perovskites (MHPs) have gained attention for their potential in producing cost-effective and efficient solar cells and LEDs. Notably, lead halide perovskite-based solar cells have seen a remarkable increase in efficiency, surpassing 25% for single-junction devices and even higher for tandem configurations. However, concerns about the toxicity of lead and its recycling have sparked a search for lead-free MHPs with similar performance. While lead-free MHP-based solar cells have made significant strides, the development of lead-free MHP-based LEDs and other optoelectronic devices lags behind. This gap highlights the challenge of fabricating Pb-free perovskite optoelectronic devices using scalable techniques.

Materials & Methods

For solar cell fabrication, MHPs with a 3D framework are preferred due to their low exciton binding energies, while 2D MHPs are promising for perovskite-based LEDs. Tin-based MHPs, in particular, show potential for lead-free LEDs, although challenges such as oxidation-induced p-doping persist. Strategies such as the addition of SnF₂ and doping with Cl have shown promise in mitigating these challenges. Inkjet printing

has emerged as a promising technique for fabricating perovskite devices at scale, offering advantages such as precise deposition and reduced precursor wastage. Additionally, 2D tin iodide perovskites exhibit narrow two-band excitonic photoluminescence, though structural strains may cause spectral inhomogeneity. Photoconductivity studies of thin films deposited via inkjet printing have shown promising characteristics for photodevices, with stable performance over time. These findings suggest the potential of inkjet-printed perovskite devices for practical applications, albeit with ongoing challenges in stability under ambient conditions.

Results and Discussion

In the present work, thin films of TEA₂SnI₄ were deposited on a flexible polyimide substrate by inkjet-printing of chemically stabilized molecular precursors and both room and low temperature PL properties of the material were investigated. TEA₂SnI₄ thin films demonstrated narrow two-band excitonic PL both at room and low temperatures, while micro-PL measurements revealed a noticeable inhomogeneity of the excitonic bands spectral positions over the sample surface. We suggest that structural strains, especially at the flat-grain boundaries, may be responsible for the presence of these two bands in PL spectra of TEA₂SnI₄ thin films. Photoconductivity was also measured in thin films deposited on top of ITO interdigitated electrodes prepatterned in glass and flexible photodevices. These devices were encapsulated using an appropriate epoxy and measured over several days without any degradation. Responsivities of the order of 1 and 20 A/W using flexible and glass devices, respectively, were extracted under very low excitation powers (< 10 nW), whereas a slow frequency response was measured by using an electrically modulated laser source, which is consistent with a non-exponential time response compatible with fast and slow time response components, which is consistent with the presence of trap levels spanning over a relatively large energy range.

References

- [1] HP Adl, J Sánchez-Díaz, G Vescio, A Cirera et al.; *Tailoring single-mode random lasing of tin halide perovskites integrated in a vertical cavity*, Advanced Materials, 2024
- [2] Vescio G., J. Sanchez-Diaz, J.L. Friero, et al.; *2D PEA₂SnI₄ Inkjet-Printed Halide Perovskite LEDs on Rigid and Flexible Substrates*, ACS Energy Letters 2022
- [3] W. Żuraw, F. Vinocour Pacheco, G. Vescio et al., *Large-Area, Flexible, Lead-Free Sn-Perovskite Solar Modules* ACS Energy Letters 2023
- [4] Vescio G., G. Mathiazhagan, S. González-Torres, et al., *Fully Inkjet-Printed Green-Emitting PEDOT:PSS/NiO/Colloidal CsPbBr₃/SnO₂ Perovskite Light-Emitting Diode on Rigid and Flexible Substrates*; Adv. Engineering Mat., 2023

P53 GUIDING LIGHT DEEP IN SCATTERING MEDIA WITH SHAPED ULTRASOUND WAVES

✉ blanca.mestretora@ub.edu

B. Mestre-Torà¹, M. Duocastella^{1,2}

¹ Department of Applied Physics, University of Barcelona, 08028 Barcelona, Spain

² Institut de Nanociència i Nanotecnologia (IN²UB), University of Barcelona, 08028 Barcelona, Spain

Optical methods are extensively used as non-invasive techniques for diagnoses and treatment procedures in life sciences. However, limited by the scattering of light, most optical techniques can only be applied inside biological tissue or other tissue-like constructs at depths of a few hundred microns [1]. This is a key constraint toward the further development of personalized medicine or the in-vivo monitoring of biomolecular processes. Several strategies have been developed to address this challenging issue, including endoscopy and wavefront shaping methods, but they typically come at the cost of losing spatiotemporal resolution or becoming invasive [2]. Here, we propose an alternative method based on using ultrasound waves to rapidly and safely guide light deep inside scattering media. Our approach is based on using pressure waves to directly modulate the optical properties of the medium of interest. In particular, a refractive index modulation is induced which effectively acts as an embedded waveguide inside the scattering medium, helping

redirect scattered photons toward deeper sections. We implement our strategy using ultrasound resonant elements filled with a turbid fluid. First, we employed a cylindrical piezoelectric cavity, as shown in Figure 1a. When driven in resonance, it generates a virtual waveguide inside the medium. Supported by Monte Carlo simulations, our results demonstrate that ultrasound modulation enables focusing and preserving light confinement up to a depth of around 15 mean free paths (MFP). Notably, combined with a point-by-point scanning system, this approach is suitable for visualizing samples inside scattering media that would remain hidden with conventional imaging methods [3]. To enhance and parallelize the guiding effect, we changed the geometry of the ultrasound source by using two perpendicularly oriented piezoelectric plates, as shown in Figure 1b. This configuration generates multiple parallel virtual waveguides within the medium, facilitating the guidance of light to multiple regions simultaneously over an area of 3x3 mm². Using this approach, we successfully demonstrated a 42% enhancement of the light intensity delivered at a depth of 2 cm within a 12.5 MFP scattering sample. These results open the door to delivering light at depths not currently accessible in applications as relevant as photoacoustic tomography, optical coherence tomography, or photodynamic therapy.

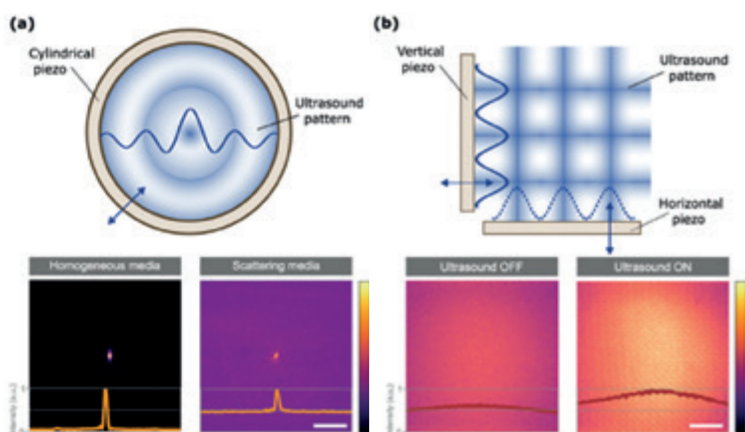


Figure 1. Light guiding in scattering media with shaped ultrasound waves. (a) Schematic representation of the cylindrical piezoelectric used to generate a single virtual waveguide embedded in a medium. The images exemplify the ultrasound-induced focused beam in a homogeneous medium (left) and a scattering medium with $\tau = 14.5$ (right). Scale bars are $130 \mu\text{m}$. (b) Schematic representation of the piezoelectric plates used to generate the multiple virtual waveguides embedded in a medium. The images illustrate the beam at the output of a scattering medium of $\tau = 12.5$ with ultrasound OFF (left) and ON (right). Scale bars are $680 \mu\text{m}$.

References

- [1] V. Ntziachristos. Going deeper than microscopy: The optical imaging frontier in biology. *Nature Methods* 7, 603–614 (2010).
- [2] X. Yu, S. Zhang, M. Olivo, N. Li. Micro- and nano-fiber probes for optical sensing, imaging, and stimulation in biomedical applications. *Photonics Res* 8, 1703 (2020).
- [3] B. Mestre-Torà, M. Duocastella. Enhanced light focusing inside scattering media with shaped ultrasound. *Scientific Reports* 13, 11511 (2023).

P54 STRUCTURAL AND OPTICAL CHARACTERIZATION OF INKJET-PRINTED CsCu₂I₃ THIN FILMS

✉ jdiagofu@ub.edu

J. D. Forero^{1,2}, J. Mari-Guaita^{1,2}, G. Vescio^{1,2}, F. Palacio^{1,2}, B. Garrido^{1,2}, S. Hernandez^{1,2}, A. Cirera^{1,2}

¹ MIND, Department of Electronics and Biomedical Engineering, Universitat de Barcelona, Martí i Franquès 1, E-08028, Barcelona, Spain.

² Institute of Nanoscience and Nanotechnology (IN²UB), Universitat de Barcelona, Av. Joan XXIII S/N, E-08028, Barcelona, Spain.

Inorganic Halide Perovskites (inorganic HPs) represent a class of novel materials that stand out for their unique properties such as high carrier mobility, broad-band emission wavelengths, and extended lifetime [1]. They are typically composed of two different cations and an anion, where iodide (I⁻), bromide (Br⁻), or chloride (Cl⁻) are the anion, along with cesium (Cs⁺) and lead (Pb²⁺) as the cations. Nevertheless, despite the excellent compatibility of Pb in the IHP, it presents significant toxicity concerns [2]. As a result, the research for non-toxic alternatives has led to investigations for replacing the Pb with elements such as copper (Cu⁺), that led to the development of compounds exhibiting an intriguing emission mechanism: self-trapped exciton (STE) mechanism [3].

In this study, CsCu₂I₃ inorganic HP was synthesized via precursor chemistry and transferred to a substrate as a thin film by inkjet-printing technique. The deposited films were structurally characterized by X-ray

diffraction (XRD) and their optical properties were assessed by transmittance/reflectance spectroscopy and photoluminescence (PL) spectroscopy.

The ink preparation process involved dissolving CsI (0.47 mol) and CuI (0.94 mol) in Dimethylsulfoxide (DMSO, 4 ml) at 60 °C for 2 hours. Subsequently, 1.5 ml of the solution was filtered through a 0.22 μm PTFE filter and loaded into a Dimatix cartridge, which is equipped with a 21-μm nozzle-diameter, enabling the ejection of 10 pl droplets. Inkjet printing, either on silicon or fused silica substrates, was performed using a Fujifilm Dimatix Inc. printer, varying the number of layers for controlling the film thickness. After deposition, the films underwent annealing at 100 °C for 5 minutes, under a vacuum of 65 mbar. In the case of XRD, the film presented 12 layers, whereas a comparison between 6 and 12 layers was done in the case of transmittance/reflectance and PL spectroscopies. In all cases, the drop spacing employed is 80 μm to achieve a high compact and homogeneous film.

The XRD analysis revealed major diffraction peaks at 13.45°, 27.06°, 41.08°, and 55.77°, which is consistent with the *Cmcm*-CsCu₂I₃ phase [4]. On the other hand, the analysis by transmittance/reflectance spectroscopy exhibits a band gap energy of 3.79 eV. By exciting the films at 3.81 eV, there is a broad emission centered at 2.17 eV, indicating a large Stoke shift, which is compatible with the self-trapped exciton mechanism.

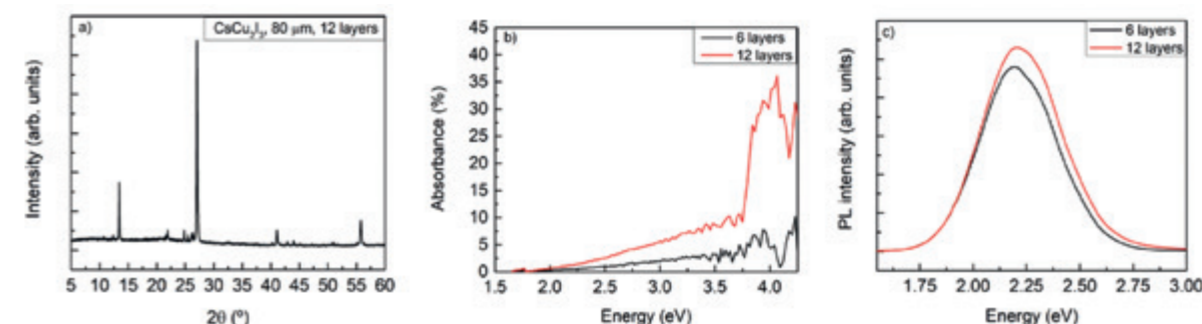


Figure 1. Optical and structural characterization of CsCu₂I₃ thin films. a) XRD spectra, b) Absorbance-energy graph and c) PL spectra.

References

- [1] H. Dong *et al.*, *eLight* 3, 3 (2023).
- [2] M. V. Kovalenko *et al.*, *Science* 358, 745 (2017).
- [3] Z. Ma *et al.*, *Adv. Mater.* 35, 2300731 (2023).
- [4] N. Jouini *et al.*, *Revue de Chimie Minerale* 17, 486 (1980).

P55 TRIPHENYLENE METAL-ORGANIC FRAMEWORKS AS A PLATFORM FOR CATALYSIS APLICATIONS

✉ yuzelfymendoza@ub.edu

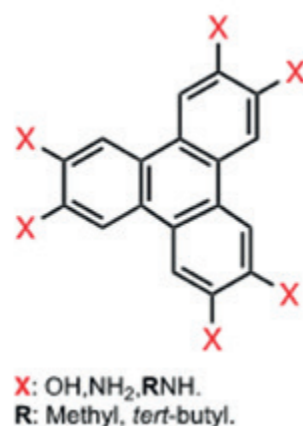
Y. Mendoza-Gamero^{1,2,3}, S. Gonzalez-Martinez³,
A. Romano-Rodriguez^{1,2}, D. Sainz-García^{2,3}

¹ Electronic and Biomedical Engineering Department,
Universitat de Barcelona, Barcelona, Spain.

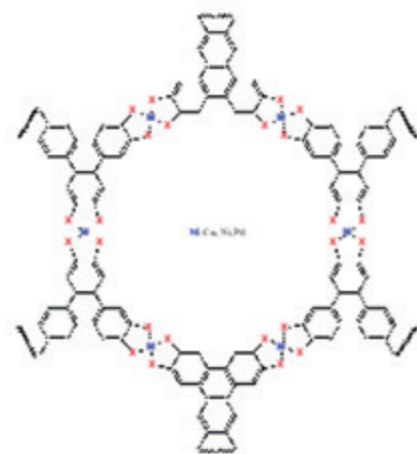
² Institute of Nanoscience and Nanotechnology
(IN²UB), Universitat de Barcelona, Barcelona, Spain.

³ Inorganic and Organic Chemistry Department,
Universitat de Barcelona, Barcelona, Spain.

High levels of greenhouse gases and the high demand for fossil-based chemicals are among the biggest environmental problems today. That is why the control of these gases, and the use of new materials from outside the carbon cycle, are crucial to mitigate this environmental catastrophe. Thus, on the one hand, sensitive, selective, and energy-efficient equipment must be developed. On the other hand, it is important to know new methods of biomass conversion through electrochemical mechanisms to avoid the excessive use of fossil fuels. Therefore, the aim of this study is the development of advanced metal-organic frameworks (MOF) materials. These materials have a high porosity and a reasonable conductivity to be used as gas detectors in a selective way. In addition, MOFs, which have a large surface area, and the ability to modulate their pore size, are materials with high capabilities for catalytic applications.



The functionalization of ligands in MOF is beneficial to increase the selectivity, catalytic performance, and improve their stability. It also allows the incorporation of additional functionalities and facilitates the synthesis and processing. Up to now, much attention has been focused on MOFs consisting of functional groups, being amine-functionalized MOFs the most investigated due to their basic amine being able to generate active sites for catalysis and display a strong affinity to acidic gas molecules [1].



We have synthesized hexa-amino-triphenylene ligands using tert-butylamine via Buchwald-Hartwig reaction, and 4-(4,4,5,5-Tetramethyl-1,2,3-dioxoborolan-2-yl) aniline via Suzuki reaction according to the methods reported in the literature [2, 3]. The resulting MOFs have been characterized using techniques such as PXRD, SEM, and EDS to confirm their crystalline nature, morphology, and components.

The synthesized MOFs present unique structures that allow the immobilisation of catalytically active metal centres, such as palladium, copper or nickel, within the structure. The resulting MOF-based catalysts show high activity and selectivity in Suzuki-Miyaura coupling reactions with NADES (Natural Deep Eutectic Solvents) and in electro-catalytic reactions [4] due to its great pore size. The performance of these MOFs in catalysis applications will be presented.

References

- [1] Liu, J, et al. *Coordination Chemistry Reviews*. 2018, 376, 518-535.
- [2] Gonell, Sergio, et al. *Angew. Chem. Int. Ed.* 2013, 52, 7009-13.
- [3] Mircea Dincă, et al. *J. Am. Chem. Soc.* 2020 142 (28), 12367-12373.
- [4] Hapeng Zhang, et al. *ASC Catal.* 2024, 14, 449-462.

P56 SYNCHRONIZATION DYNAMICS IN OPTOMECHANICAL CRYSTAL CAVITIES

✉ dnavarro@ub.edu

D. Alonso-Tomás¹, D. Navarro-Urrios¹

¹ MIND-IN²UB, Departament d'Enginyeria Electrònica i Biomèdica, Facultat de Física, Universitat de Barcelona, Martí i Franquès 1, Barcelona, Spain

Although nature presents a tendency toward disorder, systems that adjust their rhythms to oscillate in harmony, usually referred to as synchronization, can be found everywhere. In fact, synchronization emerges wherever oscillating systems and weak interactions among them exist, from planetary orbits, to cardiac rhythms, the human brain, and even chemical reactions. Due to advancements in the electronics industry, this phenomenon has found important applications in enhancing the performance of digital processing elements. Now, with integrated photonic technology aiming to process optical signals on a chip, there is a need for reference signals to synchronize actions, thereby preventing errors in processing optical systems or communication interfaces. In this context, optomechanics, the branch of physics that studies the interaction between light and mechanical excitations, can play a critical role, since optomechanical oscillators can generate coherent mechanical motion of high amplitude using the radiation pressure force exerted by light [1].

From the entire subset of devices present in the literature, in this work, we utilize silicon one-dimensional optomechanical crystal cavities (see Fig. 1a). These are suspended nanobeams capable of generating optical confinement through the use of periodic structures, which support mechanical modes that oscillate at frequencies of tens of MHz, particularly in the case of the flexural ones (Fig. 1a). The alternation of regions of high and low dielectric constant (silicon and air) gene-

rates a certain range of frequencies of light that are not allowed to pass through the geometry, acting as a mirror. By introducing a defect at the center of the structure, we can create an optical mode that is allowed there but not outside of it, thereby preventing leakage and increasing the force that light exerts on the mechanical structure [2]. In this way, light plays an active role in providing amplification to the mechanical modes supported by the geometry, but also a passive one as the mechanical oscillation influences the light itself.

To introduce light into this geometry, we employ an optical fiber thinned down to a diameter of around 1 μm (see Fig. 1b), ensuring it possesses a large evanescent field. A loop is performed on its thinnest region to facilitate the probing of the structures. When the geometries are placed in the near field of the fiber and laser light resonates with the optical mode, light is coupled. The output light, containing information about the mechanical oscillation of the geometry, can be detected and analyzed using electronic equipment. Fig. 1c provides a transmission spectrum obtained by averaging output power of light when a sweep in the incident laser wavelength is performed. Here, the coupling of light to the geometry is clearly observed as a dip in the transmission. Using this setup, we conduct synchronization experiments where these geometries are coupled through the optical or the mechanical domain. Results show that it is possible to synchronize the motion of a pair of optomechanical nanobeams using a mechanical link between them or providing an external feedback to the input light that arrives at one of the cavities. These observations lay the groundwork for the distribution of reference signals in future photonic integrated circuits and the understanding of the nonlinear behavior that could emerge in those systems.

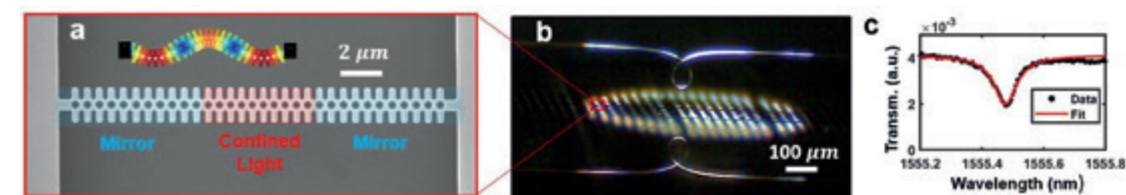


Figure 1. (a) SEM image of the optomechanical structure used in this work. Confined optical mode lies in the center of the geometry. Inset: Three-antinode mechanical flexural mode computed by FTDT simulations. (b) Micro-loop shaped tapered fiber approaching the sample. (c) Optical transmission spectra corresponding to one of the cavity modes. A Lorentzian fit is performed to data.

References

- [1] T. J. Kippenberg, H. Rokshari, T. Carmon et al. Analysis of the radiation-pressure induced mechanical oscillation of an optical microcavity. *Phys. Rev. Lett.* 95, 033901 (2015).
- [2] M. Aspelmeyer, T. J. Kippenberg and F. Marquardt. Cavity optomechanics, *Rev. Mod. Phys.* 86, 1391 (2014).

P57

STUDYING TRIPHENYLENE DERIVATIVE MOFS FOR ROOM-TEMPERATURE GREENHOUSE GAS SENSING

✉ ignfortgra_9@ub.edu

I. Fort-Grandas^{1,2,3}, Y. Mendoza-Gamero^{1,2,3},
G. Domènech-Gil^{1,2}, P. Pellegrino^{1,2}, M. Moreno-Sereno^{1,2},
A. Vidal-Ferran^{2,3,4}, A. Romano-Rodríguez^{1,2}

¹ Department of Electronic and Biomedical Engineering, University of Barcelona (UB), 08028 Barcelona

² Institute of Nanoscience and Nanotechnology (IN²UB), University of Barcelona (UB), 08028 Barcelona

³ Department of Inorganic and Organic Chemistry, Section of Inorganic Chemistry, University of Barcelona (UB), 08028 Barcelona

⁴ Catalan Institute for Research and Advanced Studies (ICREA)

Recent droughts and extreme climate events have stressed on the already established importance of monitoring Greenhouse Gases (GHGs) levels. Being able to follow with accuracy and precision the emissions of these gases is essential in order to develop effective climate change strategies based on reliable models. In that endeavour, sensors play a key role to provide the necessary data. Current available systems for GHGs sensing are complex, bulky and expensive, which means they are bound to few fixed locations. Therefore, the need arises of developing efficient miniaturized sensing devices with low power consumption and good sensing properties such as response, sensitivity and selectivity.

Most solid-state gas sensing technologies come from devices that are made from semiconducting metal oxides (MOX), which despite improved properties through intensive research still face two major drawbacks: their relatively high operating temperature

(above 150 °C) and their poor selectivity. We study the use of metal-organic frameworks (MOFs) to overcome the aforementioned limitations: room-temperature chemoresistive sensing has been achieved via conductive MOFs [1]. MOFs are organic-inorganic hybrid crystalline materials consisting in a regular array of metal “nodes” surrounded by organic “linker” molecules that form a cage-like structure with extremely high surface area and porosity. The huge structural and chemical diversity provided by the available metals and linkers allows al-most infinite possibilities of tuning the properties of MOFs. This porosity, together with the strong interaction between the material and the surrounding ambient, has made MOFs ideal material for gas capture and conversion [2], as well as very interesting candidates for sensing. Among the different properties that MOFs can present, a reduced subfamily, known as conductive MOFs, present an electrical conductivity which is comparable to that of solid-state semi-conducting materials. In addition, some of them present the ability to change their conductance by the chemical atmosphere surrounding them [3].

We have synthesized triphenylene derivative MOFs, using 2,3,6,7,10,11-hexahydroxytriphenylene (HHTP) and 2,3,6,7,10,11-hexaaminotriphenylene (HITP) as ligands and Co(II), Ni(II), Cu(II), Zn(II) to yield M₃(HOTP)₂ and M₃(HITP)₂ respectively. The obtained MOFs were deposited onto interdigitated electrodes (IDE) for the sensor fabrication. The deposition was performed by drop-casting a suspension of the MOF directly on top of the IDE, yielding a thin layer of the material in the device which allows for electrical characterization and gas sensing studies. In this work we will present the results of our study of triphenylene derivative MOFs for chemiresistive gas sensing of CO₂ and CH₄.

References

- [1] Y. Li, A. Xiao, B. Zou, H. Zhang, K. Yan, Y. Lin, *Advances of metal-organic frameworks for gas sensing*, *Polyhedron* 154, 83-97 (2018); doi: 10.1016/j.poly.2018.07.028.
[2] M. Ding, R. Flaig, H. Jiang, O. Yaghi, *Carbon capture and conversion using metal-organic frameworks and MOF-based materials*, *Chem Soc Rev* 48, 2783-2828 (2019); doi: 10.1039/C8CS00829A.
[3] E. Miner, L. Wang, M. Dincă, *Modular O₂ electro-reduction activity in triphenylene-based metal-organic frameworks* *Chem. Sci.* 9, 6286-6291, (2018); doi: 10.1039/c8sc02049c.

P58

TWO-DIMENSIONAL TRANSITION METAL DICHALCOGENIDES FOR GAS SENSING APPLICATIONS

✉ gboafobo7@alumnes.ub.edu

G. Asew Boafo¹, A. Romano-Rodríguez^{2,3},
D. Sainz-García^{1,3}, D. Navarro-Urrios^{2,3}

¹ Inorganic and Organic Chemistry Department, Universitat de Barcelona, Barcelona, Spain

² Electronic and Biomedical Engineering Department, Universitat de Barcelona, Barcelona, Spain.

³ Institute of Nanoscience and Nanotechnology (IN²UB), Universitat de Barcelona, Barcelona, Spain.

Climate change is one of the most pressing global challenges of our time, with the emission of greenhouse gases (GHGs) being a significant contributor. To effectively combat climate change, accurate and reliable monitoring of these gases is crucial. Detecting GHGs like carbon dioxide, methane, nitrous oxide, and ozone constitutes the primary and principal phase in discovering solutions to effectively control and diminish the concentrations of these gases in the Earth's atmosphere [1]. The most widely employed materials in gas sensing applications, semiconducting metal oxides, show significant drawbacks such as high-power consumption, poor long-term stability, limited selectivity, hindering their efficiency in providing real-time data critical for climate change mitigation strategies.

The utilization of two-dimensional (2D) nanomaterials holds immense promise in gas sensing endeavours due to their layered structures. In particular, 2D transition metal dichalcogenides (TMDs) exhibit noteworthy features such as high surface areas and distinctive semiconductor properties characterized by tuneable band gaps, with potential to improve the sensing parameters, such as sensitivity, selectivity, stability, and speed (response-recovery time) of gas-sensitive materials. [2]. Although TMDs offers several advantages and excellent properties, surface functionalization of 2D TMDs is a potential route for further enhancing their properties and adding extra functionalities to the surface of the fabricated sensor. The incorporation of novel metals, metal oxides into

2D TMDs is an approach for improving the gas sensing performance of these materials by the synergistic effects of the hybridization [3].

Though various methods exist in literature for fabricating 2D layered materials, achieving an edge-enriched morphology is vital for gas sensing applications. In this regard, a facile synthesis route was developed via a combination of liquid-phase exfoliation and lithium(Li) intercalation exfoliation to develop TMDs materials, such as MoS₂, WS₂, MoS₂/ZnO, WS₂/Pt, MoS₂/Pt, WS₂/SnO, MoS₂/SnO, WS₂/ZnO. We have synthesized and functionalized two-dimensional layered materials with enriched edge morphology, intending to utilize them as chemoresistive gas sensors.

The synthesized and functionalized TMDs have been characterized using methods such as X-ray diffraction spectroscopy, field emission scanning electron microscopy (FESEM), and transmission electron microscopy (TEM) to validate their crystalline structure and morphology. Changes observed in the X-ray diffraction (XRD) patterns confirm the production of few-layered TMDs and exhibit excellent crystallinity and chemical purity. The performance of these, 2D transition metal dichalcogenides (TMDs) in sensing greenhouse gases will be presented.

References

- [1] Gautam, Y. K., Sharma, et al. (2021). In *Royal Society Open Science* (Vol. 8, Issue 3).
[2] Lee E., Yoon, Y. S., & Kim, D. J. (2018). *ACS Sensors*, 3(10), 2045–2060.
[3] Shin, Dain, et al. *ACS Applied Nano Materials*, (2023) 6, 19327–19337.

NanosMat

P59

PHOSPHANE GOLD (I) COMPLEXES: STRUCTURAL CONFIGURATION VS. LUMINESCENT PROPERTIES

✉ aatences19@alumnes.ub.edu

A. P. Atencio, A. de Aquino, G. Zhuchkov, I. Angurell, L. Rodríguez

Department of Inorganic and Organic Chemistry, Universitat de Barcelona, Martí Franquès 1-11, 08028 Barcelona (Spain)

There are several factors that have been observed to affect the resulting luminescence of gold(I) complexes such as the type of ligand coordinated to the metal atom and the possible establishment of Au...Au interactions. Hence, the tuneability of their photophysical properties through structural modifications can be easily performed [1].

Regarding the type of ligand, the use of phosphanes allows the introduction of complementary electronic properties, together with several different types of coordination geometries, in transition-metal center, improving the predictable emission. Also, the phosphanes are suitable ligands to modulate the solubility and supramolecular assemblies of gold(I) complexes [2].

The adequate choice of the chromophores coordinated to the gold(I) atom play a key role on the resulting emission properties. Some interesting chromophores that we have used in our work are triphenylene, phenanthrene and carbazole. They are particularly interesting since they can display tendency to present stacking interactions providing an efficient structure for one-dimensional charge mobility, induce the enhancement of the room-temperature phosphorescence

phenomenon and obtain long-lived luminescence in the aggregate states[3], [4], [5].

Therefore, we present herein the synthesis, structural and photophysical characterization of three series of gold(I) compounds (Figure 1), which differ in the type of chromophore and the position of coordination of the gold(I) atom. The main differences remain on the position of the chromophore, that can be: i) directly coordinated to the metal center; ii) as a part of the phosphane chemical structure; iii) in both positions. The main objective is to determine if there is a relationship between the structural position of the chromophore and the change in the luminescent properties. So that the form and extent of the influence of the heavy atom on the system is determined.

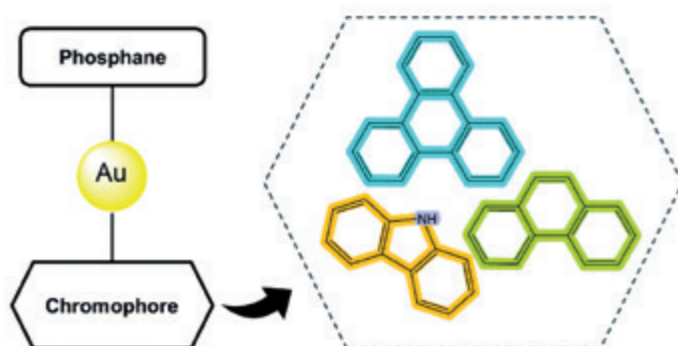


Figure 1. Chemical structure of the different chromophores.

References

- [1] A. De Aquino, J. S. Ward, K. Rissanen, G. Aullón, J. C. Lima, and L. Rodríguez. Intra- vs Intermolecular Auophilic Contacts in Dinuclear Gold(I) Compounds: Impact on the Population of the Triplet Excited State. *Inorg. Chem.* **2022**, 61, 20931–20941.
- [2] C. Cunha, A. Pinto, A. Galvão, L. Rodríguez, and J. S. Seixas De Melo. Aggregation-Induced Emission with Alkynylcoumarin Dinuclear Gold(I) Complexes: Photophysical, Dynamic Light Scattering, and Time-Dependent Density Functional Theory Studies. *Inorg. Chem.* **2022**, 61, 6964–6976.
- [3] R. Nandy, S. Sankararaman. Donor-acceptor substituted phenylethynyltriphenylenes -Excited state intramolecular charge transfer, solvatochromic absorption and fluorescence emission. *Beilstein J. Org. Chem.* **2010**, 6, 992-1001.
- [4] A. de Aquino, F. Caparrjs, G. Aullón, J. C. Lima, and L. Rodríguez. Effect of Gold(I) on the Room-Temperature Phosphorescence of Ethynylphenanthrene. *Chem. Eur. J.* **2021**, 27, 1810–1820.
- [5] X. Y. Wang, J. Gong, H. Zou, S. H. Liu, and J. Zhang. Aggregation-induced conversion from TADF to phosphorescence of gold(I) complexes with millisecond lifetimes. *Aggregate.* **2023**, 4, 1-7.

P60

SYNTHESIS AND PHOTOPHYSICAL CHARACTERIZATION OF NOVEL HETEROMETALLIC GOLD(I)-COPPER(I) COMPLEXES

✉ jahmadah89@alumnes.ub.edu

J. Ahmad, A. P. Atencio, A. de Aquino, I. Angurell, L. Rodríguez

Department of Inorganic and Organic Chemistry, Universitat de Barcelona, Martí Franquès 1-11, 08028 Barcelona (Spain)

The strategic selection of chromophores and their coordination with metal centers has a substantial impact on the emission characteristics of luminous materials. This study investigates the creative development and synthesis of a heterometallic complex that showcases a unique chromophore (2-ethynyltriphenylene), it is chosen due to its robust π -conjugation and inflexible planar structure, which greatly boost its capacity to absorb light and impact emission characteristics [1]. The chromophore is chemically bonded to a gold(I) core attached to a strong ligand, diphenylpyridine phosphine, which not only stabilizes the gold(I) center, but also enhances efficient electrical communication between the gold and copper centers due to its electron-donating properties and structural adaptability [2]. We examined the photophysical conse-

quences of combining this gold(I) complex with five different copper(I) salts: Cu(MeCN)₄PF₆, Cu(MeCN)₄OTf, Cu(MeCN)₄BF₄, CuCl, and CuI, that enable the creation of diverse coordination environments and impact the photophysical characteristics of the complexes through metallophilic interactions[3]. The heterometallic assemblies underwent thorough characterization utilizing several techniques including NMR, FTIR, ESI-MS, X-ray crystallography, and various spectrophotometric techniques both in solid and solution. This work offers an understanding of how changes in the copper(I) counterions affect the luminous characteristics of the complexes. It emphasizes the possibility of adjusting these characteristics by selecting the metal centers and their organic ligands with caution. This study adds to the overall comprehension of the connections between the structure and properties of heterometallic luminous complexes, which will facilitate specific improvements in optoelectronic applications.

Keywords

Heterometallic complexes, Luminescence, Au(I)-Cu(I) complexes, Metallophilic interactions

References

- [1] Yersin, H., & Rausch, A. F. (2011). High color purity, high efficiency OLEDs with d- and f-metal centers: The impact of molecular environment. *Organic Light Emitting Materials and Devices XV*, 8117, 81170B.
- [2] Balzani, V., Ceroni, P., & Juris, A. (2008). Photochemistry and photophysics of coordination compounds: Gold. *Photochemistry and Photophysics of Coordination Compounds I*, 280, 117-214.
- [3] Barbour, L. J. (2006). Single-crystal X-ray diffraction studies of metallophilic interactions. *Chemical Society Reviews*, 35(4), 291-305.

P61

BOOSTING SUPERCAPACITIVE PERFORMANCE USING DEFECT-ENGINEERED ZnO NANORODS ANCHORED ON GRAPHENE NANOWALLS HYBRID ELECTRODES

✉ ebertran@ub.edu ✉ ymamaxx147@ub.edu

Y. Ma^{1,2}, S. Chaitoglou^{1,2}, G. Farid^{1,2}, R. Amade^{1,2}, R. Ospina^{1,3}, A. L. Muñoz-Rosas¹, E. Bertran-Serra^{1,2}

¹ Department of Applied Physics, University of Barcelona, C/Martí i Franquès, 1, 08028 Barcelona, Catalunya, Spain / ² ENPHOCAMAT Group, Institute of Nanoscience and Nanotechnology (IN²UB), University of Barcelona, C/Martí i Franquès, 1, 08028 Barcelona, Catalunya, Spain / ³ Escuela de Física, Universidad Industrial de Santander, Carrera 27 calle 9 Ciudad Universitaria Bucaramanga, Colombia

Supercapacitors are considered the superior choice for energy storage in electric vehicles and wireless technology due to their exceptional power density, cycle stability and charge-discharge efficiency compared to conventional batteries [1]. However, their low energy density limits their ability to serve as a primary energy source. As a result, current research efforts are focused on nanostructured materials, particularly carbon-based materials such as activated carbon, carbon nanotubes (CNTs) and carbon aerogels, to increase specific capacitance [2]. Supercapacitors work through electrochemical double layer capacitors (EDLCs) and pseudocapacitors. EDLCs store energy at the electrode/electrolyte interface via ion adsorption, primarily using carbon-based electrodes [3]. Despite graphene's excellent electrical and thermal conductivity, its theoretical capacitance is limited, which recent studies aim to overcome by changing the graphene orientation from horizontal to vertical, resulting in a 38% increase in capacitance [4]. Vertical graphene nanowalls (GNWs) synthesised by plasma-enhanced chemical vapour deposition (PECVD) offer superior electrical conductivity and a three-dimensional structure, making them excellent scaffolds for supercapacitor electrodes [5]. Pseudocapacitors composed of metal oxides and polymers have higher specific capacitance than EDLCs, but require a carbon substrate for efficient charge transfer [6]. Combining carbon materials with metal oxides demonstra-

tes a synergistic effect and meets crucial requirements for innovative energy storage devices. Nonetheless, the high cost and toxicity associated with most metal oxides pose challenges. Zinc oxide (ZnO) emerges as a promising electrode material for supercapacitors due to its abundance, eco-friendliness, cost-effectiveness, and prolonged cycle life [7]. Enhancing the specific capacitance of ZnO involves preserving oxygen vacancies, achievable through annealing in inert atmospheres. While integrating ZnO with graphene-based structures has shown significant advancement, the process remains intricate and costly.

In this investigation, we explore the potential of GNWs as a promising porous structure, providing ample surface area for active sites and facilitating rapid ion diffusion. To elevate their specific capacitance, we introduce a supercapacitive enhancement by arranging defect-engineered ZnO nanorods (ZNRs) hierarchically anchored onto the GNWs. This hierarchical configuration is synthesized through a multi-step process involving inductively coupled plasma-chemical vapor deposition, magnetron sputtering, and hydrothermal techniques. The induction of oxygen vacancy (OV) defects within the ZNRs, achieved via argon annealing, is characterized using X-ray photoelectron spectroscopy. The appearance of OV defects below the conduction band of the ZNRs leads to a reduction in the bandgap within the hybrid structure, thereby enhancing its conductivity and augmenting the reaction sites. When utilized as supercapacitor electrodes, the ZNRs/GNWs hybrids are assessed in an aqueous KOH electrolyte solution, operating within a voltage range of 0.5 V and at a current density of 0.1 mA cm⁻². This evaluation reveals an area capacitance of 21.45 mF cm⁻², indicating a 1.5-fold increase in capacitance compared to GNWs grown on graphite sheets. The ZNRs/GNWs hybrid showcases outstanding electrochemical performance, underscoring its significant potential for energy storage applications. Our study is poised to offer valuable insights for enhancing electrochemical properties in various composite and hybrid materials.

References

- [1] Lethien, C.; Le Bideau, J.; Brousse, T. Challenges and Prospects of 3D Micro-Supercapacitors for Powering the Internet of Things. *Energy Environ. Sci.* 2019, 12, 96-115. [2] Zhang, Y.; Sun, X.; Pan, L.; Li, H.; Sun, Z.; Sun, C.; Tay, B. K. Carbon Nanotube-ZnO Nanocomposite Electrodes for Supercapacitors. *Solid State Ionics*. 2009, 180, 1525-1528. [3] Wen, S.; Jung, M.; Joo, O.-S.; Mho, S.-i. EDLC Characteristics with High Specific Capacitance of the CNT Electrodes Grown on Nanoporous Alumina Templates. *Curr. Appl. Phys.* 2006, 6, 1012-1015. [4] Zhang, Y.; Zou, Q.; Hsu, H. S.; Raina, S.; Xu, Y.; Kang, J. B.; Chen, J.; Deng, S.; Xu, N.; Kang, W. P. Morphology Effect of Vertical Graphene on the High Performance of Supercapacitor Electrode. *ACS Appl. Mater. Interfaces*. 2016, 8, 7363-7369. [5] Chi, Y.-W.; Hu, C.-C.; Shen, H.-H.; Huang, K.-P. New Approach for High-Voltage Electrical Double-Layer Capacitors Using Vertical Graphene Nanowalls with and without Nitrogen Doping. *Nano Lett.* 2016, 16, 5719-5727. [6] Zhou, Y. K.; He, B. L.; Zhang, F. B.; Li, H. L. Hydrous Manganese Oxide/Carbon Nanotube Composite Electrodes for Electrochemical Capacitors. *J. Solid State Electrochem.* 2004, 8, 482-487. [7] Zhou, X.; Ma, L. MnO₂/ZnO Porous Film: Electrochemical Synthesis and Enhanced Supercapacitor Performances. *Thin Solid Films*. 2015, 597, 44-49.

P62

OPTICAL STUDIES ON ANISOTROPIC Bi₂S₃ AND HYBRID Bi₂S₃@Au THERAGNOSTIC NANOCOMPOSITES

✉ jruiz-torres@ub.edu

J. Ruiz-Torres^{1,2}, C. Moya^{1,2}, M. Escoda-Torroella^{1,2}, A. Fraile Rodríguez^{1,2}, A. Labarta^{1,2}, X. Batlle^{1,2}

¹ Departament de Física de la Matèria Condensada, Martí i Franquès 1, 08028 Barcelona, Spain,

² Institut de Nanociència i Nanotecnologia, Universitat de Barcelona, 08028 Barcelona, Spain

Theragnostic nanoparticles (NPs) are multifunctional nanosystems that combine diagnostic and therapeutic capabilities into one single agent [1]. Although numerous types of theragnostic NPs, both organic and inorganic, have been developed in the last decade for treating cancer, there is still a big gap between fundamental and applied research. In this regard, hybrid Bi₂S₃@Au nanocomposites have been drawing much attention due to their superior performance in both computed tomography and photothermal therapy [2, 3]. In this work, we synthesized stoichiometric Bi₂S₃ and sulphur deficient Bi₂S_{3-x} NPs using a previously reported method [4]. Additionally, the samples were centrifuged to separate particle agglomerates from stable individual particles. All UV-vis

spectra of individual NPs were independent of morphology and volume, strongly absorbing in the UV and decaying to zero towards the IR, while uncentrifuged samples and pellet samples exhibited a broad maximum in their absorbance around 500-600 nm due to particle agglomeration. Furthermore, sulphur deficient particles showed a slightly higher relative IR absorption compared to stoichiometric samples. In a separate step, samples composed of individual NPs were functionalized with Au at room temperature for a reaction time of 30 min. Interestingly, both Bi₂S₃@Au and Bi₂S_{3-x}@Au nanocomposites yielded an increased NIR absorption as compared to their non-functionalized counterparts. Finally, selected samples of all types were transferred from an organic solvent to water by coating them using DMSA through a ligand exchange process. The as-prepared samples show good stability in water, with DLS measures showing average diameters below 200 nm, low polydispersity, and a negative ζ-potential. These final samples were later irradiated with a 808 nm laser to study their photothermal efficiency, showing promising temperature increases.

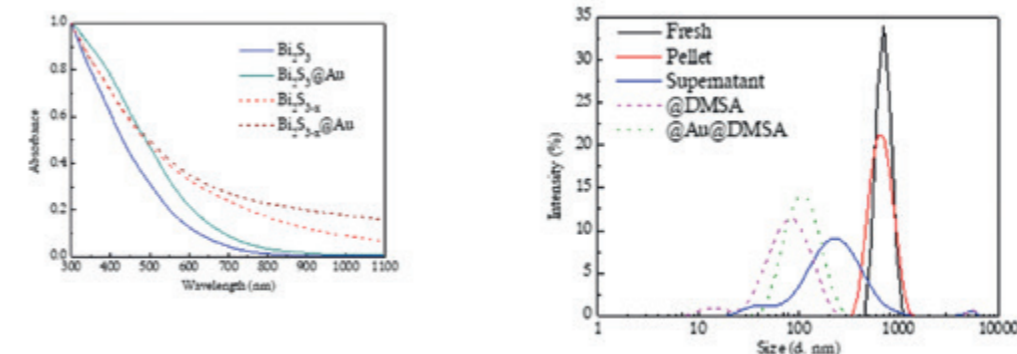


Figure 1. Left panel) Normalized optical absorption spectra of stoichiometric and sulphur deficient samples with and without Au functionalization. Right panel) DLS measurements of fresh (as prepared), pellet, supernatant, DMSA-coated individual Bi₂S₃ NPs, and DMSA-coated individual Bi₂S₃@Au NPs.

References

- [1] Xue, Y. et al., *Cancer Biol Med.* 18, 336 (2021),
 [2] Wang, X. et al., *ACS Nano* 13 (5), 5947-5958 (2019),
 [3] Cheng, Y. et al., *Angew. Chem. Int. Ed.*, 57, 246-251 (2018),
 [4] Escoda-Torroella, M., et al., *Phys. Chem. Chem. Phys.*, 25, 3900-3911 (2023).

P63

LUMINESCENT GOLD(I) NAPHTHALIMIDE DERIVATIVES

✉ aracelideaquino@ub.edu

A. de Aquino¹, E. Romero¹, J. C. Lima², L. Rodríguez¹¹ Departament de Química Inorgànica i Orgànica, Secció de Química Inorgànica, Universitat de Barcelona, Martí i Franquès, 1-11, E-08028, Barcelona, Spain.² LAQV-REQUIMTE, Departamento de Química, Universidade Nova de Lisboa, Monte de Caparica.

Gold(I) complexes present a high versatility due to their emission properties that can make these compounds suitable for obtaining advanced materials [1,2], therapeutic drugs, photodynamic therapy, and sensors.[3,4]

The presence of the gold(I) metal centre can modify this emission by increasing the population of the triplet state, responsible for the phosphorescence emission [5].

Previous studies of our group showed how the phosphorescence emission of some gold(I) derivatives containing naphthalimide as a ligand, worked for the detection of PAHs [6]. In this work, we have synthesized gold(I) derivatives that contain naphthalimides to study their photophysical properties. In this occasion, the second coordination position of the gold(I) atoms is occupied by a diphosphane, instead of phosphanes, in order to favour π - π interactions. This could approach both gold(I) atoms and induce aurophilic interactions as well as π - π interactions between two naphthalimide groups of neighbour molecules resulting in modifications of the emission spectra.

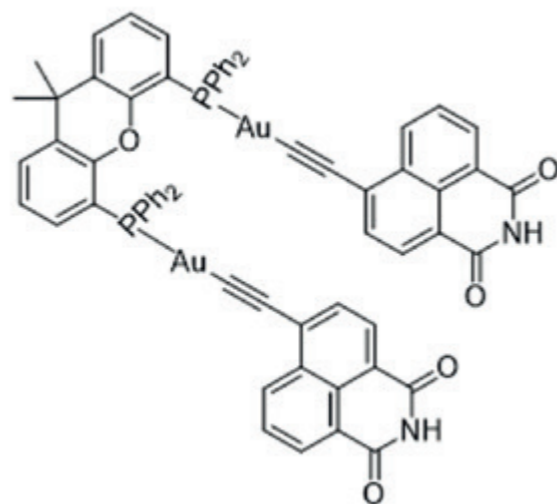


Image 1. Example of the gold(I) complexes studied in this work

References

- [1] A. de Aquino, F. J. Caparrós, G. Aullón, J. S. Ward, K. Rissanen, Y. Jung, H. Choi, J. C. Lima, L. Rodríguez, *Chem. Eur. J.*, **2021**, 27, 1810.
- [2] A. de Aquino, F. J. Caparrós, K.-N. Truong, K. Rissanen, M. Ferrer, Y. Jung, H. Choi, J. C. Lima, L. Rodríguez, *Dalton Trans.*, **2021**, 50, 3806.
- [3] M. B. Nielsen, *Synthesis*, **2016**, 48, 2732.
- [4] X. He, V. W.-W. Yam, *Coord. Chem. Rev.*, **2011**, 255, 2111.
- [5] E. Aguiló, A. J. Moro, M. Outis, J. Pina, D. Sarmiento, J. S. Seixas de Melo, L. Rodríguez, J. C. Lima, *Inorg. Chem.*, **2018**, 57, 13423.
- [6] M. Rosental, R. N. Coldman, A. J. Moro, I. Angurell, R. M. Gomila, A. Frontera, J. C. Lima, L. Rodríguez, *Molecules*, **2021**, 26, 2444.

P64

SiNWs-MoOX HYBRID ELECTRODES: ADVANCING Li-ion BATTERY TECHNOLOGY THROUGH SURFACE MODIFICATION

✉ olga.b.bantysh@ub.edu

G. Farid^{1,2}, R. Amade-Rovira^{1,2}, Y. Ma^{1,2,3}, R. Ospina^{1,2,3}, S. Chaitoglou^{1,2}, S. Majumdar^{1,2}, E. Bertran-Serra^{1,2}¹ Department of Applied Physics, University of Barcelona, C/Martí i Franquès, 1, 08028 Barcelona, Catalunya, Spain² ENPHOCAMAT Group, Institute of Nanoscience and Nanotechnology (IN²UB), University of Barcelona, C/ Martí i Franquès, 1, 08028 Barcelona, Catalunya, Spain³ Escuela de Física, Universidad Industrial de Santander, Carrera 27 calle 9 Ciudad Universitaria Bucaramanga, Colombia

The burgeoning demand for high-energy-density lithium-ion (Li-ion) batteries, fueled by the widespread adoption of electric vehicles and portable electronic devices, necessitates continuous advancements in electrode materials [1-7]. Silicon (Si) has emerged as a frontrunner for negative electrodes owing to its exceptionally high theoretical capacity compared to conventional graphite [4]. Among Si-based nanostructures, silicon nanowires (SiNWs) have garnered substantial interest due to their unique morphology and superior electrochemical properties, including one-dimensional electron transport and large surface area, which are conducive to enhancing Li-ion battery performance [8-10].

Methods and materials

In this study, we delve into the potential of integrating molybdenum oxide (MoO₃) nanoparticles as functional additives to augment the electrochemical performance

and cycling stability of SiNW-based Li-ion battery anodes. The methodology involves the deposition of MoO₃ nanoparticles via Drop-casting onto pre-fabricated SiNW arrays synthesized via a facile one-step metal-assisted chemical etching (MACE) process [11].

Results and discussion

The core objective is to evaluate the viability and efficacy of MoO₃@SiNWs hybrid architectures as advanced anode materials for high-capacity and long-cycle-life energy storage devices. When assessing the effectiveness of SiNW arrays decorated with Mo oxide nanoparticles as anodes for Li-ion batteries, it became evident that the hybrid electrode outperformed the bare SiNW arrays electrode. The MoO₃@SiNWs hybrid electrode exhibited a notably higher initial discharge capacity of 1.34 mA·h·cm⁻² compared to the bare SiNW arrays electrode, which only achieved 0.35 mA·h·cm⁻² at a scan rate of 1C. Over 200 charge-discharge cycles, the MoO₃@SiNWs hybrid electrode maintained a consistent reversible specific capacity of 1.23 mA·h·cm⁻², whereas the bare SiNW arrays electrode experienced a significant decrease in capacity to 0.20 mA·h·cm⁻² under the same cycling conditions. Additionally, the coulombic efficiency of the MoO₃@SiNWs hybrid electrode progressively improved from 96% to 99.4% over the initial five cycles, demonstrating stable performance thereafter. This exceptional electrochemical performance is attributed to the synergistic interaction between MoO₃ nanoparticles and the SiNW arrays, showcasing the potential of this hybrid structure for advanced Li-ion battery applications.

References

- [1] G. Farid, R. Amade, S. Chaitoglou, I. Alshaiikh, R. Ospina, Y. Ma, E. Bertran-Serra, *Journal of Alloys and Compounds*, (2023) 172109.
- [2] G. Farid, G. Murtaza, M. Umair, H.S. Arif, H.S. Ali, N. Muhammad, M. Ahmad, *Materials Research Express*, 5 (2018) 055044.
- [3] A. Ayyaz, G. Murtaza, A. Ahmed, S.M. Ramay, A. Usman, G. Farid, M. Naeem, *Computational Condensed Matter*, 38 (2024) e00885.
- [4] G. Farid, R. Amade-Rovira, R. Ospina, E. Bertran-Serra, *Journal of Energy Storage*, 78 (2024) 110104.
- [5] G. Farid, R. Amade-Rovira, Y. Ma, S. Chaitoglou, R. Ospina, E. Bertran-Serra, *Arabian Journal of Chemistry*, (2024) 105631.
- [6] M.A. Shafique, G. Farid, F. Shaheen, Z. Zaheer, G. Murtaza, S. Sharif, R. Ahmad, *Chemical Physics Letters*, (2024) 141213.
- [7] Y. Ma, S. Chaitoglou, G. Farid, R. Amade, R. Ospina, E. Bertran, *Proceedings of MATSUS Spring 2024 Conference (MATSUS24)*, 2023.
- [8] G. Farid, S. Chaitoglou, R. Amade, R. Ospina, E. Bertran-Serra, *Surface Science Spectra*, 31 (2024).
- [9] C. Huo, J. Wang, H. Fu, X. Li, Y. Yang, H. Wang, A. Mateen, G. Farid, K.Q. Peng, *Advanced Functional Materials*, 30 (2020) 2005744.
- [10] H. Ali, A.S. Alghamdi, G. Murtaza, H. Arif, W. Naeem, G. Farid, S. Sharif, M.G.B. Ashiq, S.A. Shabbir, *Materials*, 12 (2019) 821. [11] G. Farid, Y. Yang, A. Mateen, C. Huo, H. Wang, K.-Q. Peng, *ACS Applied Nano Materials*, 5 (2022) 2779-2786.

P65

Mo₂C NANOSTRUCTURES ANCHORED ON CARBON NANOTUBES FOR ENHANCED ELECTROCATALYTIC HYDROGEN EVOLUTION

✉ shmajumm110@alumnes.ub.edu

S. Majumdar^{1,2}, S. Chaitoglou^{1,2}, G. Farid^{1,2},
R. Ospina^{1,2,3}, Y. Ma^{1,2}, E. Bertran-Serra^{1,2},
R. Amade Rovira^{1,2}

¹ Department of Applied Physics, University of Barcelona, C/Martí i Franquès, 1, 08028 Barcelona, Catalunya, Spain

² ENPHOCAMAT Group, Institute of Nanoscience and Nanotechnology (IN²UB), University of Barcelona, C/ Martí i Franquès, 1, 08028 Barcelona, Catalunya, Spain

³ Escuela de Física, Universidad Industrial de Santander, Carrera 27 calle 9 Ciudad Universitaria Bucaramanga, Colombia

As the demand for clean, sustainable energy is rising, there is an increased interest in the use of hydrogen, owing to its high energy density and for being an efficient energy storage and conversion option. This study focuses on electrochemically extracting hydrogen from water, by using a carbon felt electrode, decorated with carbon nanotubes (CNTs). CNTs have excellent mechanical and chemical stability and possess a large surface area for reactions to take place. Nevertheless, CNTs are not inherently active towards catalytic reactions and therefore require functionalization [1]. Here, electrocatalytically active pristine Mo and Mo₂C nanostructures are anchored on the CNTs to functionalize them. The research compares the performance of Mo on CNTs to that of Mo₂C on CNTs as an efficient electrode for water splitting [2].

Materials and Methods

CNTs are deposited on carbon felt by sputtering of catalytic Fe layer, followed by chemical vapor deposition growth. Mo is deposited on the CNTs by magnetron sputtering, followed by in-situ thermal annealing.

References

- [1] Chaitoglou, S.; Amade, R.; Ospina, R.; Bertran-Serra, E. Hybrid Nanostructured Compounds of Mo₂C on Vertical Graphene Nanoflakes for a Highly Efficient Hydrogen Evolution Reaction. *ACS Appl. Energy Mater.* **2023**, 6 (11), 6120–6131. <https://doi.org/10.1021/acsaem.3c00625>.
- [2] Farid, G.; Amade, R.; Chaitoglou, S.; Alshaiikh, I.; Ospina, R.; Ma, Y.; Bertran-Serra, E. Efficient Flexible Electrodes for Lithium-Ion Batteries Utilizing Well-Dispersed Hybrid Mo₂C Nanoparticles on Vertically-Oriented Graphene Nanowalls. *J. Alloys Compd.* **2023**, 968, 172109. <https://doi.org/10.1016/j.jallcom.2023.172109>.
- [3] Chaitoglou, S.; Ospina, R.; Ma, Y.; Amade, R.; Vendrell, X.; Rodríguez-Pereira, J.; Bertran-Serra, E. Deposition and In-Situ Formation of Nanostructured Mo₂C Nanoparticles on Graphene Nanowalls Support for Efficient Electrocatalytic Hydrogen Evolution. *J. Alloys Compd.* **2024**, 972, 172891. <https://doi.org/10.1016/j.jallcom.2023.172891>.

We used SEM, TEM, XRD, and Raman Spectroscopy to study the fabricated CNTs and subsequent deposition of molybdenum and molybdenum carbide. We also performed electrochemical analysis of the fabricated electrodes to measure and compare their performance towards hydrogen evolution reaction (HER).

Results and Discussion

The morphology of the fabricated electrode is studied using SEM. The successful functionalization of the CNTs with molybdenum is confirmed by SEM and EDS. XRD is used to study the physical properties of the crystal structure of the CNTs and confirms the formation of molybdenum carbide after the annealing process. The XRD data is further supported by TEM imaging where the FFT analysis of the image gives us the accurate d-spacing to confirm the various carbide phases. Raman spectroscopy gives us valuable information about the carburization process. The Raman spectra confirms the in-situ carburization of molybdenum to molybdenum carbide, without using any external precursors [3]. Electrochemical analysis of the samples reveals the efficiency of electrodes towards HER. The as-deposited Mo on CNTs exhibit an onset potential of -300 mV for the generation of -1 mA/cm² and an overpotential of -393 mV for the generation of -10 mA/cm². Mo₂C on CNTs exhibits an onset potential of -103 mV for the generation of -1mA/cm² and an overpotential of -176mV for the generation of 10 mA/cm². Tafel slope is plotted for Mo on CNTs, exhibiting a value of 105mV/dec. Mo₂C on CNTs exhibit a Tafel slope value of 95mV/dec. From the data obtained by calculating the onset and over potentials and Tafel slopes, it is concluded that the CNTs functionalized with Mo₂C performs as a better electrode for HER when compared with bare Mo on CNT electrode.

P66

CoFe₂O₄/Cu- AND Ce-DOPED SnO₂ COMPOSITES FOR SONOPHOTO-CATALYTIC DEGRADATION OF ORGANIC POLLUTANTS

✉ juditlloreda@ub.edu

J. Lloreda^{1,2}, R. Bujaldón^{1,2}, E. Gómez^{1,2}, A. Serrà^{1,2}

¹ Grup d'Electrodeposició de Capes Primes i Nanoestructures (GE-CPN), Departament de Ciència de Materials i Química Física, Universitat de Barcelona, Martí i Franquès 1, E-08028, Barcelona, Spain

² Institut of Nanoscience and Nanotechnology (IN²UB), Universitat de Barcelona, Barcelona, Spain

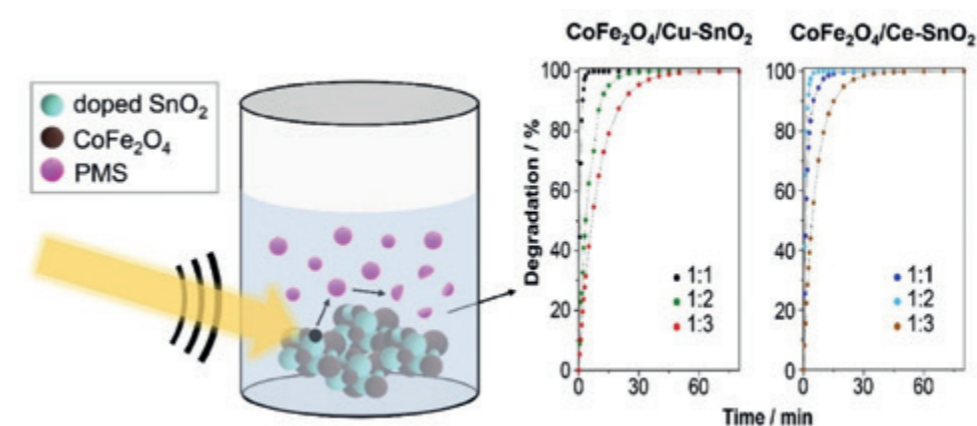
For years, large quantities of apparently innocuous compounds have been released into aquatic environments, with limited understanding of their long-term effects for both the ecosystem and human health. The emergence of these organic pollutants has raised concerns about their persistence after the application of conventional wastewater treatments. Addressing the need for effective degradation, wide-spectrum catalysts together with environmentally friendly oxidative radicals have gained prominence.

In this context, we have developed and utilized multicomponent composite materials under sonophotocatalytic conditions [1], and employing peroxy-monosulfate (PMS) as a radical source [2]. These composites elaborately combine cobalt ferrite with Cu- or Ce-doped SnO₂, two independently promising components. To assess their individual abilities for

degrading organic pollutants, using rhodamine-B as a target molecule, we conducted tests with and without PMS, employing sonocatalytic, photocatalytic, and combined sonophotocatalytic conditions. The nanocomposites were carefully synthesized by meticulously adjusting the doping metal percentage in SnO₂ and the ratio mixture with CoFe₂O₄. Under sonophotocatalytic conditions with PMS, the most effective composites showed significant degradation within 3 minutes, and a prominent 70% mineralization within 5 minutes. These outstanding nanocomposites were further evaluated in a complex multipollutant solution, achieving a 75% mineralization after 150 minutes. The stability and reusability of the composites were also assessed, being the cerium-doped one slightly more reusable after 15 cycles. In conclusion, the proposed CoFe₂O₄/Cu- and Ce-doped SnO₂ composites emerge as heterogeneous catalysts for the mineralization of organic pollutants through PMS activation.

Acknowledgments

Grant PID2020-115663GB-C32 funded by MCIN. J.L.L. thanks the support of the Industrial Doctorates Program of the Department of Research and Universities of the Generalitat de Catalunya (project 2022 DI 035).



References

- [1] Bembibre, A. et al. *Chem. Eng. J.* **2022**, 427, 132006.
- [2] Ni, T. et al. *J. Colloid Interface Sci.* **2022**, 615, 650.

P67

ELECTROCHEMICAL FABRICATION AND FUNCTIONALIZATION OF BiOI FOR PHOTOCATALYTIC WATER DECONTAMINATION

✉ l.huidobro@ub.edu

L. Huidobro^{1,2}, Q. Bautista¹, E. Gómez^{1,2}, A. Serrà^{1,2}¹ Grup d'electrodeposició de Capes Primes i Nanoestructures (GE-CPN), Departament de Ciència de Materials i Química Física, Universitat de Barcelona. Martí i Franqués 1, E-08028, Barcelona² Institut de Nanociència i Nanotecnologia (IN²UB), Universitat de Barcelona. E-08028, Barcelona

The research on new materials plays an essential role in the progress of solutions aimed at water decontamination. In this context, a study focused on the fabrication of a thin film of BiOI using electrochemical techniques has been carried out, with the aim of creating a material with photocatalytic properties to enhance water purification through the activation of peroxydisulfate (PMS).

This study research electrochemical synthesis of BiOI via p-benzoquinone reduction, resulting in thin film formation. Characterization techniques reveal varied BiOI morphology (FE-SEM) with applied potential, showing nanoplates (-0.1V to -0.3V) and compact structures (<-0.3V). XPS analysis detects [Bi₂O₂]²⁺ signals at lower deposition potentials (according with BiOI presence), shifting to Bi(0) for the prepared at more negative potentials, confirmed by XRD technique. Heat treatment induces structural transformation of BiOI to Bi₇O₉I₃ and Bi₅O₇I based on temperature.

The resulting material exhibits significant visible light absorption and photocatalytic activity, particularly when combined with PMS activation. Heat treatment at different temperatures yields distinct species, with Bi₅O₇I (420°C) proving most effective for degradation, demonstrating both stability and reusability [1]. The versatility of these materials is highlighted by their effectiveness in mineralize various pollutants, supporting their potential for scalable applications and the development of advanced photocatalysts.

The study coming to compare the properties of prepared films by electrochemical techniques with more commonly used BiOI synthesis methods like solvothermal method. Additionally, it suggests subsequent functionalization to optimize the material. For this purpose, next step is to prepare hybrid composites capable of maintaining the photocatalytic activity attaching other properties as magnetic, catalytic, etc. Moreover, it lays the groundwork for material optimization through nanostructure creation (nanowires, nanotubes, etc.).

Acknowledgment

L.H. acknowledges the support of the project PID2020-115663GB-C32 funded by the Ministry of Science and Innovation and of the University of Barcelona through the PREDOCS-UB predoctoral program.

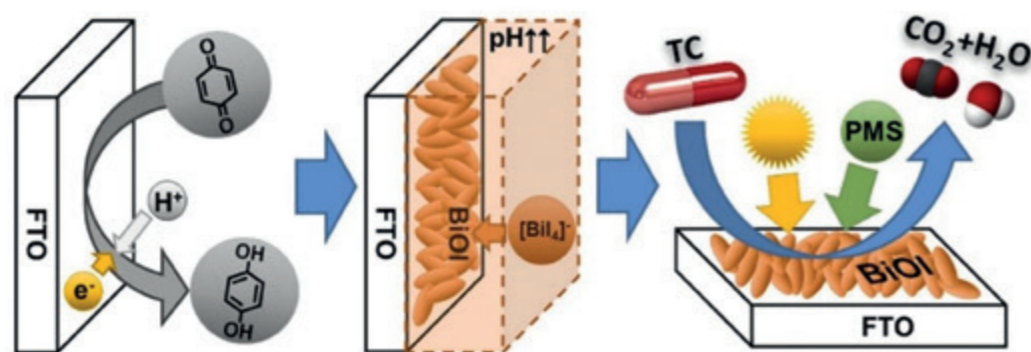


Figure 1. Graphical abstract of electrodeposition process obtained from reference 1.

References

[1] Huidobro, L., Bautista, Q., Alinezhadfar, M., Gómez, E., Serrà, A., J. Environ. Chem. Eng., 12 (2024) 112545.

P68

DOPED ZnO/Ni PHOTOCATALYSTS FOR THE REMOVAL OF PHARMACEUTICAL POLLUTANTS VIA PMS ACTIVATION

✉ r.bujaldon@ub.edu

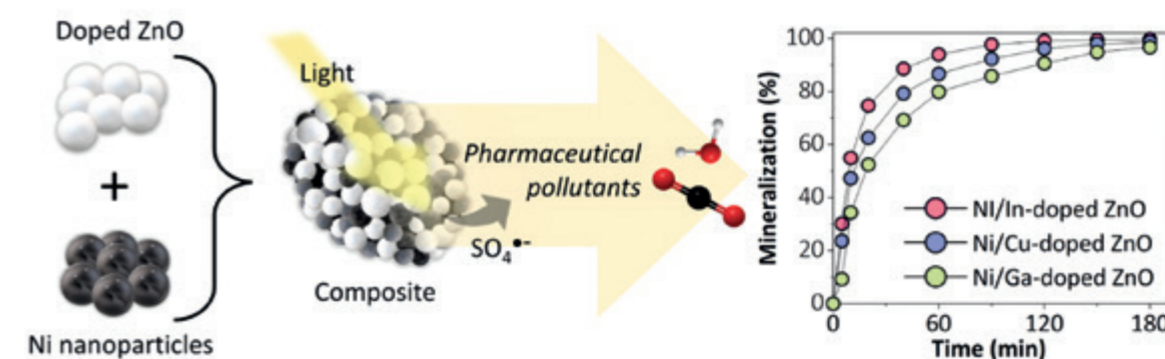
R. Bujaldón^{1,2}, E. Gómez^{1,2}, A. Serrà^{1,2}¹ Grup d'Electrodeposició de Capes Primes i Nanoestructures (GE-CPN), Departament de Ciència de Materials i Química Física, Universitat de Barcelona, Martí i Franqués, 1, E-08028, Barcelona, Spain.² Institute of Nanoscience and Nanotechnology (IN²UB), Universitat de Barcelona, Barcelona, Spain.

The proliferation of pharmaceutical products in aqueous media, stemming from both industry and waste waters throughout decades, has evolved into a major environmental issue [1]. The concerns go beyond their immediate potential toxicity, since their long-term impact on ecosystems is still rather unexplored. Hence, water treatment technologies are compelled to overtake the current release of organic pollutants and ensure the access to drinking water. Current methodologies, however, are still costly and, oftentimes, insufficient. In this context, novel catalysts capable of mineralizing a wider spectrum of pharmaceuticals via friendlier and lower-consuming strategies are highly sought-after. ZnO, especially once doped, is a well-known semicon-

ductor that also shines in the photocatalytic disposal of recalcitrant organic pollutants [1][2]. Herein we evaluated the effect of doping ZnO with either indium, copper or gallium on its morphology, structure, properties and catalytic performance. The suitability of these materials was tested on a complex, multipollutant solution comprising tetracycline, levofloxacin and lansoprazole as model pharmaceuticals. The activation strategy combined photocatalysis with peroxydisulfate (PMS) as an eco-friendly source of highly oxidative sulfate radicals [3]. Further, they were merged with nickel nanoparticles to confer a ZnO/NiO heterojunction. Both components revealed outstanding synergy, greatly ameliorating their separate activities. Particularly, indium-containing composites outperformed the other proposed metal dopants, exceeding a 93% mineralization after 1 hour and achieving a complete mineralization after 3 hours. All materials displayed excellent reusability with no catalytic loss after 10 consecutive cycles, supporting their potential in water remediation.

Acknowledgements

Grant PID2020-115663GB-C32 funded by MCIN.



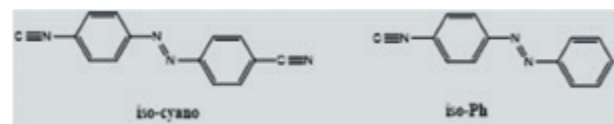
References

[1] Serrà, A. et al. *Appl. Catal. B* **2020**, 268, 118745.
 [2] El Golli, A. et al. *Sci. Rep.* **2023**, 13, 20809.
 [3] Hjiri, M. et al. *Chemosphere* **2024**, 354, 141656.

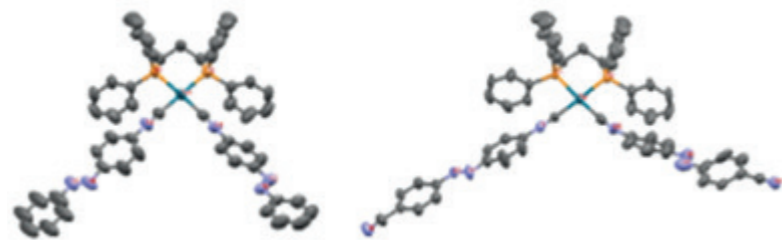
P69

NO SWITCHING COOPERATIVITY ON COMPLEXES WITH *BIS*-COORDINATED AZO LIGANDS HAVING A {M^{II}(DPPP)}²⁺ (M = Pd, Pt) SCAFFOLD

✉ oraichpa7@alumnes.ub.edu

O. Raïch¹, J. Jover¹, C. Puigjaner², M. Ferrer^{1,3}, M. Martínez^{1,3}¹ Secció de Química Inorgànica, Departament de Química Inorgànica i Orgànica, Universitat de Barcelona, Martí i Franquès 1-11, 08028 Barcelona, Spain² Unitat de Difracció de RX, Centres Científics i Tecnològics de la Universitat de Barcelona (CCiTUB), Universitat de Barcelona, Solé i Sabarís 1-3, 08028 Barcelona, Spain³ Institute of Nanoscience and Nanotechnology (IN²UB), Universitat de Barcelona, 08028 Barcelona, Spain

Azobenzenes and their derivatives are compounds that can be photoisomerised by the action of light and returned to their thermodynamic form reversibly. Following our interest in the variations occurring on solvent conditions [1,2] and coordination of these units to metal centres, [3] we have prepared square planar complexes containing the {M^{II}(dppp)}²⁺ (M = Pd, Pt) frameworks, and the azoderivatives 4-((4-isocyanophenyl)diazenyl)benzotrile, CN(C₆H₄)-N=N-(C₆H₄) (iso-cyano) and 4-((4-isocyanophenyl)diazenyl)phenyl, CN(C₆H₄)-N=N-(C₆H₅) (iso-Ph) as ligands, in order to



study the effect of their attachment on the switching behaviour.

The preparation of the compounds was conducted by a one-pot procedure from the [M(dppp)(H₂O)₂](TfO)₂ precursors and the appropriate amount (2-fold) of the azoderivatives. All compounds were fully characterised by RMN, IR, ESI (+) and UV-vis and for [Pd(dppp)(iso-cyano)₂]²⁺ and [Pd(dppp)(iso-Ph)₂]²⁺ the structure was elucidated by XRD. The robustness of the photoswitching process was followed carrying several cycles and monitored by UV-Vis spectroscopy. The presence of a clean isosbestic point in the UV-Vis photoisomerisation profile indicates a single step profile despite the existence of the [M(dppp)(trans-azo)₂]²⁺, [M(dppp)(trans-azo)(cis-azo)]²⁺ and [M(dppp)(cis-azo)₂]²⁺ structures as determined by NMR monitoring. This fact indicates that the process occurs statistically individually on each one of the ligands. Clearly, there is a lack of cooperativity between the two azo ligands attached to the metal centre.

Furthermore, the spontaneous back *cis*-to-*trans* reaction was also studied at different temperatures, pressures and solvent conditions to determine possible changes in the mechanism operating during the process. By doing so, the possible differences between the behaviour of the free and coordinated ligands would be signalled. Effectively, the derived thermal and pressure activation parameters indicate that the attachment of the azoderivatives to a positive moiety favours the rotational (charge separated) trans state over the inversion transition state.

References

- [1] García-Amorós, J.; Stopa, G.; Stochel, G.; van Eldik, R.; Martínez, M.; Velasco, D., Activation volumes for *cis*-to-*trans* isomerisation reactions of azophenols: a clear mechanistic indicator? *Physical Chemistry Chemical Physics* **2018**, 20, 1286-1292.
- [2] García-Amorós, J.; Martínez, M.; Velasco, D., High-Pressure Kinetics of Azo Dyes in Nematic Liquid Crystals. *The Journal of Physical Chemistry C* **2019**, 123, 30578-30583.
- [3] Martínez, M.; Ferrer, M.; García-Cirera, B.; Gallen, A.; Font-Bardia, M.; Bardaji, M., Iron complexes of bridging azo ligands in aqueous solution; changes in the thermal switching mechanism on coordination and oxidation state of metal centres. *Dalton Transactions* **2023**, 52, 1720-1730.

P70

FLOWER-LIKE HYDROXYAPATITE: HYDROTHERMAL PREPARATION AND FUNCTIONALIZATION WITH AMINOPHOSPHATE COMPOUNDS

✉ mohandes@ub.edu

F. Mohandes^{1,2}, E. Gómez^{1,2}, A. Serrà^{1,2}¹ Grup d'Electrodeposició de Capes Primes i Nanoestructures (GE-CPN), Departament de Ciència de Materials i Química Física, Universitat de Barcelona, Martí i Franquès, 1, E-08028, Barcelona, Catalonia, Spain² Institute of Nanoscience and Nanotechnology (IN²UB), Universitat de Barcelona, Barcelona, Catalonia, Spain

Surface modification of hydroxyapatite (HAP; Ca₁₀(PO₄)₆(OH)₂) in both chemical and physical features has been attracted much attention due to the wide biomedical applications of HAP in tissue engineering and drug/gene carriers [1]. The use of chelating agents including carboxylate and amine groups can control the growth of HAP, causing the formation of different morphologies of HAP. Moreover, the chemical properties of surface biomaterials should be modified, as the surface is the first region that comes into contact with the physiological environment. For this purpose functionalization of biomaterials can develop their chemical and physical properties to establish efficient interface with biomolecule [2]. In this study, HAP was

hydrothermally deposited on substrate in the presence of calcium and phosphate precursors. For the first time, trisodium nitrilotriacetic acid (NTA) was used as chelating agents to promote the formation of hierarchical HAP microparticles composed of nanorods. The effect of preparation parameters on the HAP morphology and its crystalline phase was also studied. Figure 1 shows SEM images of the as-synthesized HAP in the presence of NTA and after thermal treatment. In order to functionalize HAP, peeling of the deposited layer was carried out with the aid of water-soluble polymers to obtain HAP powders. After peeling and purification process, HAP powders were treated by alendronate (AL) molecules. Fourier transform infrared (FTIR) spectroscopy and Brunauer-Emmett-Teller (BET) analysis confirmed the surface modification of HAP with AL molecules. The AL-HAP flower-like can be introduced as multifunctional biomaterial for future bio-applications.

Acknowledgments

Grant PID2020-115663GB-C32 funded for MCIN/AEI and the contribution of Dr. Lluïssa Pérez-García for advisor. FM thanks for grant of María Zambrano postdoctoral fellowship (UNI/551/2021).

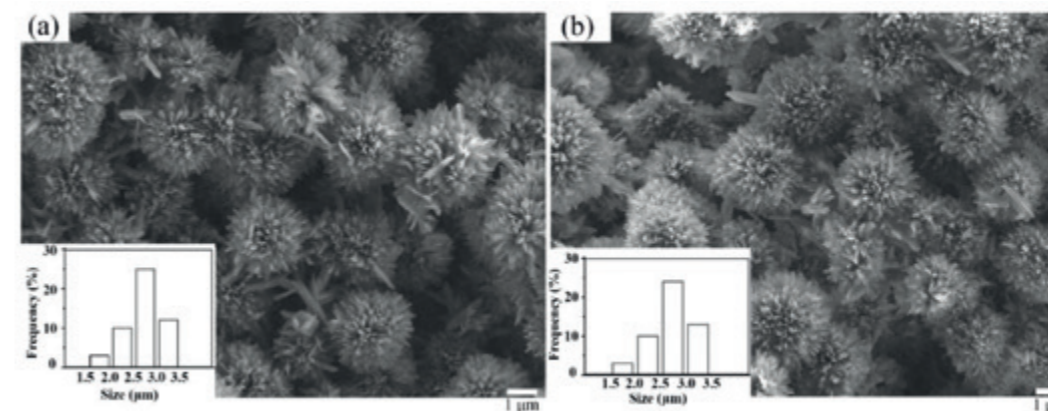


Figure 1. SEM images of HAP synthesized via hydrothermal at 180 °C for 24 h in the presence of NTA (a) and the corresponding sample after thermal treatment at 400 °C for 30 min (b). Molar ratios of NTA/Ca and Ca/P are 1:1 and 1.67:1, respectively. The insets show particle size distribution.

References

- [1] Haider, A., Haider, S., Han, S.S., Kang, I.K., *RSC Adv.*, **7**, 7442 (2017).
- [2] Wang, G., Lv, Z., Wang, T., Hu, T., Bian, Y., Yang, Y., Liang, R., Tan, C., Weng, X., *Adv. Sci.* **10**, 2204234 (2023).

P71

BIOMIMETIC SUNFLOWER POLLEN-BASED HETEROSTRUCTURED PHOTOCATALYST FOR ENHANCED VISIBLE-LIGHT-DRIVEN PHOTOCATALYTIC DEGRADATION OF PHARMACEUTICALS

✉ a.serra@ub.edu

A. Serrà^{1,2}, M. Ortiz¹, E. Gómez^{1,2}

¹ Grup d'Electrodeposició de Capes Primes i Nanoestructures (GE-CPN), Departament de Ciència de Materials i Química Física, Universitat de Barcelona, Martí i Franquès 1, E-08028, Barcelona.

² Institut de Nanociència i Nanotecnologia (IN²UB), Universitat de Barcelona, Barcelona.

Recent research has highlighted the water crisis facing over 1 billion people in arid regions due to contamination of water sources by emerging and/or persistent organic pollutants. This necessitates the development of innovative water treatment methods. This research integrates principles of green and circular chemistry by employing pollen to synthesize three-dimensional onion-like pollen-Cu@Cu₂O@CuO@CuS photocatalysts with exceptional degradation and mineralization capabilities. Importantly, the photocatalyst is recycled to fabricate biopellet for waste-to-energy conversion. The resulting ashes after combustion are utilized as peroxymonosulphate (PMS) activators for mineralizing drugs from wastewater. This proposes a comprehensive circular process to minimize waste production.

The study presents a pioneering approach to synthesizing a highly efficient pollen-Cu@Cu₂O@CuO@CuS photocatalyst through a sequential and scalable electrochemical production method. The process of utilizing sunflower pollen's distinctive echinate and tricolporate structure involves several steps, including pollen pretreatment, palladization, electroless deposition, thermal treatment, and chemical sulfidation. It is noteworthy that the pollen's structural integrity and size uniformity are preserved throughout the process, which enhances its potential for practical applications.

The work examines the stability and degradation of the antibiotic TC under varying pH conditions. It also assesses the effectiveness of pollen-Cu@Cu₂O@CuO@CuS hybrids as photocatalysts for TC degradation and mineralization. The photocatalytic experiments reveal rapid TC degradation, particularly in alkaline conditions, with over 99% mineralization achieved after 90 minutes of visible light irradiation. The efficiency of the photocatalyst is maintained over multiple cycles, especially in basic conditions, indicating excellent resistance to photocorrosion.

The study shows how used photocatalysts can be recycled into pollen pellets, which aligns with the principles of the green and circular economy. The pellets meet strict criteria for commercial biofuels, with low ash and moisture content and a high calorific value.

The ash residue, despite being a small fraction of the original photocatalyst mass, can be utilized as an activator for PMS to efficiently mineralize organic pollutants in wastewater. The mineralization rates for a multicomponent drug solution exceed 99% under both dark and visible light conditions, demonstrating the effectiveness of the ash as a PMS activator. Moreover, the ash maintains consistent mineralization rates over ten consecutive cycles, demonstrating its robustness as a reusable PMS activator without requiring additional treatment.

This approach highlights the potential for sustainable waste management and resource utilization in water treatment, providing a practical solution for pollutant removal while minimizing waste production.

Acknowledgment

Grant PID2020-115663GB-C32 funded by MCIN/ AEI /10.13039/501100011033.

P72

ENHANCING ORGANIC FIELD-EFFECT TRANSISTORS: A STUDY ON TRIINDOLE-BASED SEMICONDUCTORS USING ADVANCED PROCESSING TECHNIQUES AND DEVICE ARCHITECTURES

✉ dvelasco@ub.edu

C. Fabregat^{1,2}, L. Fijahi³, M. Mas-Torrent³, J. García-Amorós^{1,2}, D. Velasco^{1,2}

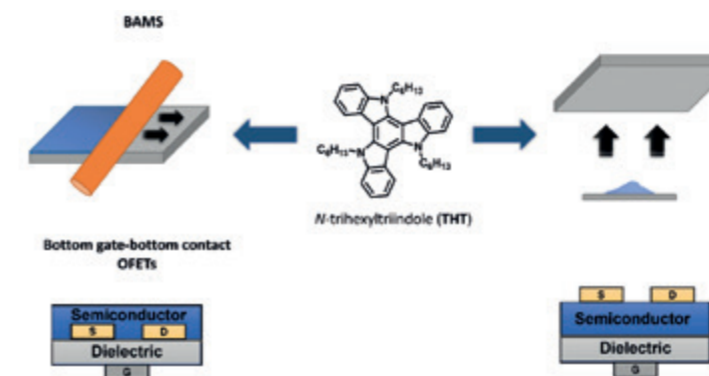
¹ Grup de Materials Orgànics, Departament de Química Inorgànica i Orgànica, Secció de Química Orgànica, Universitat de Barcelona, Martí i Franquès 1, E-08028, Barcelona, Spain.

² Institut de Nanociència i Nanotecnologia (IN²UB), Universitat de Barcelona.

³ Institut de Ciència de Materials de Barcelona, ICMAB-CSIC, Campus UAB, 08193 Bellaterra.

The ongoing evolution of technology in the 21st century necessitates the development of advanced materials, such as organic semiconductors for Organic Field-Effect Transistors (OFETs). These three-terminal devices control the current flow in a semiconductor layer between the source and drain electrodes (S and D, respectively) using the voltage applied to the gate electrode (G). Unlike the traditional silicon-based transistors, organic semiconductors offer significant advantages for applications requiring flexibility and miniaturization of the final technologies, such as in sensors and photodetectors.[1]

This study explores the compound 5,10,15-trihexyl-10,15-dihydro-5*H*-diindolo[3,2-*a*:3',2'-*c*]carbazole (hereafter referred to as N-trihexyltriindole, **THT**), which was selected for its superior hole-transporting properties and strong π - π stacking interactions, both of which are critical for efficient charge transport. [2-3] This organic compound was processed using two distinct methods: vacuum evaporation and solution processing with Bar Assisted Meniscus Shearing (BAMS) technique. The research further investigates the influence of different device architectures, including bottom gate-top contact and bottom gate-bottom contact configurations to assess their impact on the electrical performance and morphology of the semiconducting layer. The results focus on examining the film morphology and electrical characterization of THT in different OFET architectures. This study aims to contribute to the broader integration and functionality of organic semiconductors in cutting-edge electronic devices.



References

- [1] H. Li, W. Shi, J. Song, H.J. Jang, J. Dailey, J. Yu, H.E. Katz. *Chem. Rev.* 2019, **119**, 1, 3–35.
- [2] M. Reig, G. Bagdziunas, A. Ramanavicius, J. Puigdollers, D. Velasco. *Phys. Chem. Chem. Phys.*, 2018, **20**, 17889-17898.
- [3] M. Reig, J. Puigdollers, D. Velasco. *J. Mater. Chem. C*, 2015, **3**, 506-513.

AUTHOR INDEX



AUTHOR INDEX

A

Abad Galán, L. 60
 Aballe, L. 56
 Aguilà, D. 58, 60, 66, 82
 Ahmad, J. 101
 Alff, L. 43
 Alonso-Tomás, D. 97
 Álvarez-Berbel, I. 68, 75, 77
 Alvarez-Braña, Y. 28
 Amade-Rovira, R. 19, 102, 105, 106
 Amazian, M. 55
 Andreu, T. 55
 Angurell, I. 100, 101
 Ara, J. 59
 Arango-Restrepo, A. 37, 39
 Aromí, G. 57, 58, 60, 65, 66
 Arteaga, O. 91
 Asew Boafo, G. 99
 Atencio, A. P. 100, 101
 Aviñó, A. 31

B

Bagherpour, S. 69, 73
 Baiutti, F. 41
 Barrios, L. A. 57, 60, 65
 Barthel, J. 41
 Basabe-Desmots, L. 28
 Batalla Ferrer-Vidal, I. 56
 Battle, X. 20, 24, 56, 59, 87, 103
 Bautista, Q. 108
 Beirampour, N. 70
 Ben-Abdallah, P. 40
 Benavent-Claró, A. 28
 Benito-Lopez, F. 28
 Bertran-Serra, E. 14, 102, 105, 106
 Bescós, L. 72
 Blanco-Portals, J. 26
 Bocher, L. 26
 Bonilla-Vidal, L. 74, 78
 Borrell, J. H. 46
 Borrisé, X. 24
 Boter, J. 55
 Botet-Carreras, A. 46
 Boulehjour, H. 65
 Buch-Palasi, J. 63
 Bujaldón, R. 107, 109
 Busquets, M. A. 68, 75, 77
 Bustos Salgado, P. 79

C

Caballero, A. B. 82
 Calpena, A. C. 46, 70, 71, 79
 Calvino J., J. 41
 Calvo-de la Rosa, J. 30
 Cambor, L. 52
 Capó, N. 65
 Carnicer, A. 15
 Carreras-Vidal, L. 48, 50
 Casals, B. 21, 67
 Castaño, O. 53

Cerrato-Serrano, P. 62
 Chaitoglou, S. 19, 102, 105, 106
 Chekir, L. G. 79
 Chiabrera, F. 41
 Chillón, M. 31
 Chirvony, S. V. 88, 93
 Cian, A. 24
 Cirera, A. 88, 93, 95
 Cirisano, F. 76
 Ciudad, C. J. 31, 47, 102, 105, 106
 Coll, C. 26, 43
 Colom, M. 90
 Costa, V. 26
 Costache, M. V. 62, 63, 64
 Cuillamat, P. 45
 Cullell, J. 47

D

D'Amico, F. 36
 de Aquino, A. 63, 100, 101
 del Pozo Bueno, D. 26, 43
 del Pozo Carrascosa, A. 80
 Dell'Anna, R. 24
 Dias, F. B. 61
 Díaz-Torres, R. 58, 66
 Dimaki, M. 85
 Dirin, D. 88, 93
 Domènech-Gil, G. 18, 84, 85, 98
 Domènech, Ò. 46
 Dong, Y. 53
 Duch, M. 69
 Duocastella, M. 27, 90, 92, 94
 Duran-Sindreu, F. 25

E

Engel, E. 53
 Eritja, R. 31
 Escoda-Torroella, M. 56, 103
 Escribano Ferrer, E. 80
 Espargaró, A. 68, 75, 77
 Espina, M. 25, 74, 78, 81, 83
 Espinoza, L. C. 71
 Estany-Macià, A. 18, 85
 Esteruelas, G. 74, 78, 83
 Estradé, S. 26, 41, 43

F

Fabregat, C. 113
 Farid, G. 102, 105, 106
 Farré, R. 49
 Fenoglio, I. 36
 Ferchichi, A. 82
 Fernández-Pradas, J. M. 92
 Ferrari, M. 76
 Ferrer, M. 110
 Figueroa, A. 20, 56, 59
 Fijahi, L. 113
 Fikry, H. 64
 Filgaira, I. 74
 Font-Bardía, M. 61
 Forero, J. D. 20, 95

Fort-Grandas, I. 18, 85, 98
 Fraile Rodríguez, A. 24, 56, 59, 87, 103

Franzese, G. 36

G

Gallo-Cordova, A. 56
 Gamez, P. 82
 García Celma, M. J. 80
 García del Muro, M. 59
 García-Amorós, J. 113
 García-Martín, A., 87
 García-Santiago, A. 30, 62
 García, Í. 56
 García, M. L. 25, 74, 78, 81, 83
 Garrido, B. 20, 88, 93, 95
 Garrós, N. 70
 Gavara, N. 48, 50
 Gil, M. 32
 Giubertoni, D. 24
 Gliszczyńska, A. 78, 83
 Gómez, E. 107, 108, 109, 111, 112
 Gong, R. C. 74
 González Sánchez, J. A. 25
 Gonzalez-Martinez, S. 96
 González-Torres, S. 88
 Guerrero, A. 24
 Guyot, Y. 60

H

Halbaut, L. 25
 Hernandez-Machado, A. 28
 Hernández, J. M. 30, 62, 63, 64, 67
 Hernández, S. 20, 88, 93
 Homs, N. 19, 32
 Huidobro, L. 108

I

Idrobo, J. C. 24
 Ingés-Mullo, J. 29

J

Jover, J. 110

K

Kaiser, N. 43
 Kakabadze, T. 80
 Kociak, M. 26
 Kohlmann, H. 62
 Kosksi, T. 79
 Kovalenko, M. 88, 93

L

Labarta, A. 20, 24, 56, 59, 87, 103
 Lakshmi Kavya Anguluri, N. V. 73
 Latella, I. 40
 Lima, J. C. 104
 Lloreda, J. 107
 Llorente, X. 74
 López-Conesa, L. 43
 López-Haro, M. 41
 Lopez-Ramajo, D. 74

Lopez-Villegas, J. M. 30
 López, M. 18, 84

M

Ma, Y. 19, 102, 105, 106
 Macià, F. 21, 62, 67
 Madariaga Burgos, J. 81
 Maddaleno, A. S. 72
 Majumdar, S. 105, 106
 Mallandrich, M. 46, 70, 71
 Maluenda, D. 54
 Maniaki, D. 60
 Manils, J. 74
 Marchese, A. 27
 Marchetti, G. 36
 Mari-Guaita, J. 95
 Martí Jerez, E. 92
 Martín-Badosa, E. 52
 Martínez-Blanco, Á. 48, 50
 Martínez-Herrero, R. 54
 Martínez-Serra, A. 36
 Martínez, M. 110
 Martínez, O. 66
 Mas-Torrent, M. 113
 Maury, O. 60
 Mendoza-Gamero, Y. 96, 98
 Mestre-Torà, B. 90, 94
 Mitjans, M. 72
 Mohammadi, R. 70
 Mohandes, F. 110
 Molina-Luna, L. 43
 Monopoli, M. P. 36
 Montero, M. T. 46
 Montes-Usategui, M. 52
 Mora-Seró, I. 88
 Morán, M. C. 76
 Moreno-Sereno, M. 18, 84, 85, 98
 Moro-López, M. 49
 Morral Ruíz, G. 80
 Moya, C. 20, 56, 59, 103
 Muñoz-Rosas, A. L. 102

N

Nandi, P. 41, 43
 Nasiou, D. 43
 Navarro-Urrios, D. 97, 99
 Nielsen, H. H. 58
 Noé, S. 48, 50
 Noé, V. 31, 47
 Nogales-Altozano, P. 31
 Noguera-Monteagudo, A. 53
 Nogués, J. 26

O

Olivé-Palau, S. 49
 Ortiz, M. 112
 Ospina, R. 19, 102, 105, 106
 Otero, J. 49, 50
 Öz, S. 88, 93

P

Palacio, F. 95

Pander, P. 61
 Pardo, I. 91
 Pascual, E. 91
 Pastor, J. 88, 93
 Peiró, F. 15, 26, 41, 43
 Pellegrino, P. 18, 84, 98
 Pérez-Murano, F. 24
 Pérez-García, Ll. 69, 73
 Pieres Termes, R. 84
 Plaza, J. A. 69
 Puerto Morales, M. 56
 Puigjaner, C. 110
 Pujol, M. 74, 81
 Putriüté, G. 68, 75, 77

R

Raïch, O. 110
 Ramírez de la Piscina, P. 19, 32
 Reta, D. 65
 Ricci, P. 27, 90
 Rincón, M. 71
 Riobé, F. 60
 Rodríguez Abreu, C. 80
 Rodríguez-Álvarez, J. 24, 47, 56
 Rodríguez-Lagunas, M. J. 70
 Rodríguez-Suné, L. 27
 Rodríguez, G. 58
 Rodríguez, L. 61, 100, 101, 104
 Rodríguez, R. 53
 Roig, X. 25
 Rojas, J. M. 31
 Romano-Rodríguez, A. 84, 85, 98
 Romero, E. 104
 Rosales Rivera, L. C. 80
 Rossi, B. 36
 Roubeau, O. 57, 58, 60, 65
 Roviola, M. 62, 67
 Rubi, J. M. 39
 Rubi, M. 37
 Ruiz-Torres, J. 20, 103

S

Sabaté, R. 68, 77
 Saggau, P. 27
 Sagués, F. 29, 45
 Sainz-García, D. 96, 99
 Sánchez López, E. 74, 81
 Sanchez-Díaz, J. 88
 Sánchez, A. 32
 Sarango-Granda, P. 71
 Sarret, M. 55
 Sepulveda, B. 26
 Serafin, J. 32
 Serrà, A. 107, 108, 109, 111, 112
 Serra, P. 92
 Sevilla, N. 31
 Sickinger, A. 60
 Soler, C. 74
 Sosa, L. 71
 Sotirakopoulos, K. A. 65
 Spinelli, G. 82

Sturza, M. I. 62
 Suarez, I. 88, 93
 Suárez, T. 69
 Sunyer, R. 49
 Svendsen, W. E. 85

T

Tarancón, A. 41
 Teat, S. J. 57
 Tejada, J. 30
 Tejedor, I. 65
 Tiana-Alsina, J. 52
 Toledo-García, N. 52
 Torrenegra-Rico, J. D. 37, 39
 Torres-Andrés, J. 29
 Trepard, F. 58
 Tubau, À. 61

V

Valiuska, S. 31
 Van Durme, B. 53
 Van Vlierberghe, S. 53
 Vargas, B. 43
 Vazquez-Aige, M. 30
 Vázquez, P. 69
 Velasco, D. 113
 Vélez-Cerón, I. 45
 Vendrell, X. 19
 Vescio, G. 88, 93, 95
 Vicente, R. 61
 Vidal-Ferran, A. 18, 98
 Vilariño, P. 58
 Vilche, A. 53
 Vinardell, M. P. 72

W

Weatherill, L. 61

X

Xiulan Aribó, M. 59
 Xuriguera, E. 53

Y

Yedra, Ll. 41, 43

Z

Zhuchkov, G. 100



Institut de Nanociència
i Nanotecnologia



UNIVERSITAT DE
BARCELONA

UNIVERSITAT DE BARCELONA
in²ub - Institut de Nanociència i Nanotecnologia

in2ub@ub.edu

www.ub.edu/in2ub

in²

Institut de Nanociència
i Nanotecnologia



UNIVERSITAT DE
BARCELONA